Development of a Novel Cam-based Infinitely Variable Transmission

Derek Lahr

Thesis submitted to the faculty of the Virginia Polytechnic Institute and State University in partial fulfillment of the requirements for the degree of

Master of Science
In
Mechanical Engineering

Dennis Hong, Chair
Bob Sturges
Robert West

November 6th, 2009
Blacksburg, Virginia

Keywords: Infinitely Variable Transmission, IVT, CVT, Cammoid, Ratcheting Drive

Development of a Novel Cam-based Infinitely Variable Transmission

Derek F. Lahr

(ABSTRACT)

An infinitely variable transmission (IVT) is a transmission that can smoothly and continuously vary the speed ratio between an input and output from zero to some other positive or negative ratio; they are a subset of continuously variable transmissions (CVTs), which themselves do not have the ability to produce a zero gear ratio. In this thesis, the operation, analysis, and development of a novel, highly configurable, Cam-based Infinitely Variable Transmission of the ratcheting drive type is presented.

There are several categories of CVTs in existence today, including traction, belt, and ratcheting types. Drives of these types, their attributes, and associated design challenges are discussed to frame the development of the Cam-based IVT. The operation of this transmission is kinematically similar to a planetary gearset, and therefore, its operation is described with that in mind including a description of the six major components of the transmission, those being the cam, followers, carriers, planet gears, sun gears, and one way clutches. The kinematic equation describing its motion is derived based on the similarities it shares with a planetary gearset. Additionally, the equations for the cam design are developed here as the operation of the CVT is highly dependent on the shape of the cam. There are six simple inversions of this device and each inversion has special characteristics and limitations, for example, the available gear range. A method was developed to select the most suitable inversion, gearing, and follower velocity for a given application.

The contact stress between the rollers and cam is the limiting stress within the transmission. A parametric study is used to quantify the relationship between this stress and the transmission parameters. Based off those results, two optimization strategies and their results are discussed. The first is an iterative brute force type numerical search and the second is a genetic algorithm. The optimization results are shown to be similar and successfully reduced the contact stress by 40%. To further improve the transmission performance, several mechanisms were developed for this unique transmission. These include a compact and lightweight differential mechanism based on a cord and pulley system to reduce the contact force on the rollers. In addition, a unique external/inverted cam topology was developed to improve the contact geometry between the rollers and said cam. A prototype was built based on both the optimization strategies and these mechanisms and is described within. Finally, a Prony brake dynamometer with cradled motor was constructed to test the transmission; the results of those tests show the Cam-based IVT to be 93% efficient at low input torque levels.

Acknowledgements

This thesis is dedicated to my mother, Debra Frei-Lahr. She was an incredibly supportive woman who was always there to give thoughtful and intelligent advice when I doubted, whether it be on friends, school, or my career. She became sick soon after I started graduate school, and even during her illness, maintained a great interest in my work as only the most wonderful and caring mother could. She is dearly missed.

I would also like to thank my father, Chris Lahr, for his unending supply of support, constant praise, and wise (if not bold) advice. It is only due to him, that during my junior year as an undergraduate I went to my advisor, Dr. Hong, with a Lego model of the transmission and the desire to make it into a senior design project. During the five years since, he has contributed a huge amount to this project and it could easily be said that without him, I would not have made it this far.

It goes without saying that my advisor, Dennis Hong, deserves a great deal of gratitude. If not for him and his endless supply of opportunities, this thesis would not have been. From the first undergraduate competition I entered on his advice, to the numerous grants and travel opportunities he has made possible, and his willingness to take time from his schedule to give me guidance, his support too has been unending. I continue to be thankful for the chance to work with him, and look forward to the continued success of RoMeLa.

I thank the members of my graduate committee, Dr. Robert West and Dr. Bob Sturges, who have given me their time and support to better my education and research.

Thanks to everyone in RoMeLa. I look forward to coming in every day because of the great friends I have here and the amazing and fun work we do together. Special thanks go to several design teams, the 2005/06 team of Jesse, Akira, Matt, Michael, Mike, and Ryan for the help in making the first working CVT prototype. Also, the second team of 2008/09 of Nick, Carl, Andrew, Kenny, Jake, and Matthew, for building a functioning dynamometer on which to test the transmission. It was a pleasure working with all of you.

Table of Contents

1 Introduction 1
1-1 Motivation 1
1-2 Background and Prior Art 2
1-3 Mapping 6
2 Operation 8
2-1 Components 8
2-1 Operation 8
2-2 Operation via the conservation of energy 11
2-3 Shifting 13
2-4 Conclusions 14
3 Kinematic Analysis of the Cam-based IVT 16
3-1 Introduction 16
3-2 Derivation of Kinematic Equation 16
3-3 Cam Profile Design 19
3-4 Inversion Characteristics 21
3-5 Gear Range Investigation 25
3-6 Inversion selection criteria 30
3-7 Conclusions 31
4 Numerical Optimization of the Cam-based IVT 32
4-1 Parametric Study 33
4-2 Numerical Search 36
4-3 Genetic Algorithm 40
4-3-1 Chromosome Coding 40
4-3-2 Fitness Scoring 42
4-3-3 Fitness Scaling 43
4-3-4 Selection and Mutation rate 44
4-3-5 Stop Criteria 44
4-4 Results 45
5 Mechanical Design Improvements 46
5-1 Contact Stress Model 47
5-1-1 Methods Contact Stress Reduction 47
5-2 Dual active follower system 48

5-2-1 Benefits 48
5-2-2 Differential System Requirements 49
5-2-3 Prior Art 49
5-2-4 Cable Differential Design 50
5-2-5 Kinematic Equation 52
5-3 Mechanical Design 52
5-4 External Inverted Cam 54
5-4-1 Benefits 55
5-4-2 Incorporation of the External Cam 56
5-5 Conclusions 57
6 Prototype Testing 58
6-1 Prototype History 58
6-2 Gamma Prototype Design 59
6-2-1 Sun Assembly 63
6-2-2 Input Assembly 64
6-2-3 Carrier 64
6-2-4 Shifter 65
6-2-5 Assembled Transmission 67
6-1 Dynamometer Design 67
6-2 Testing procedure 68
6-3 Results 69
6-4 Scalability of the Cam-based IVT 70
6-5 Conclusions 72
7 Conclusions 73
8 References 75
9 Appendix 78
9-1 Nomenclature 78
9-2 Inversion Analysis Continued 79

List of Figures

Figure 1-1. A) Torroidal , B) Kopp, C) Milner, D) Beier CVTs 3
Figure 1-2. Schematic of a Belt type CVT. [21] 3
Figure 1-3. Schematic of Benitez's ratcheting CVT. 5
Figure 1-4. The "Zero-Max" ratcheting CVT. 5
Figure 2-1. Major components of a simplified representation of the Cam-based IVT on left, and the complete prototype on right. The version on left has its sprag clutches in the planet gears while the version on right has them in the sun gears. 9
Figure 2-2. Displacement and Velocity profile. 9
Figure 2-3. Three velocity profiles overlaid out of phase. 10
Figure 2-4. Schematic of IVT with round cam. One of the carriers and the base has been removed from the figure on right for clarity. 10
Figure 2-5. Free body diagram of the forces on the follower/planet pulley assembly. 12
Figure 2-6. Isometric and front view of a 3-D cammoid model installed in the first prototype. 13
Figure 2-7. The front and isometric view of a concept transmission showing the shifting mechanism. 14
Figure 3-1. Displacement profile of the cam profile. 17
Figure 3-2. Overlay of the two velocity profiles showing the constant velocity motion that results from the out of phase followers. 18
Figure 3-3: Planet gearset representative of the Cam-based IVT. 18
Figure 3-4. The follower's velocity and position as a function of cam rotation. 20
Figure 3-5. The follower's acceleration as a function of cam rotation. 21
Figure 3-6. Binary search algorithm for finding the level of acceleration, a, for given $\omega_{p.}$ 22
Figure 3-7. Power flow with one-way clutch. 23
Figure 3-8. Power flow with one-way clutch. 24
Figure 3-9. Configurations necessary to change the sign of θ_L. 25
Figure 3-10. Transmission ratio versus the internal ratio while using the sun gear as the input and the carrier as the output. 26
Figure 3-11. Viewing angle taken for the transmission ratio analysis. A clockwise rotation of any component is considered as positive. 27
Figure 3-12. Transmission ratio versus internal ratio using the cam as the input and the carrier as the output. 28
Figure 4-1. Reference for contact force equations. 34
Figure 4-2. Sum of the moments on the follower about its axis of rotation. 35
Figure 4-3. Contact force between roller and cam versus follower velocity and initial follower position. 36
Figure 4-4. Graphical representation of a two dimensional search area and the effect δ has on the search area. 38
Figure 4-5. Contact force between roller and cam versus follower velocity and initial follower position 39
Figure 4-6. Flowchart of the Genetic Algorithm process. 40
Figure 4-7. Variable relationships to the transmission model. 41
Figure 4-8. Fitness function used to evaluate individual fitness based on the contact stress. 43
Figure 4-9. Fitness scaling used to promote healthy competition. 44
Figure 5-1. Model of Naude's cam driven IVT with cylindrical rollers [33]. 48
Figure 5-2. The current follower system on the left and the dual roller follower concept. 49
Figure 5-3. Cable driven differential drive mechanism. [41] 50
Figure 5-4. The cable differential system used in the CVT, right, is an adaptation of a conventional pulley system. 51

Figure 5-5. Two optional cable routes for the cable differential, one through the middle of the sun pulley, one which is routed around the sun. 51
Figure 5-6.Transmission prototype with cable differential. 53
Figure 5-7. Comparison of the single follower cam profile to that of the dual follower design. 53
Figure 5-8. Maximum offset of followers during normal operation. 54
Figure 5-9. Partial CAD model of transmission including the external cam, followers, and carriers. 55
Figure 5-10. CAD model of the follower and roller assembly to be used with the external inverted cam design. 56
Figure 5-11 Points on the inactive profile of the cam of zero draft, also where the shifter guides should be located to minimize shifting loads. 57
Figure 6-1. Prototypes from left to right: one speed Lego, three speed 'Alpha', fully functional 'Beta' version. 59
Figure 6-2. Gamma prototype with external cam and cable differential gear mechanism. 59
Figure 6-3. The maximum external radius of the cam surface was computed to allow for .1[in] at the thinnest section. 61
Figure 6-4. CAD model of the follower and roller assembly used with the internal cam design. 61
Figure 6-5. CAD model of the follower and roller assembly used with the external inverted cam design. 62
Figure 6-6. Gamma prototype with cam removed for clarity. 62
Figure 6-7. Sun assembly on left, and individual sun pulley on right. 63
Figure 6-8. Schematic of cable routing from one planet pulley to another around the sun and differential pulleys. 64
Figure 6-9. Carrier of the Cam-based IVT. 65
Figure 6-10. Shifter mechanism of the 'Beta' prototype on left, and its inherent compliance on right used to reduce shifting loads. 66
Figure 6-11. Shifter mechanism of the 'Gamma' prototype on left, and its position in the transmission on right. 66
Figure 6-12. Assembled transmission on base with input and output cogs shown. 67
Figure 6-13. The current dynamometer setup including the current CIVT design. The three components of the design are connected together by a chain. 68
Figure 6-14. Unfiltered raw data on left, versus the data that has been averaged using a discrete time low-pass filter with a break frequency of 30 [Hz]. 69
Figure 6-15. Filtered torque data from the dynamometer versus the sample number. 70
Figure 9-1. Input Carrier, Output Cam 79
Figure 9-2. Input cam, Output sun 80
Figure 9-3. Input sun, Output cam 81
Figure 9-4. Input carrier, Output sun 82

List of Tables

Table 1: Acceleration, Velocity, and Position functions for a transmission having *n* followers 19
Table 2: Possible ratio range of the various inversions. 21
Table 3. Possible ratio range of the various inversions. 30
Table 4: Possible ratio range of the various inversions. 31
Table 5: Design specifications for optimization algorithms. 33
Table 6: Parameter bounds for the numerical search and genetic algorithm. 37
Table 7: Parameter bounds for the numerical search and genetic algorithm. 41
Table 8: Final parameter values resulting from the optimizations. 45
Table 9: Design specifications for optimization algorithms. 60
Table 10: Final parameter values resulting from the optimizations. 62

1 Introduction

A continuously variable transmission (CVT) is a system which allows a user to vary the angular velocity between an input and output progressively from one positive value to another. Unlike conventional transmissions, the selection of gears is not restricted to a finite number of ratios. An infinitely variable transmission (IVT), such as the Cam-based IVT presented here, is a particular type of CVT which can also achieve a transmission ratio of zero, commonly referred to as a geared neutral.

These transmissions, which date back to at least 1877 [1], are sometimes referred to as one of the "Holy Grails" of mechanical engineering, because firstly, they can transmit power at an infinite number of gear ratios, and secondly, it is extremely difficult to design and produce a transmission competitive with their non-continuously variable cousins. The lack of commercially successful instances is not a result of a lack of trying; on the contrary, the US Patent Office can provide examples of nearly every possible iteration. Therefore the difficulty in penetrating the transmission market with a CVT reflects mostly upon the difficulty of designing a competitive one. This work details the four years of research and development undertaken to create an IVT through the careful creation, selection, design and optimization of different concepts and mechanisms. It is hoped that this work will contribute to the knowledge, understanding, and success of all continuously variable transmissions.

1-1 Motivation

One of the main motivations behind the nearly 150 years of development of CVT's is the performance advantages they can bring to rotary motion applications. Electric motors, internal combustion engines, generators, and pumps have and still are being adapted with CVTs [2]. They are promoted in all these applications as a method of improving the performance, economy and functionality of components that operate together but at independent and often varying speeds. Probably the most common example given to support the development of a CVT is the automobile transmission. In such an application, a CVT allows the car engine to operate at its maximum efficiency, independent of the speed at which the car is travelling. Therefore fuel efficiency gains of 10% are possible [3].

Another such example is that of variable speed wind turbines. These are the latest generation in wind turbine technologies which, as the name suggests, allow the turbine rotor to spin at variable speeds in accordance with wind speed fluctuations. Therefore, the rotors operate at maximum aerodynamic efficiency at all times, producing 10% more energy per year [4]. Current variable speed wind turbine designs use expensive power electronics to convert a variable AC power to the constant voltage and frequency necessary for the nation’s electrical grid. Replacing these electronics with a mechanical transmission can significantly decrease the cost, up to 6.8% with

little or no loss in reliability [5]. The Cam-based IVT presented here was motivated by similar applications.

The driving force behind the development of the Cam-based IVT was the concept of a lightweight and self contained bicycle transmission with the ability to shift under power. Such an application has no shortage of challenges and restrictions, all of which have shaped the outcome of this work. To name a few, a bicycle transmission must be small and lightweight so as to not encumber the rider significantly. It must be efficient to keep energy losses to a minimum, and probably most importantly, the transmission should be able to handle the large torques generated by the rider. While the application of a bicycle transmission may appear narrow in scope, the design challenges are quite broad and demanding. Therefore the outcome of this work is relevant to any other application in which the weight, size and torque requirements are relaxed. To highlight the solutions developed for this application, particular attention will be paid to the decisions that shaped the design to meet these restrictions.

1-2 Background and Prior Art

As mentioned previously, there is a substantial amount of prior work in the field of continuously variable transmissions. In general, these drives can be separated into 4 different categories [6]: traction, belt, ratcheting, and hydrostatic drives. Additionally, sometimes electrical couplings (generator/inverter/motor) are considered to be CVTs. Of these, only the hydrostatic and electrical drives depend on power transmission devices which are not mechanically linked and therefore less attention will be given to these.

Traction drives will be addressed first. Their single unifying characteristic is the transmission of power through rolling contact. As one can imagine then, much of their success depends upon the careful design of the contact patch geometry and kinematics through the gear range. The several most common and successful types of traction drives are the Full or Half Toroidal [7-10], the Kopp Variator [11-14], the Milner CVT [15-18] and the Beier Variator [19].

The full and half torroidial drives are perhaps the oldest designs, dating back to the 1877 patent by Hunt [1]. They are comprised of at least two traction discs with a toroidal shape connected through one or more rollers. By varying the angle at which the rollers contact the toroidal discs, the effective gear ratio can be changed. There has been an extensive amount of research on these drives, and some have been commercially successful [20]. Both the Kopp Variator and the Milner CVT use planet balls instead of rollers to transmit power between the input and output races. While the Kopp Variator actively positions these rollers to control the transmission ratio, the Milner CVT moves the races axially instead. Finally, the Beier Variator relies on intermeshing disks whose radial separation can be adjusted to vary the transmission ratio.

There are several challenges which traction CVT designers face. One of the most significant is the high contact force necessary between the rotating elements [3] required to transmit torque through a thin film of oil. Enormous pressures (up to 3.5[GPa]) [16] are necessary to compress the film of oil to the point that it nearly solidifies, and only then can it efficiently transmit motion. Therefore the power transmission components must be manufactured from a suitably strong material (such as AISI 4340, 8620, or 9310) with suitably fine surface finish [20]. In addition, care must be taken to reduce the losses in the bearings that generate the clamping forces between the elements. Great efforts are also taken to reduce the losses within that contact patch due to viscous sliding, the greatest culprit being spin, which is the rotation of the rolling elements about an axis perpendicular to the contact patch. The penalties which these drives incur in terms of cost, complexity, and weight were meant to be avoided while developing the Cam-based IVT.

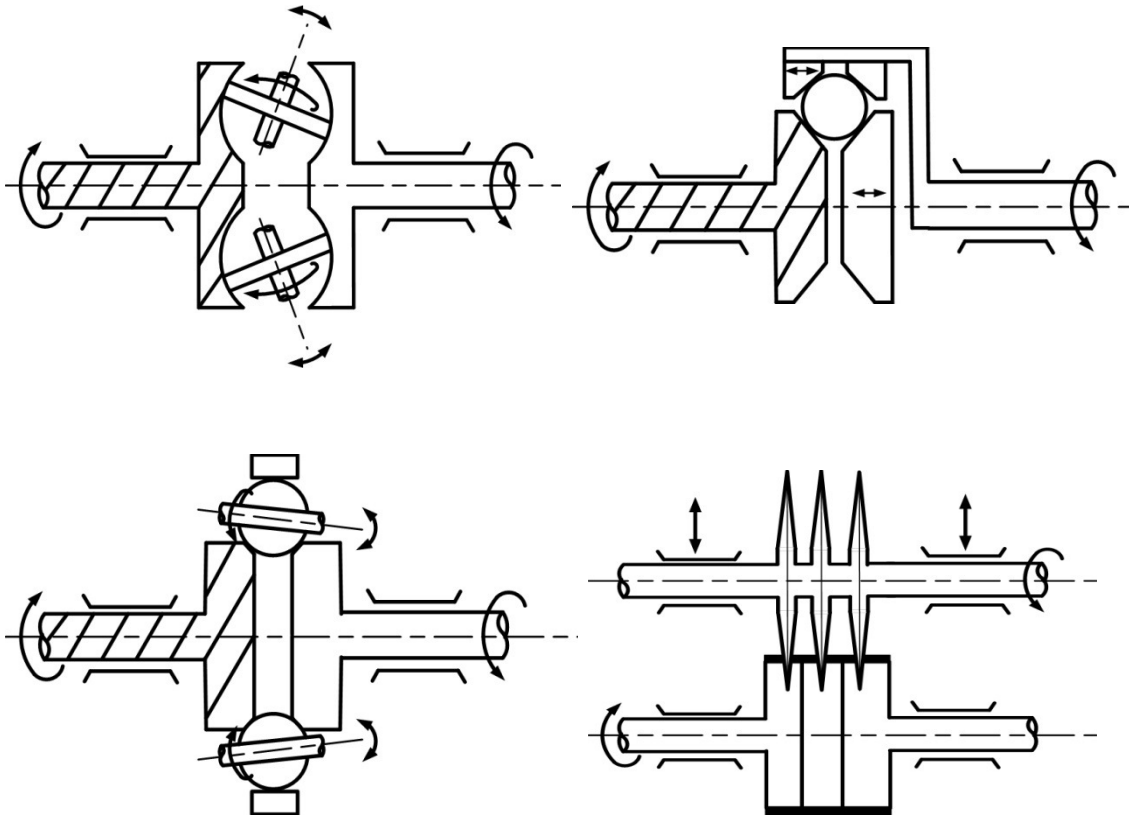

Figure 1-1. A) Torroidal , B) Kopp, C) Milner, D) Beier CVTs

Belt drives are another class of continuously variable transmissions. They are notable because they are the most common CVT developed for commercial production, being used by Honda, Ford, Nissan and Toyota as well as many small tractor and ATV manufacturers. In principle, their operation has changed little since their inception. This transmission uses a pair of 'V' shaped pulleys arranged so that one half of the pulley can be moved axially in relation to the other to vary the gear ratio. A matching belt which rides in the pulleys transmit power between the driven and driving pulley, as can be seen in Figure 1-2.

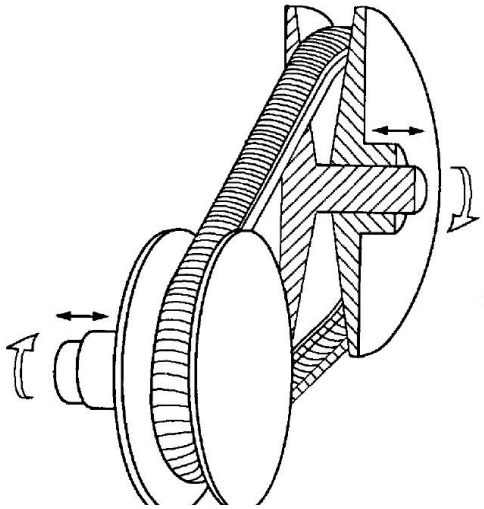

Figure 1-2. Schematic of a Belt type CVT. [21]

Belt drives have been developed into a unique mechanical device, one in which a belt is pushed between two pulleys, as opposed to pulled. The problem is analogous to the cliché of "pushing a rope". Such a motion is accomplished with a number of flat plates mounted on a metal band or belt; when put under a load, the plates are compressed together and form a rigid column between the two pulleys. Unfortunately, with as much development as they have undergone, belt CVTs are still unable to produce efficiency gains in automobiles predicted by their makers. In fact, some are often worse than their manual transmission counterparts. [21,22]

The losses present in belt CVT's can be contributed to three sources. First, like the traction drives presented earlier, there are losses due to the viscous slip between the belt and the pulleys. Secondly, to generate the clamping forces on the belt while controlling the gear ratio often requires complex hydraulic systems whose pumping losses represent a significant energy cost. [10] Finally, there are belt related frictional losses which occur as a result of the sliding motion of the belt as it enters and leaves the v-groove in the pulley. Regardless, because of the significant development these transmissions have undergone and the relative simplicity of low power versions, they have seen widespread acceptance.

The ratcheting drive is the final class of mechanically driven continuously variable transmissions. All ratcheting CVTs, of which the Cam-based IVT is one, converts a rotary input into at least two out of phase oscillations of adjustable magnitude. Through the use of several one-way clutches, these oscillations are then converted back to a rotation. By varying the magnitude of the oscillations, the ratio between the input and output angular velocities can be changed. If these adjustments can be made infinitely small, the transmission will be continuously variable. Up to now, one of the main limitations of ratcheting CVT's has been their propensity for producing a nonuniform output for a uniform input [23-27]; therefore, their applications have been limited, but there are several examples of such transmissions.

The prior work in ratcheting drives includes that by Benitez. He presents a transmission whose operation is similar to the concept presented here, but it is characterized by its non-uniform output for a uniform input [23,24]. It is similar in that there is a device that varies the amount of rotation of several planetary gears with respect to a carrier. As seen in Figure 1-3, this particular design uses a slotted plate to drive a number of planet gears around a sun gear. By varying the eccentricty, e, of the slotted plate with respect to the "guide groove", the angular velocity of the planet gears will vary as they travel around the sun. Each planet gear is connected to a second planet through a one way clutch; the planet with the largest velocity will then transmit motion to the ring gear. Similarly, Pires [25,26] incorporates a number of levers, shafts, and a slotted plate to accomplish the same task. Similar in concept to both Pires and Benitez, but different in implementation, is a design used by Matsumoto[27] which is commercially available under the name "Zero-Max" [29]. This transmission uses several reciprocating four bar linkages to oscillate the indexing clutches. One of the several linkage systems can be seen in Figure 1-4. An input is applied to the crank mechanism on the left which oscillates the first four bar mechanism. A second four bar loop converts these oscillations to a continuous output rotation through a number of one way clutches. Like Benitez's and Pires' CVTs though, it exhibits a non-uniform output for a uniform input.

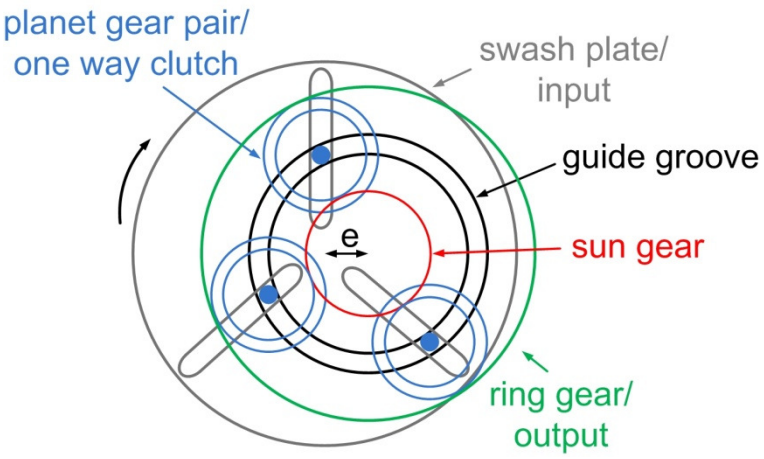

Figure 1-3. Schematic of Benitez's ratcheting CVT.

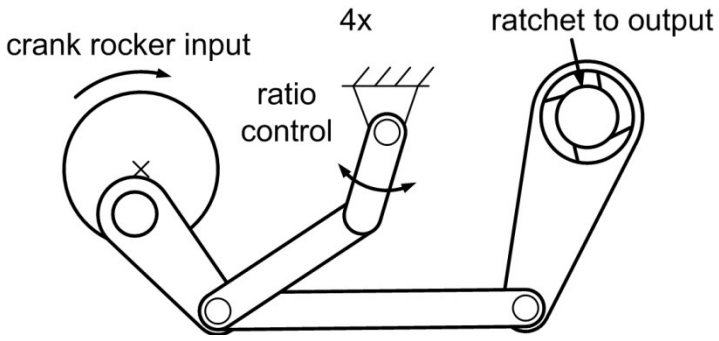

Figure 1-4. The "Zero-Max" ratcheting CVT.

Because of ratcheting drives unique power transmission mechanisms, they do not exhibit the typical loss mechanisms of other CVTs. For instance, the frictional elements which transmit power in all ratcheting CVTs are of the diode type. That is, they are either locked or freewheeling, and when transmitting power in the locked state they do so with no losses because there is no relative motion between components. The losses during freewheeling are also relatively small and independent of the transmitted power. Therefore large rolling frictional losses and viscous slipping losses are avoided. Secondly the clamping forces necessary to generate the friction is self-contained within commercially available sprag clutches. This keeps manufacturing costs and weight to a minimum. In addition, the shifting mechanisms can be designed to shift only the unloaded side of the drive, the particular mechanism which is freewheeling at that instant. Therefore the inefficient and complex shifting mechanisms of belt drives can be avoided.

While ratcheting drives avoid the common sources of inefficiencies, the limited amount of available research references and commercially available examples can in part be attributed to the nearly universal trait of these transmissions, their non-uniform output for a uniform input. That is, given a constant input velocity, the output of most ratcheting drives will exhibit some sort of rippling effect. Up to now this limitation has relegated these drives to vibration tolerant applications only, such as farm equipment [32]. The Cam-based IVT presented within though has the ability to produce a continuous and uniform output. Therefore it is hoped that this transmission will be able to bridge the gap between research only studies and real world applications for both ratcheting drives and CVT's in general. It should be noted that only one other similar transmission as been recently developed, that by Jan Naude, covered under US and

international patents [33] although no academic literature is available. While similar, significant differences exist as both designs overcome problematic areas with different solutions.

The capability of the Cam-based IVT to produce a smooth and continuous output given a smooth input comes as the name suggests, from a cam and follower mechanism. Only this mechanism gives the designer sufficient freedom to eliminate any output velocity ripples unlike the linkage driven systems used by Benitez, Pires, and Matsumoto. Cams of course are not new in this regard, but the development of three dimensional cams with varying profiles along their lengths are a relative new development only made feasible with the development of computer controlled machining operations. Although not impossible, it would have been very difficult to achieve such a shape prior to the development of this technology.

In the same vein as other ratcheting drives, Cam-based IVT uses such a three dimensional cam to produce oscillations in a number of followers. By varying the profile on which the followers travel, the magnitude of these oscillations can be changed, thereby producing a different transmission ratio. And through the careful design of the cam profiles, the smoothness of the output velocity can be ensured.

1-3 Mapping

Up to this point, this work has discussed the background art that exists in continuously variable transmission design. Traction, belt, and ratcheting drives were discussed. The remaining work will focus specifically on the Cam-based IVT. The report is predominantly divided into two sections, Chapters 2 and 3 discuss the analysis and operation of the transmission, while the latter half specifically addresses the optimization and development work that was performed.

In theory, the kinematics of ratcheting drives is obvious. It would seem their complexity should not exceed that of a crank rocker mechanism. The same is true for some inversions of the Cam-based IVT. However, in its functioning form, the opposite is true, and in the authors experience it often takes several explanations and a live demo for most to grasp the kinematics of this transmission. Therefore careful attention is given to the Operations section of this thesis with the hopes that the explanation is as thorough and as well illustrated as possible.

A kinematic analysis is then presented which builds off the principles of operation. In this section, the equations governing the motion of the CVT are derived from those of a planetary gearset, and for a constant output case, are shown to be relatively simple. Additionally, the equations for the cam design are also first presented here, as the operation of the CVT is obviously highly dependent on the shape of the cam. The derivations presented here are used to study the inversion characteristics in the next section.

Following the description, attention is given to the six possible simple inversions of the Cam-based IVT. This section is included to elaborate on the special capabilities and limitations of each inversion with particular details given on the available gear ratio. This is particularly important with the Cam-based IVT as each inversion has a unique possible gear ratio range; therefore deciding on the appropriate inversion to satisfy the constraints of the application should be the first step of a design process. The reasoning behind the selection of the particular inversion for this work will also be explained.

As with many power transmission devices, the problem of contact stress is an issue with the Cam-based IVT as well. In this case, the problem arises as a result not of the frictional members in the transmission, but between the cam and follower rollers. A broad study of the factors influencing

this stress is presented as a way of understanding the results from two optimization strategies which were implemented. The first strategy presented is that of a numerical search, in which a broad design space is systematically searched for an optimum. A genetic algorithm is then elaborated on as a comparison.

In addition to the optimization schemes, several mechanical solutions were developed as a way of reducing the contact stress. Firstly, a cable differential was designed to double the number of rollers under load at any time, nearly halving the stress. Secondly an external cam was devised to provide a more complementary contact surface for the roller, further reducing the stress. Both these innovations are presented along with the appropriate design considerations.

The achievable efficiency of a CVT is often used as its defining characteristic. In that light, a test rig was developed by a senior design team under the guidance of the author. Using an electric gear motor and several load cells, the efficiency was experimentally determined. The design of the experiments and the results are presented here. Some final thoughts and possible future directions are presented lastly.

2 Operation

2-1 Components

In its simplest form, this transmission contains six unique components. Each component is described here briefly and illustrated in the following figures. While their function may be alluded to here, it is more completely described in Section 2-1. The heart of this transmission is a centrally located three dimensional cammoid. It is sometimes referred to as simply "cam" but this is somewhat undescriptive as a cammoid has a continuously varying profile along its length. The cammoid is most often fixed to ground, but can also serve as the input or output. Around the cammoid are a number of followers. Each follower interacts with the cammoid through a spherical or ellipsoidal roller mounted on said follower. The followers are held to the cam surface when not under load by a return spring.

The followers are rotatably mounted to one or two carrier plates, the third major unique component of the transmission. The carriers are used to support the followers as well as transmit the input and output torques in some inversions. This is analogous to a carrier's function in a planetary gearset. When designed to rotate, the carriers do so about the central axis of the cam. On each follower, is fixed a planet gear or pulley which meshes with a sun gear. The sixth and final unique component of the Cam-based IVT is a one way clutch located inside each of the planet gears or the sun gears. These clutches are responsible for rectifying the oscillations generated by the cam and followers and can be connected on the race opposite the sun gear to either the input, output, or ground depending on the inversion specified. The shaft connected to this inner race of the sun gears is simply called the sun gear shaft and its sole purpose is to transmit torques from an external source to both of the sun gears (however usually not at the same time). If however the sprag clutches are located in the planet gears, the sun shaft is directly connected to only one sun gear. These components are labeled on both a simplified representation and a prototype CAD model in Figure 2-1.

2-1 Operation

Attention is now given to the operation of the Cam-based IVT, specifically, how the major components detailed above interact to generate a smooth output motion at infinitely many transmission ratios. There are six different inversions of the Cam-based IVT, and while the majority of this work is focused on one particular inversion, the operation of the transmission is better first illustrated with a dynamically simpler one. Therefore the configuration first presented here uses the cam as the input and the sun gear shaft as the output.

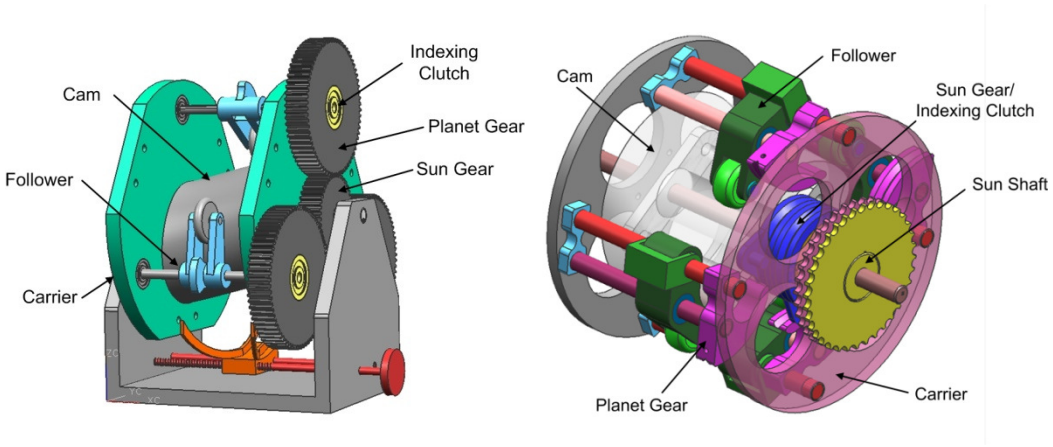

Figure 2-1. Major components of a simplified representation of the Cam-based IVT on left, and the complete prototype on right. The version on left has its sprag clutches in the planet gears while the version on right has them in the sun gears.

Consider now the simplest inversion the Cam-based IVT which can be thought of as simply a cam and follower system with an attached geartrain. Therefore the cam will serve as the input and the sun gear shaft as the output while the carriers remain fixed to ground. In such a configuration, a rotational input to the cam causes the followers to simply oscillate up and down as they are held to the cam with the return springs. In this case the followers do not rotate around the cam because the carrier is fixed. Due to the shape of the cam and the position of the followers around the cam, the followers oscillate out of phase of one another, that is, one follower will rotate clockwise, while the other rotates predominately counter clockwise.

The out of phase oscillations of the followers drives the planet gears and their respective sun gears back and forth. It follows then that one direction of the oscillations of the sun gears will be transmitted to the sun gear shaft through the one way clutches. Because one sun gear will always be moving faster in the locking direction of the clutches, one sun will transmit torque to the sun gear shaft. With a carefully designed cam profile, the velocity of the sun gears can be shaped to produce a smooth and continuous output of the sun gear shaft with no velocity ripples. Such a velocity profile would look something like that in Figure 2-2. When overlaid with the velocity profile of the other out of phase followers, it would appear as in Figure 2-3.

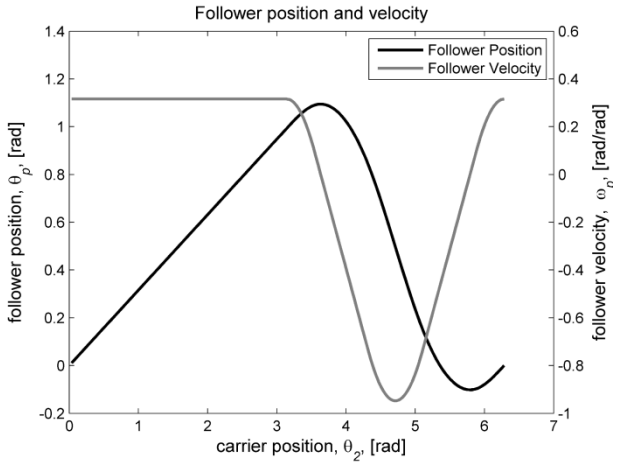

Figure 2-2. Displacement and Velocity profile.

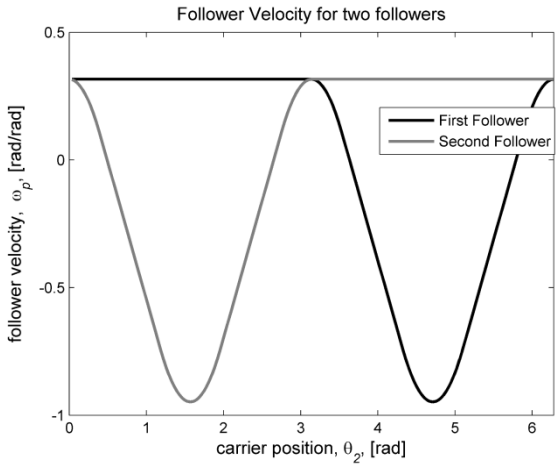

Figure 2-3. Three velocity profiles overlaid out of phase.

The inversion studied for the majority of this work utilizes the sun gear shaft as the input, and the carriers as the output. As will be elaborated on later, this particular inversion was chosen because it provides higher gear ratios as well as a larger gear ratio range for a given cam eccentricity. It has been experienced that this inversion is more difficult to visualize then others, but much clarity can be gained by picturing something similar and much more familiar, a planetary gearset. To fully describe its motion, first a circular cam is considered. This will decouple the motion of the carrier and the followers around the cam, from the oscillations of the followers. Once these dynamics are understood, it is only a small step to superimpose follower oscillations and their effects on the carrier motion to understand the full system.

To begin, first consider a perfectly circular cam as in Figure 2-4. A clockwise rotation applied to the sun gear is transmitted by all one way clutches as a counter clockwise rotation on the planet gears. Such a motion will force the follower down onto the cam and because they cannot rotate in this direction (due to the cam reaction force) the carrier will then rotate around the cam. The carrier rotates with a 1:1 ratio to the sun gear.

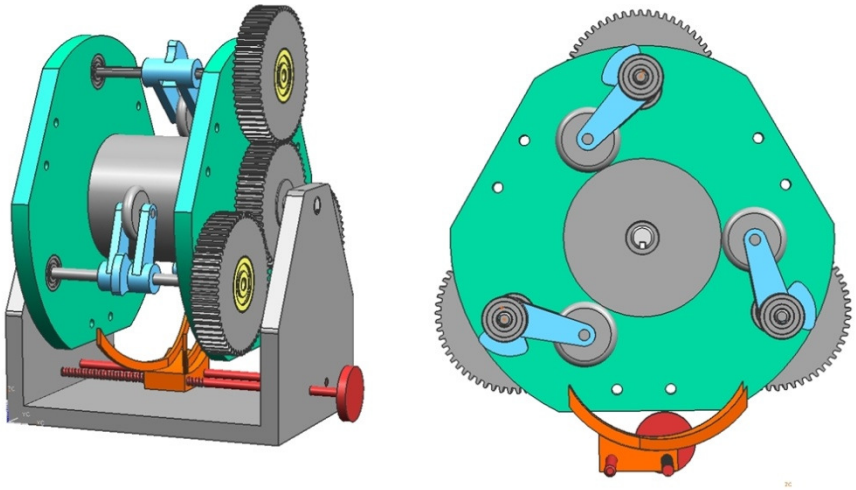

Figure 2-4. Schematic of IVT with round cam. One of the carriers and the base has been removed from the figure on right for clarity.

Now consider a non-circular cam. The operation is nearly the same as above; a clockwise rotation on the sun gear shaft forces one of the followers down onto the cam. Since the follower cannot rotate in this direction, the sun gear rotation causes the carrier to rotate about the cam just as above. Except this time, as the carrier rotates around the cam, the follower will rotate in relation to the carrier as it follows the lobes of the cam. For example, when the follower moves up onto a cam lobe, it and the attached planet gear will rotate in a clockwise direction in relation to the carrier. Here the operation is similar to a planetary gearset, where the rotation of the carrier depends upon both the sun gear and the planet gear rotations. Specifically, the relative clockwise rotation of the planet gears forces them to rotate (or walk) around the sun gear in a clockwise direction. As the planet gears orbit the sun gear they move the carrier along with them, advancing its position with respect to the sun gear. Because the carrier is the output, a non circular cam will create transmission ratios greater than unity.

The reader will note that only one follower was considered in the above analysis. This follower, the one under load, is called the active follower. This is because while the active follower is moving up a cam lobe, the second or third followers, called the inactive followers, should be moving down a lobe and will be rotating in a counterclockwise direction with respect to the carrier as a result. A counterclockwise rotation of the attached planet gear will rotate the meshing sun gear further clockwise, in a direction that disengages the one way clutch. (Because the sun gear shaft rotates clockwise, they are installed such that they lock up with a counter clockwise application of torque on the sun gear race.) Therefore as one sun gear transmits torque to the carrier and cam, the second is freewheeling faster in the same direction, but one gear is always engaged with the sun gear shaft.

2-2 Operation via the conservation of energy

An alternative explanation of the operation is possible that utilizes free body diagrams and conservation of energy principles to understand the interaction between components and the result that has on their motion. Because the planet gear and follower assembly interacts with all the remaining major components (sun gear, cam, and carrier), it is the focus of this analysis.

Figure 2-5 shows the follower and planet gear assembly. There exist three significant reaction forces on the assembly, that of the sun gear (f_s), the carrier bearing (f_{car}), and the cam (f_{cam}). Assume a clockwise torque is applied to the sun gear as the input, which will exert a force to the right and a counter clockwise torque on the planet gear. This force that generates this torque is given as Equation 2-1:

$$f_s = \frac{\tau_s}{r_s} \tag{2-1}$$

where τ_s is the torque on the sun, and r_s is the radius of the sun gear.

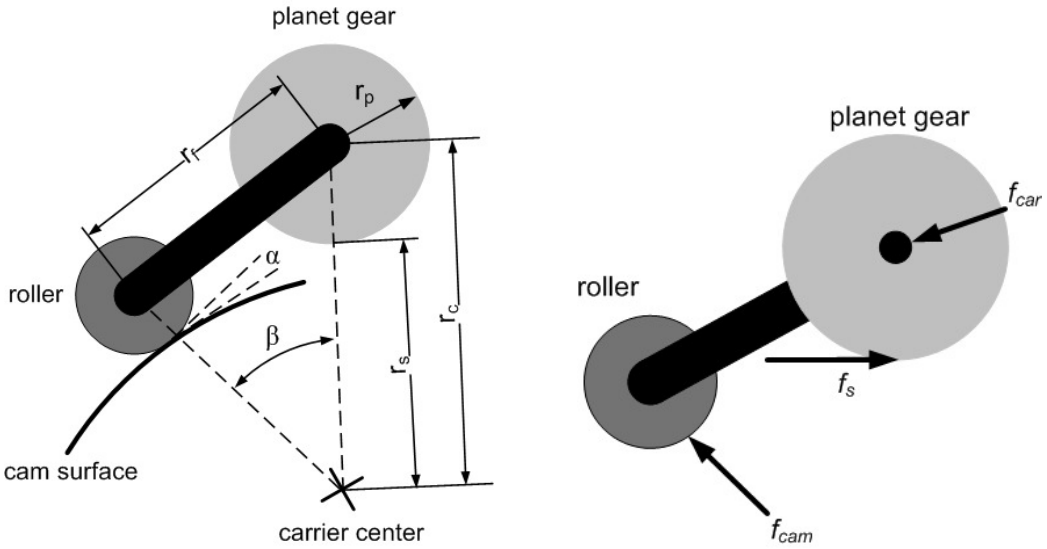

Figure 2-5. Free body diagram of the forces on the follower/planet pulley assembly.

An equal and opposite torque is exerted on the follower by the cam due to the reaction force between the cam and roller. This force, f_{cam}, is given by:

$$f_{cam} = f_s \frac{r_p}{r_f} \tag{2-2}$$

where r_p is the radius of the planet pulley. Now the only reaction left to consider is that from the carrier, f_{car}. Summing the forces in the *x*-direction, setting equal to zero, and solving for the force due to the carrier will produce:

$$f_{car} = f_s - sin\,(\beta + \alpha) f_{cam} \tag{2-3}$$

where α is the pressure angle of the cam and β is the angle between the roller center, carrier center, and planet gear center. Combining Equations 2-1, 2-2, and 2-3 and putting in terms of the carrier torque, τ_{car}, produces Equation 2-4:

$$\frac{\tau_{car}}{r_c} = \frac{t_s}{r_s}\left(1 - \frac{r_p}{r_f} sin\,(\beta + \alpha)\right). \tag{2-4}$$

Because the term $sin(\beta+\alpha)$ can be shown to be greater than r_f/r_c for small α>0 by simple trigonometry, Equation 2-4 can be rewritten as Equation 2-5:

$$\frac{\tau_{car}}{r_c} < \frac{\tau_s}{r_s}\left(1 - \frac{r_p}{r_f}\frac{r_f}{r_c}\right) \tag{2-5}$$

where the magnitude of the inequality is determined by the magnitude of α. As α grows, the right side of the equation will become larger with respect to the left. If α becomes too large, Equation *2-5* may not hold, but this indicates the pressure angle of the cam is larger than is feasible with this inversion of the transmission. Rearranging terms yields Equation 2-6:

$$\tau_{car} < \tau_s \frac{r_c}{r_s}\left(\frac{r_c - r_p}{r_c}\right) = \tau_s. \tag{2-6}$$

where r_c-r_p=r_s as can be seen in Figure 2-5.

Conservation of energy states that if there are no energy storage devices, the input energy must equal the output energy. Similarly, the input power equals the output power, where the input power is given as $\tau_s \cdot \omega_s$ and the output by $\tau_{car} \cdot \omega_{car}$ in which ω_s and ω_{car} are the angular velocities of the sun and carrier respectively. Because τ_{car} is less than τ_s, ω_{car} must be larger than ω_s indicating a transmission ratio larger than 1 for the transmission. Therefore when the pressure angle, α, is zero for a circular cam, the transmission ratio will be 1:1 and as α increases, the transmission ratio will also increase.

2-3 Shifting

The shifting capabilities of the Cam-based IVT are particularly unique, especially when compared to those of traction drives. Specifically, many traction drives require large and powerful shifting mechanism to reposition components in relation to one another as they transmit power. For traction drives this can be particularly problematic because of the large normal forces necessary to generate traction. Belt and toroidal drives are noteworthy examples [3,34]. However, as with all ratcheting drives, at least one of the drive components (the follower in the case of the Cam-based IVT) is unloaded for some time. Repositioning these components when unloaded eases the task of shifting. This is a characteristic unique to the Cam-based IVT even amongst other ratcheting drives.

As mentioned before, the cam is made up of an infinite number of profiles along its length; therefore, the cam's cross section continuously changes along its length, as can be seen in Figure 2-6. It changes from a circular shape on one end to an oblong or peanut shape on the other. Shifting the transmission between gears is accomplished by positioning the followers on different profiles along the cams length. This affects the magnitude of the follower's oscillations and therefore the output of the transmission. This fact can be seen in Equation *2-4*, in which the followers' position along the cam determines the pressure angle, α, which thereby determines the torque applied to the carrier and therefore transmission ratio.

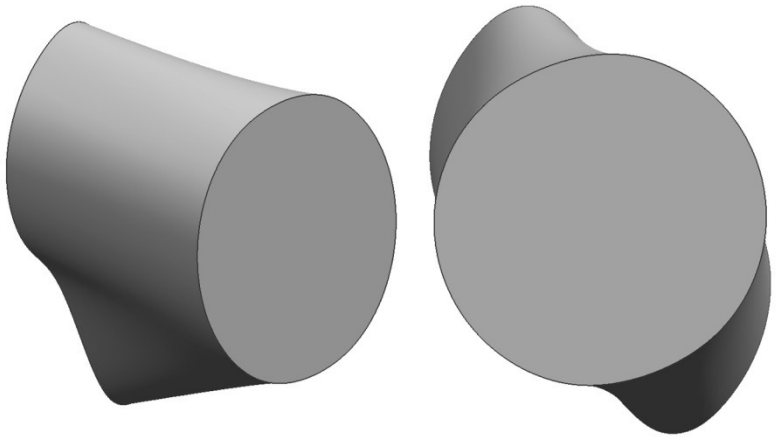

Figure 2-6. Isometric and front view of a 3-D cammoid model installed in the first prototype.

While shifting, to move either the cam or the followers under load, would require the shifter to overcome the high static friction between the roller and the cam. In addition, as a follower moves across the cam, it may also rotate as it moves onto a larger lobe. If this rotation is in the same

direction required to activate the indexing clutches, the followers will then be transmitting torque to the output, and therefore part of the shifting load will be required to drive the output.

A unique advantage of a ratcheting drive though, is that the followers are unloaded on a portion of the cam as they rotate in a direction that disengages the one way clutches. This allows them to be repositioned with less force, and therefore, the shifting mechanism must only overcome the friction between the roller and the cam produced by the return spring. As the follower then enters the active profile of the cam, it will produce a different transmission ratio. One such concept for achieving this task can be seen in Figure 2-7. In this design, each follower is built with a guiding tab, and as the carrier rotates the followers through the shifter guides, those guides will drive the follower across the cam to the desired profile. A lead screw is used to reposition the shifter guides to select different profiles. Although this design was never implemented in a prototype, it demonstrates the necessary functionality required of a shifter. A complete description of the shifting mechanism actually implemented on the prototypes is presented in the mechanical design portion of this work.

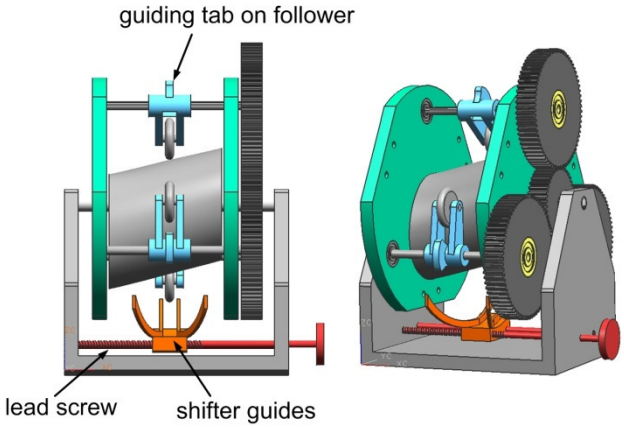

Figure 2-7. The front and isometric view of a concept transmission showing the shifting mechanism.

2-4 Conclusions

In this section the components and operation of the Cam-based IVT were presented. The seven major components the reader should be familiar with are the sun shaft, sun gears, planet gears, carrier, followers, cammoid, and one way clutches. Amongst these, the cammoid, carrier, and sun shaft can theoretically act as either the input or output for different inversions. The cammoid is at the heart of the transmission, essentially being a cam with a continuously changing profile along its length. This component gives the transmission infinitely variable transmission ratios.

The operation of the transmission was also presented, first as a simple cam/follower system with an attached geartrain. In this inversion, the cam rotates as the input, causing the followers to oscillate out of phase with one another. Two planet gears transmit this motion to two sun gears where one-way clutches rectify these oscillations to produce a continuous output. This is the simplest inversion of the transmission, and although some inversions are more difficult to visualize, it is important to remember that their operation is only an inversion of this simple system. Finally the inversion used for the majority of this work is described in which the sun shaft serves as the input, and the carrier as the output. The operation was also described in terms of the conservation of energy principle, which may yield more insight.

The shifting mechanism in the Cam-based IVT was also introduced. Unlike traction and belt CVT's in which the drive components are always loaded when under power, the nature of a ratcheting drive means one or more drive components are unloaded every cycle. These unloaded components can be shifted with relative ease, and upon entering the active portion of the cycle will transmit power at the new transmission ratio. Shifting of the Cam-based IVT is accomplished by repositioning the unloaded followers along the length of the cam. The specific mechanisms developed for shifting are described later.

3 Kinematic Analysis of the Cam-based IVT

3-1 Introduction

In this section, a kinematic analysis is presented which builds off the principles outlined in the theory of operations section. Specifically, the equations governing the motion of the CVT are derived from those of a planetary gearset, and for a constant output case, are shown to be relatively simple. Following this derivation, the equations for cam profile design are presented in which a zero acceleration active profile is combined with a trapezoidal acceleration return profile. The derivations presented here are then used to study the characteristics of each inversion, in particular focusing on the achievable gear range of each inversion.

3-2 Derivation of Kinematic Equation

As stated before the behavior of the transmission is highly dependent on the cam profile. In this section, the behavior of the transmission is described in terms of the profile developed for this transmission, which for reference can be seen in Figure 3-1. This profile combines a constant velocity section, as seen from 0[rad] to π [rad], with an appropriate return profile, from π [rad] to 2π [rad]. It is possible to generalize the kinematic equation for the transmission to work with any cam profile, but given that the constant velocity type is of the most interest as an IVT, it is the focus of this work.

Several terms must be defined to follow the analysis. The acting planet is the planet gear that is driving the output; it is often the planet gear with the maximum rotational velocity with respect to the carrier at that time. It may also be thought of as the planet gear with the largest velocity in the driving direction, the direction in which the one way clutches engage. This is to differentiate it from planet gears which may have a larger absolute velocity but are rotating in the wrong direction to engage the clutches and therefore have no effect on the output. The portion of the cam profile on which a followers, and therefore planet gears, are active is called the acting profile.

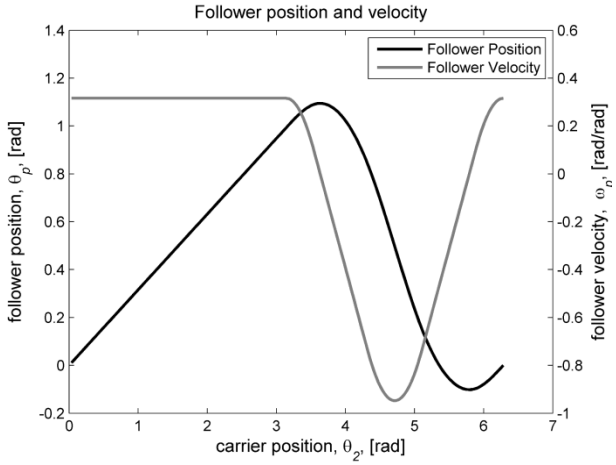

Figure 3-1. Displacement profile of the cam profile.

A generalized term is defined here called the follower lift, or θ_L. This term can be thought of as the cumulative lift of all active followers for one cycle. Therefore it is the sum of all followers rotations during the active profile of the cam for one cycle of the followers around the cam divided by the number of followers, *n*. It is a useful term to characterize both the cam profile and the kinematics and is given by:

$$\theta_L = \frac{\pm \int_0^{2\pi} \max(w_{p1}(\theta_2), w_{p2}(\theta_2), ..., w_{pn}(\theta_2)) d\theta_2}{n}, \tag{3-1}$$

where ω_p is the velocity of the planet gear. The sign of θ_L is positive if the follower rotates in the same direction of the cam as it rotates and is negative if they rotate in opposite directions. That is, if a clockwise rotation of the cam also rotates the followers clockwise, θ_L is positive, however if the followers rotate counterclockwise, θ_L is negative. When the follower velocity is constant for the acting profile, Equation 3-1 simplifies to:

$$\theta_L = \pm \max(\omega_p(\theta_2)) \frac{2\pi}{n}. \tag{3-2}$$

Such is the case in Figure 3-2 which shows *n* velocity profiles overlaid with and offset of $2\pi/n$. In this example, *n* equals two for a transmission with two followers.

To derive the kinematic equation for the entire transmission, we can apply the analogy presented earlier of a planetary gearset, as seen in Figure 3-3. Although it is not a conventional planetary geartrain because it has a second sun gear instead of a ring gear, the kinematics are very similar. This analogy is useful because of the resemblance in topology and operation that the Cam-based IVT bears to such a geartrain. The kinematic relationship of the gearset presented below is given in Equation 3-3:

$$\theta_3 = \theta_2 \left(1 - \frac{r_a r_p}{r_b r_3} \right) + \theta_1 \frac{r_a r_p}{r_b r_3}, \tag{3-3}$$

where θ_1, θ_2, and θ_3 denote the angular position of the first sun, carrier, and second sun respectively, and r_a, r_b, r_p, and r_3 denote the radii of the gears as presented in Figure 3-3.

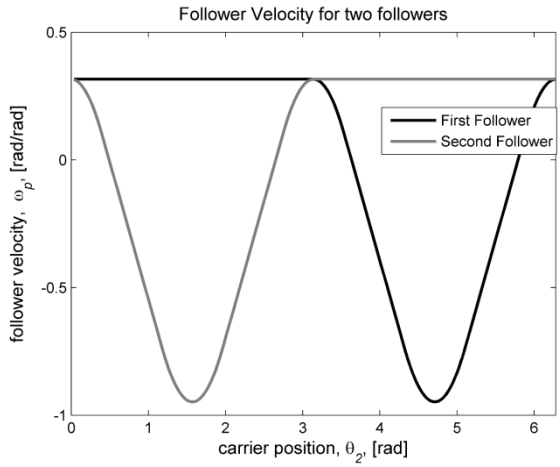

Figure 3-2. Overlay of the two velocity profiles showing the constant velocity motion that results from the out of phase followers.

Now consider the interaction between one of the sun and planet gears. The sun is centrally located, and when rotated, will cause the planet gear to rotate as well. This operation is similar to the cam and follower arrangement of the Cam-based IVT and therefore the cam and follower system can be modeled as a geartrain. The cam is centrally located, and when rotated, causes at least one follower to rotate in a direction that engages the clutches. Therefore, the relationship expressed in Equation 3 can be modified by replacing the gear ratio of one pair of sun and planet gears with an effective gear ratio between the followers and the cam. This effective ratio captures the interaction between the cam and followers during the active profile.

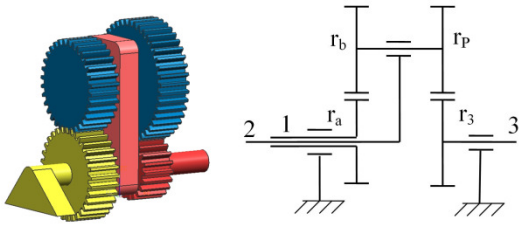

Figure 3-3: Planet gearset representative of the Cam-based IVT.

This effective ratio is essentially the collective amount the followers rotate in one direction for every revolution about the cam and is therefore analogous to the gear ratio r_A/r_B in Equation 3. It is a representation of the cam and followers as a gear train, in which the rotation between the two are coupled by a constant ratio. It should be noted that this is only possible with at least two followers that are out of phase of each other, have a constant velocity during the active profile, and are coupled through one-way clutches. In such an arrangement, their overall behavior is in fact more like a gear set because the significant portion of their rotation (the active profile) is constant and unidirectional. The effective gear ratio is given by Equation 3-4:

$$EffectiveRatio = \frac{\theta_L n}{2\pi} . \tag{3-4}$$

The relationships presented in Equation 3-4 is substituted into Equation 3-3 for r_A/r_B which becomes Equation 3-5, where θ_1 now representing the angular position of the cam instead of the second sun gear:

$$\theta_3 = \theta_2\left(1-\frac{\theta_L n r_p}{2\pi r_3}\right)+\theta_1\frac{\theta_L n r_p}{2\pi r_3}, \tag{3-5}$$

Differentiating Equation 3-5 yields:

$$\omega_3 = \omega_2\left(1-\frac{\theta_L n r_p}{2\pi r_3}\right)+\omega_1\frac{\theta_L n r_p}{2\pi r_3}. \tag{3-6}$$

Equation 3-6 can be used for any inversion of the transmission where the corresponding velocity of the stationary component is set to zero.

3-3 Cam Profile Design

The requirements for the cam profile needed only to satisfy two requirements, 1) provide a period of constant velocity for a suitable duration, and 2) ensure a smooth return profile following the constant velocity portion. To accomplish this, the cam profile was designed with a zero acceleration portion while a trapezoidal acceleration curve controlled the return profile. The trapezoidal acceleration curves were selected for their simplicity, as compared to those based on sinusoids or higher power curves, as well as the continuous velocity and finite jerk levels they produce.

This curve includes a portion of zero acceleration, to produce the constant velocity output as seen on row one of Table 2. The trapezoidal portion required for the return of the follower begins on row 2, in which the acceleration is linearly decreasing from zero to a finite level, *-a*, at which point it remains long enough for the velocity of the follower to reverse direction. At the proper time, the acceleration reverses direction and begins to slow the follower down to again reverse direction and accelerate to the proper velocity for the active profile of the cam. These transitions are represented by rows 4 and 5 of Table 2. For the trapezoidal sections, the length of the upslope was on quarter the duration of the horizontal portion to keep jerk levels to an acceptable level [46]. In addition, the trapezoidal sections are not equal in duration or magnitude. Both the positive and negative accelerations can be separately optimized to ensure the follower does not leave the cam or cause undercutting due to high accelerations. The velocity and position equations presented in Table 2 are found from the integration of the acceleration curve.

Table 1: Acceleration, Velocity, and Position functions for a transmission having *n* followers

Phase, θ_2=	Acceleration, A=	Velocity, ω_p=	Position, θ_p=
[0,2π/n]	0	ω_p	$\omega_{p*}\theta_2+\theta_p(0)$
[2π/n,b],	$-a_1\frac{(\theta_2-\frac{2\pi}{n})}{(b-\frac{2\pi}{n})}$	$-a_1\frac{(\theta_2-\frac{2\pi}{n})^2}{2(b-\frac{2\pi}{n})}+\omega_p(\frac{2\pi}{n})$	$-a_1\frac{(\theta_2-\frac{2\pi}{n})^3}{6(b-\frac{2\pi}{n})}+\omega_p(\frac{2\pi}{n})(\theta_2-\frac{2\pi}{n})+\theta_p(\frac{2\pi}{n})$
[b,c],	$-a_1$	$-a_1(\theta_2-b)+\omega_p(b)$	$\frac{-a_1(\theta_2-b)^2}{2}+\omega_p(b)(\theta_2-b)+\theta_p(b)$

[c,d],	$a_1\left[\frac{(\theta_2-c)}{(d-c)}-1\right]$	$a_1\left[\frac{(\theta_2-c)^2}{2(d-c)}-(\theta_2-c)\right]+\omega_p(c)$	$a_1\left[\frac{(\theta_2-c)^3}{6(d-c)}-\frac{(\theta_2-c)^2}{2}\right]+\omega_p(c)\cdot(\theta_2-c)+\theta_p(c)$
[d,e],	$a_2\frac{(\theta_2-d)}{(e-d)}$	$a_2\frac{(\theta_2-d)^2}{2(e-d)}+\omega_p(d)$	$a_1\frac{(\theta_2-d)^3}{6(e-d)}-\omega_p(d)(\theta_2-d)+\theta_p(d)$
[e,f],	a_2	$a_2(\theta_2-e)+\omega_p(e)$	$a_2\frac{(\theta_2-e)^2}{2}+\omega_p(d)\cdot(\theta_2-e)+\theta_p(e)$
[f, 2π]	$-a_2\left[\frac{(\theta_2-f)}{(2\pi-f)}-1\right]$	$-a_2\left[\frac{(\theta_2-f)^2}{2(2\pi-f)}-(\theta_2-f)\right]+\omega_p(f)$	$-a_2\left[\frac{(\theta_2-f)^3}{6(2\pi-f)}-\frac{(\theta_2-f)^2}{2}\right]+\omega_p(f)\cdot(\theta_2-f)+\theta_p(f)$

For any given value of ω_p, it is necessary to determine the actual level of acceleration needed to return the follower to its origin after the acting profile. Once the parameters *b* through *f* are determined for the specific transmission, the necessary level of accelerations can be found numerically using a binary search method. A numerical approach was taken for simplicity and ease of computation even though there is only one unknown and one equation, $\theta_p(2\pi)=0$; however, the derivation of this equation symbolically is unnecessarily complex and therefore avoided. The algorithm for this binary search is shown in Figure 3-6. Knowing that $a_1=0$,when $\omega_p=0$, and that a_1 and a_2, are linear function of ω_p all other values of acceleration can then be linearly interpolated from these two points. The values of a_1 and a_2 are related as in Equation 3-6

$$a_1\frac{(e-b)+(d-c)}{2}=a_2\frac{(2\pi-d)+(f-e)}{2}. \tag{3-6}$$

The position, velocity, and acceleration curves of the cam follower can be seen in Figure 3-5 and Figure 3-5.

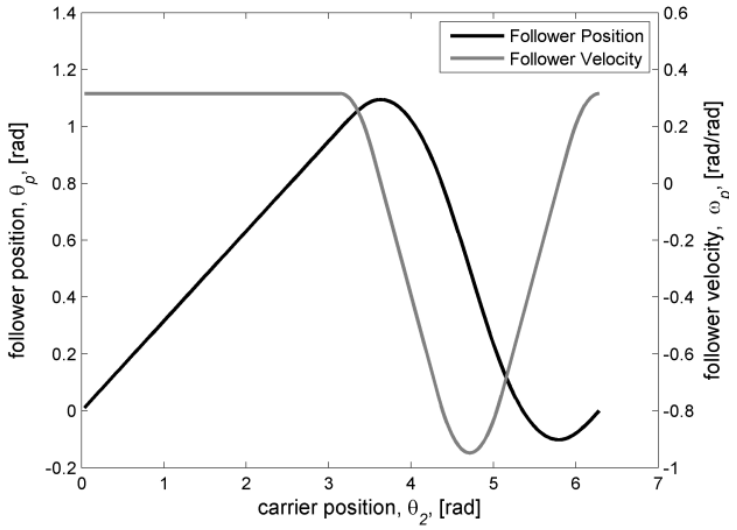

Figure 3-4. The follower's velocity and position as a function of cam rotation.

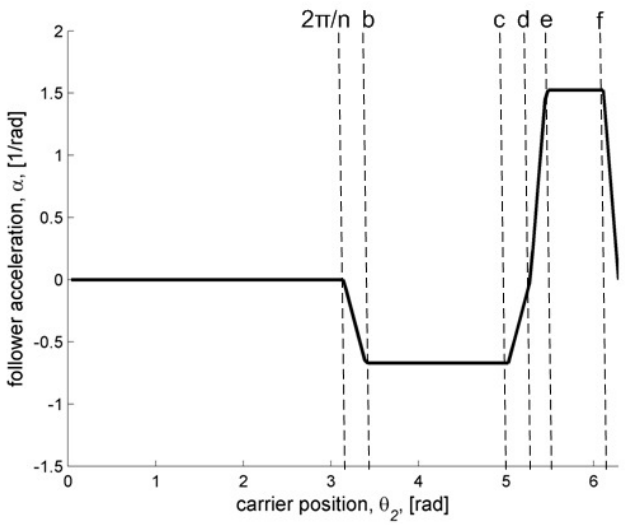

Figure 3-5. The follower's acceleration as a function of cam rotation.

3-4 Inversion Characteristics

As mentioned before, the Cam-based IVT has three primary components, the sun gear, carrier, and cam, each of which can be used as the input or output to the transmission. Each different combination of components is called an inversion. Attention is now given to the six possible simple inversions of the Cam-based IVT. The special capabilities and limitations of each inversion are discussed as well as the root cause of these unique characteristics. Particular details is given to the available gear ratio which is particularly important because each inversion has a unique possible gear ratio range; therefore deciding on the appropriate inversion to satisfy the constraints of the application should be the first step of a design process. The reasoning behind the selection of the particular inversion for this work will also be explained.

There are six possible simple inversions of the Cam-based IVT that can be studied. It will be shown that not all inversions are kinematically feasible, but all are investigated. These six inversions, which are listed in Table 1, are simply all possible permutations of the three components capable of receiving or delivering torque. That is, the input and output can be varied between the sun gear, planet carrier, or cam.

Table 2: Possible ratio range of the various inversions.

Inversion #	Input	Output
1	cam	carrier
2	cam	sun gear
3	sun gear	carrier
4	sun gear	cam
5	carrier	cam
6	carrier	sun gear

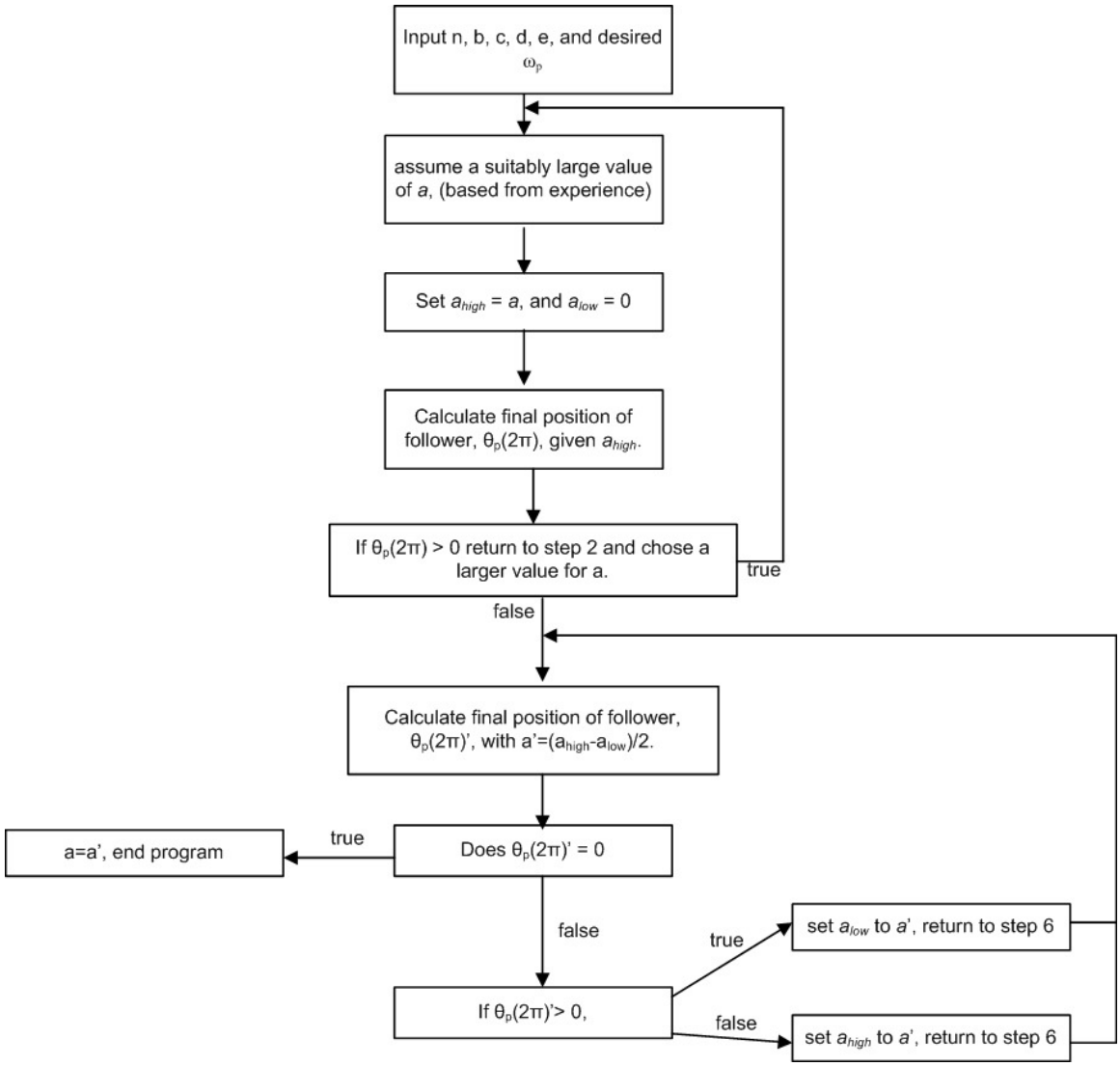

Figure 3-6. Binary search algorithm for finding the level of acceleration, *a*, for given ω_p.

For all inversions, the ratio range is limited by the engagement of the one-way clutches. Because they can only transmit force in one direction and freewheel in the opposite direction, they restrict the interaction of the followers with the cam. More specifically, the active portion of the cam must rotate the followers in the same direction as the torque exerted by the cam on the follower. This prevents the two opposite followers from exerting equal and opposite forces on the cam, thereby locking the transmission. Realistically, what this means is that the shape of the active profile is limited, and any attempt to design an active profile which does not follow this rule will result in an unexpected operation.

It should be noted that this problem can be avoided if a controllable clutch is used as opposed to a one-way clutch. If a cam or electronic circuitry were used to engage and disengage the clutch, a much larger gear range would be possible from the inversions because the direction of torque and the direction of freewheeling would not be interdependent. However due to the complexity this introduces, it is not given much consideration at this point. For automobile applications, where backdrivability is important, such an implementation should be considered as it solves both the problem of ratio range and backdrivability.

Figure 3-7 illustrates a correct configuration of the active profile and Figure 3-8 illustrates the incorrect operation. In both figures, there are two followers that rotate about the center of the inner clutch races. The races themselves are interconnected via a geartrain (not shown) and will rotate in the same direction. There is also a CCW torque on these races due to the external environment. The cam is assumed to move to the left. Linear and angular velocities are shown in blue, and forces and torques shown in green.

In Figure 3-7 the correct configuration of the active profile is illustrated; that is, the follower on the left rotates in the same direction as the torque exerted on it by the cam. Therefore this follower rotates CW and transmits a CW torque through the ratchets to the inner clutch race. The left and right inner clutch races are interconnected via a geartrain and will both rotate CW. The inactive follower on the right though is still free to move CCW down the inactive profile of the cam because the one-way clutch freewheels in this direction. This is the correct normal operation.

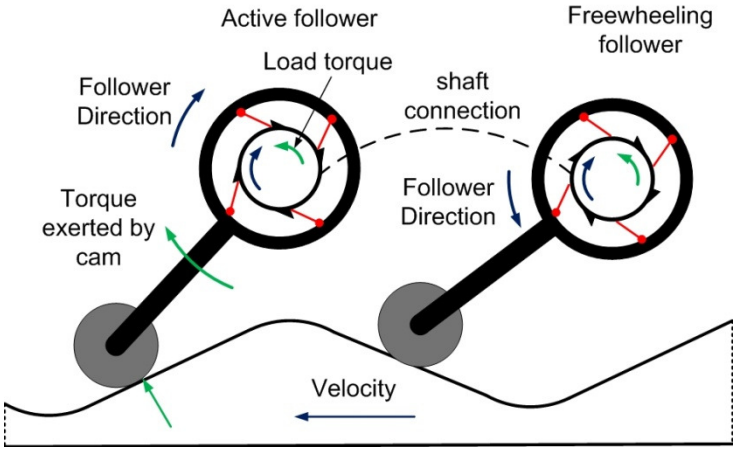

Figure 3-7. Power flow with one-way clutch.

In Figure 3-8 (d), using a proof by contradiction, it is shown that a follower cannot rotate opposite the torque applied by the cam during the active profile. Therefore any type of active profile designed in this manner will be inoperable (the mechanics of the system will automatically make this the inactive profile rather than the active, and the transmission will not operate as expected). The assumption used in this proof is that the follower on the left is the active follower and the active profile is the downsloping portion of the cam on the left. The left follower is assumed to rotate CCW while transmitting a CCW torque from the inner clutch race to the cam. The rotation and torque of this follower causes the cam to move to the left. Now consider the follower on the right. As the cam moves to the left, it causes this follower to rotate CW, which engages the one-way clutch to which it is attached and forces the right inner clutch race to rotate CW. Because the two clutch races are interconnected and cannot rotate in opposite directions, there is a contradiction with this scenario and the assumption must be wrong. The active profile can only be the profile that rotates the follower in the same direction as the torque it applies to the follower.

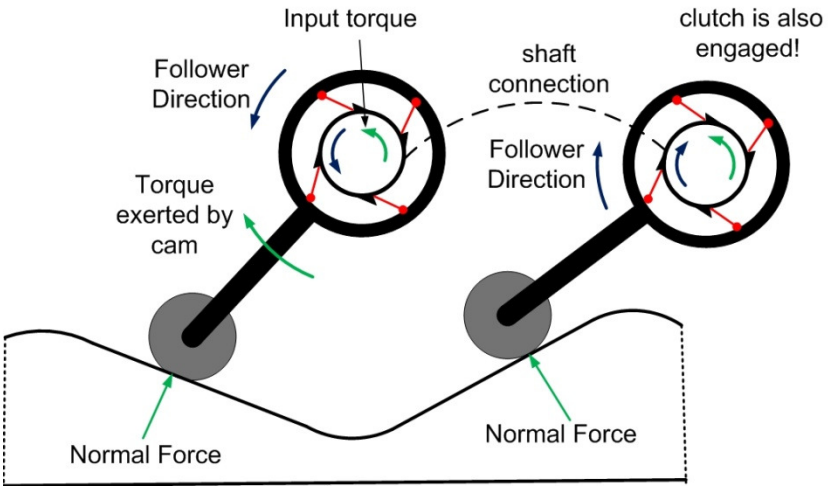

Figure 3-8. Power flow with one-way clutch.

It follows then that only the portion of the profile of the cam that rotates the follower away from the cam can be utilized. That is, the follower can only rotate so as to move the center of the roller in the same direction as the normal force on that roller. Any profile which does not follow this rule will not operate correctly. Because some profiles are not possible, not all ratios between minus infinity to positive infinity are possible, meaning the ratio range of the transmission may be limited.

In Section 3-2, it is noted that the sign of θ_L, the cumulative lift of the followers during the active profile, is determined by the relative direction of rotation between the cam and follower. Because the active profile must rotate the follower away from the cam, the only way to change the sign of θ_L is to change the physical orientation of the follower. Specifically, to generate either positive or negative values of θ_L, the follower orientation must be switched between leading and trailing, as seen in Figure 3-9. This will ensure the active portion of the cam moves the follower in the direction of the normal force. In this figure, the carrier is assumed to be stationary, and the cam rotates CW. Therefore in Figure 3-9 (a), this will generate a CW rotation in the follower, while the trailing orientation in Figure 3-9 (b) will generate a CCW. The same holds for scenarios in which the cam rotates CCW, as in Figure 3-9 (c and d).

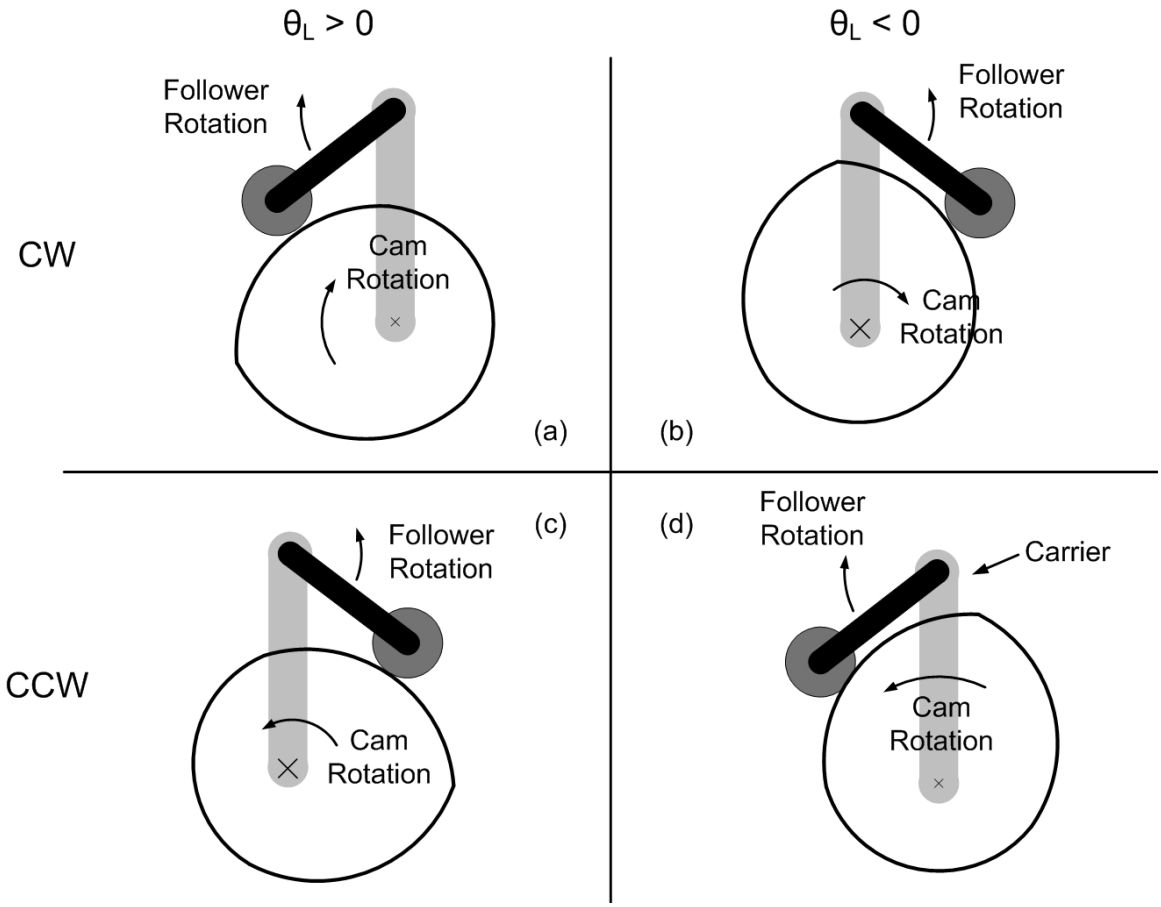

Figure 3-9. Configurations necessary to change the sign of θ_L.

3-5 Gear Range Investigation

Because of the limitations on the active profile, each of the six inversions listed in Table 1 has a range of gear ratios that are possible. For example, one inversion may be able to produce a geared neutral, while others can only produce transmission ratios greater than unity. The analysis and determination of each inversion's characteristic gear range is covered in this section. The analysis will compare the type of follower used, whether leading or trailing, and the direction of applied torque on the follower. For a feasible transmission ratio, the applied torque will rotate the follower into the cam. An infeasible ratio will cause the follower to rotate away from the cam. To determine which type of follower is used and the direction of the torque on the follower it is first necessary to define the kinematic equation specific to the inversion. Therefore the analysis begins with the kinematic equation of the transmission, reprinted here from Equation 3-6:

$$\omega_3 = \omega_2\left(1-\frac{\theta_L n r_p}{2\pi r_3}\right)+\omega_1\frac{\theta_L n r_p}{2\pi r_3}. \tag{3-8}$$

Each inversion can be modeled with this equation by setting the variable associated with the ground component equal to zero. For example, if the cam is fixed and the sun and carrier are the input and output, ω_1 should be set to zero. The gear ratio can then be defined as the output velocity over the input velocity, as in Equation 3-9:

$$TR = \frac{\omega_2}{\omega_3} = \left(1 - \frac{\theta_L n r_p}{2\pi r_3}\right)^{-1} . \tag{3-9}$$

This function can then be plotted with the overall transmission ratio, *TR*, on the y-axis, and the quantity, $\frac{\theta_L n r_p}{2\pi r_3}$ which will be called the internal ratio, on the x-axis. Therefore above the x-axis the input and output rotate in the same direction and rotate opposite on another below the x-axis. The internal ratio is basically the product of the follower lift and the ratio of the planet to sun gear radii, and is therefore a measure of the rotation of the sun gear and sprag clutch during the active profile as well as an indicator of the eccentricity of the cam profile. This plot appears in Figure 3-10. This type of plot will be studied for each inversion and contains all the necessary information to determine the type of follower used (whether leading or trailing) as well as the direction of torque on the follower. Each quadrant is analyzed independently to determine which portions of the graph are physically possible.

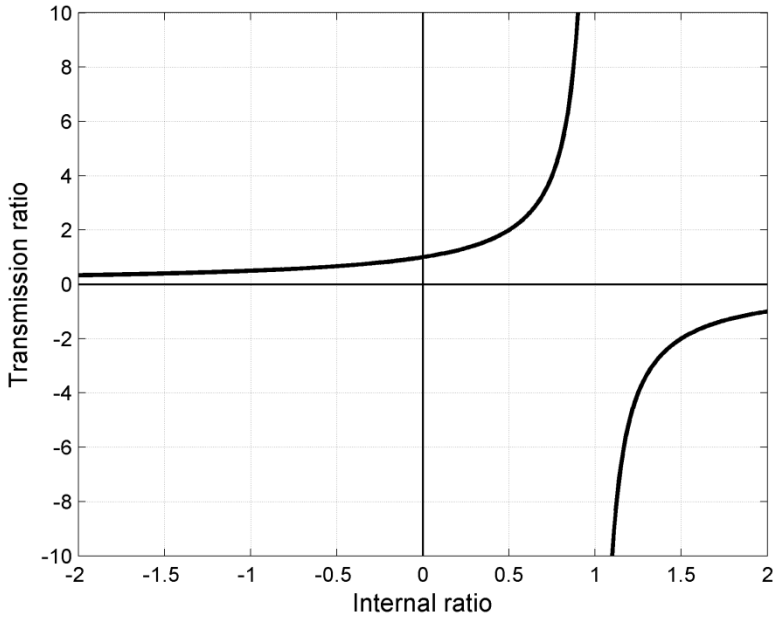

Figure 3-10. Transmission ratio versus the internal ratio while using the sun gear as the input and the carrier as the output.

The internal ratio, plotted on the x-axis can be positive or negative depending on the direction of rotation of the follower with respect to the cam (if they rotate in the same or opposite directions during the active profile as in Figure 3-9) and the direction of rotation of the planet relative to the sun (if they rotate in opposite directions, $\frac{r_p}{r_3}$, will be negative). Similarly, the transmission ratio can be either positive or negative depending on the direction of rotation of the input versus the output. Now several rules and assumptions are established which are used in the analysis.

1) The ratio, $\frac{r_p}{r_3}$, is assumed to be negative, although the arguments still hold if it is positive.

2) A positive rotation is assumed to be in the clockwise direction, as seen from the perspective of Figure 3-11.

3) The input torque and direction is positive, and the applied output torque is opposite the output direction.

4) If the cam rotates CW with respect to the carrier, follower configuration 'a' or 'b' from Figure 3-9 will be used. If it rotates CCW, configuration 'c' or 'd' should be used. This rule ensures the active profile performs as expected.

Quadrants through which the Transmission ratio curve do not pass do not need to be checked. It can be assumed the transmission will not operate in that quadrant.

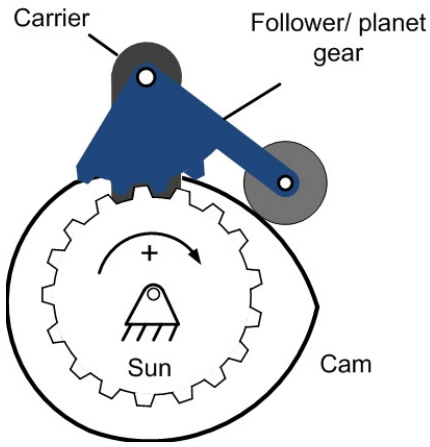

Figure 3-11. Viewing angle taken for the transmission ratio analysis. A clockwise rotation of any component is considered as positive.

The analysis takes the following approach:

5) Indentify the quadrant of interest in the plot of the transmission ratio versus internal ratio.

6) Determine the direction of rotation between the cam and the carrier using the transmission ratio in that particular quadrant.

7) Identify which follower configuration should be used in this quadrant.

8) Determine the direction of applied torque on the sun gear.

9) Check the direction of applied torque to the follower is consistent with the orientation of the follower given the configuration found in step 3.

The analysis of all four quadrants of Figure 3-10 are shown below for the inversion with the sun gear as the input and the carrier as the output.

Quadrant 1: The transmission ratio is positive, so the sun gear rotates CW as the input and the carrier rotates CW as the output. To maintain a positive internal ratio, a negative value of θ_L is necessary. By Figure 3-9, a CCW rotating cam and negative follower lift dictates that configuration 'd' must be used (rule 4). A CW torque is applied to the sun as the input (rule 3), which applies a CCW torque to the follower (rule 1). This torque pushes the follower down onto the cam, and therefore the transmission ratios in this quadrant are valid.

Quadrant 2: The transmission ratio is positive, so the sun gear rotates CW as the input and the carrier rotates CW as the output. However to maintain a negative internal ratio, a positive value of θ_L is necessary. By Figure 3-9, configuration 'c' must be used. A CW torque is still

applied to the sun as the input (rule 3), which applies a CCW torque to the follower (rule 1). This torque though rotates the follower away from the cam, and therefore the operation of the transmission in this quadrant is impossible, and the resulting transmission ratios invalid for this inversion.

Quadrant 3: There are no possible transmission ratios in this quadrant, so no analysis is necessary (rule 5).

Quadrant 4: The transmission ratio is negative, so the sun rotates CW as the input and the carrier rotates CCW as the output. To maintain a positive internal ratio, a negative value of θ_L is necessary. By Figure 3-9, configuration 'b' must be used (rule 4). A CW torque is applied to the sun as the input (rule 3), which applies a CCW torque to the follower (rule 1). This torque again rotates the follower away from the cam, and therefore the transmission ratios in this quadrant are not valid.

To summarize, for the inversion with the sun as the input and the carrier as the output, the first quadrant is the only quadrant through which the plot of transmission ratio versus internal ratio passes that produces feasible gear ratios. From Figure 3-10, it can be seen that the curve of transmission ratios starts at a value of unity, and go off to infinity; therefore this inversion is capable of gear ratios between one and infinity.

The next inversion studied here uses the cam as the input and the carrier as the output. This configuration has several unique features including the ability to produce a geared neutral. The kinematic equation governing this inversion is given in Equation :

$$TR = \frac{\omega_2}{\omega_1} = -\frac{\theta_L n r_p}{2\pi r_3}\left(1 - \frac{\theta_L n r_p}{2\pi r_3}\right)^{-1}. \tag{3-10}$$

The plot of the transmission ratio versus the internal ratio is shown in Figure 3-12.

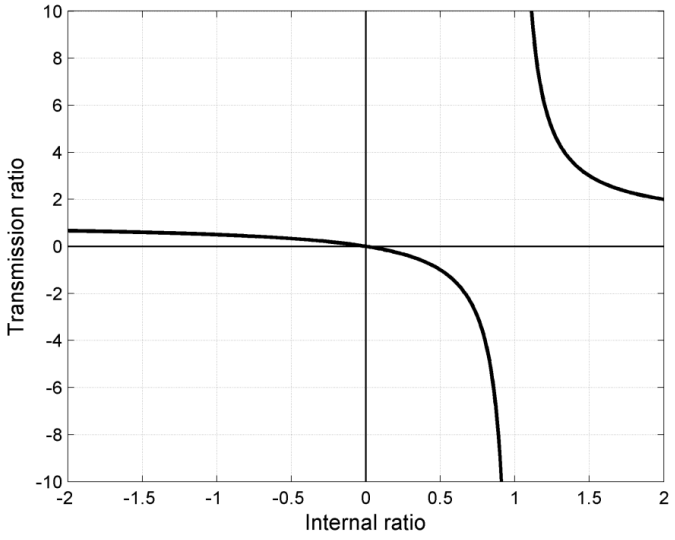

Figure 3-12. Transmission ratio versus internal ratio using the cam as the input and the carrier as the output.

The analysis of all four quadrants of Figure 3-12, in which the cam is used as the input and the carrier is the output, is detailed below.

Quadrant 1: The transmission ratio is positive and greater than one, so the cam rotates CW as the input and the carrier rotates CW at a rate faster than the cam as the output. To maintain a positive internal ratio, a negative value of θ_L is necessary. By Figure 3-9, configuration 'd' must be used (rule 4). The torque on the sun is not as straightforward as before. For this inversion, the reaction torque generated on the sun must be determined. A CW torque is applied to the cam as the input (rule 3), and a CCW torque smaller in magnitude than the input is applied to the carrier as the output. Therefore the reaction force on the sun must be in the CCW direction. This torque rotates the followers away from the cam, and therefore the transmission ratios in this quadrant are invalid.

Quadrant 2: The transmission ratio is positive and less than one, so the cam rotates CW as the input and the carrier rotates CW at a rate slower than the cam as the output. To maintain a negative internal ratio, a positive value of θ_L is necessary. By Figure 3-9, configuration 'a' must be used (rule 4). A CW torque is still applied to the input (rule 3), but a CCW torque larger in magnitude than the input is applied to the output. Therefore the reaction force on the sun must be in the CW direction. This torque rotates the followers into the cam, and therefore the transmission ratios in this quadrant are valid.

Quadrant 3: There are no possible transmission ratios in this quadrant, so no analysis is necessary.

Quadrant 4: The transmission ratio is negative, so the cam rotates CW as the input and the carrier rotates CCW as the output. To maintain a positive internal ratio, a negative value of θ_L is necessary. By Figure 3-9, configuration 'b' must be used (rule 4). A CW torque is still applied to the input (rule 3), and a CW torque is applied to the output. Therefore the reaction force on the sun must be in the CCW direction. This torque rotates the followers into the cam, and therefore the transmission ratios in this quadrant are valid.

For this inversion, quadrants 2 and 4 possess valid transmission ratios. In these two quadrants, the transmission ratio can be seen to go from positive unity to negative infinity. From Figure 3-12 it can be seen that this inversion has a geared neutral ratio. However, an interesting note is that the configuration of the follower must be changed to generate either positive or negative values of θ_L; that is the follower must switch from configuration 'b' to 'a' from quadrant 2 to 4. Therefore it is impossible to achieve transmission ratios in both quadrants with one transmission without complex gear changing mechanisms even though the transmission ratios are continuous through the origin.

At this point it may become apparent that only opposite quadrants are capable of valid transmission ratios. For example, in the first inversion studied, quadrants 1 and 3 were valid, while for the second inversion quadrants 2 and 4 were valid. This is to be expected because quadrants across the y-axis have opposite follower configurations, that is, they go from leading to trailing or vice-versa. Similarly, the torque on the follower also switches across the x-axis because the transmission ratio changes sign. Therefore only in quadrants across the origin from one another will both the torque and the follower orientation switch to maintain the same validity of the transmission ratios. It is necessary then to only study the validity of one quadrant of each inversion's kinematic equation to determine the validity of the rest. For clarity though, similar analyses as those above are given in the Appendix for the remaining four inversions. The results however are presented in Table 2.

Table 3. Possible ratio range of the various inversions.

Inversion #	Input	Output	Ratio range
1	cam	carrier	$(-\infty,0)$; (0, 1]
2	cam	sun gear	$(-\infty,0)$; $(0, \infty)$
3	sun gear	carrier	$[1, \infty)$
4	sun gear	cam	not possible
5	carrier	cam	[0, 1]
6	carrier	sun gear	$(-\infty, 0]$; $[1,\infty)$

3-6 Inversion selection criteria

Given an application, the selection of a suitable inversion depends on several factors. First and foremost is the overall transmission ratio range. For example, the necessity of a geared neutral will eliminate the inversion in which the sun is the input and the carrier is the output. Other factors include the size of the gear range, the direction of rotation between the input and the output, the torque amplification at the sun gear, as well as the relationship between a change in cam lift versus the change in transmission ratio. This section will provide some guidelines for the selection of the proper inversion as well as the reasoning for the sun gear/carrier inversion used in this work.

The selection of the inversion based on the required ratio range is straightforward and only hinges on the necessity of a geared neutral. If a geared neutral is required, inversion number 4 can be eliminated as an option because at no value of the internal ratio will this transmission produce zero output with a nonzero input. All other inversions are technically capable of a geared neutral. If a negative transmission ratio is required across the entire gear range, inversions 1, 2 and 6 may be used. Otherwise, only inversions 2 and 5 can produce a positive ratio range with a geared neutral.

One of the components that limit the torque capacity of the transmission is the sprag clutch that acts as the one way clutch of the transmission. A sprag clutch is an intricate and expensive part whose size is directly related to its torque capacity. Therefore to increase the torque capacity will increase the size, weight, and cost of the design. Ideally then, an inversion should be chosen to minimize the torque applied to these components. Assuming the sprag clutches are directly connected to the sun gear, the applied torque on the sprag can be found as a ratio of either the input or output torque. These ratios are listed in Table 4. Using either the maximum input or output torques and smallest desired transmission ratio, the maximum torque on the sprag can be computed. For inversions with a geared neutral, which can theoretically apply an infinite torque, a torque limiting devices should be used. In these cases the slip torque of this device should be used as the maximum input or output depending on where the device is placed.

The final consideration for selecting an inversion is the relationship between the cam lift, θ_L, and the transmission ratio, essentially the slope of the curve in Figure 3-10 and Figure 3-12. This value gives some indication as to the length and eccentricity of the required cam. If the slope is large, a small change in the cam lift during the active profile will result in a large change in the transmission ratio. This is desirable to minimize either the draft along the cam and thus the cam's length, or the eccentricity of a cam. Conversely, if a large change in θ_L is necessary to achieve the desired gear range, the cam may become too eccentric, resulting in undercutting, or the draft may be very severe, lead to shifting problems, less then optimal loading of the rollers and followers, or a very long cam. The two inversions with the largest derivatives across the possible transmission ratios are number 1 and 3.

Table 4: Possible ratio range of the various inversions.

			Torque on Sprag	
Inversion #	**Input**	**Output**	**Ratio of Input**	**Ratio of Output**
1	cam	carrier	$T_{in}\left(1-\frac{1}{Tr}\right)$	$T_{out}(Tr-1)$
2	cam	sun gear	$\frac{T_{in}}{Tr}$	1
3	sun gear	carrier	1	$T_{out}\cdot Tr$
4	sun gear	cam	NA	NA
5	carrier	cam	$T_{in}\left(1-\frac{1}{Tr}\right)$	$T_{out}(Tr-1)$
6	carrier	sun gear	$\frac{T_{in}}{Tr}$	1

For the remainder of this work, only the inversion in which the sun is the input and the carrier is the output is considered. The reasoning for choosing this inversion is as follows. The transmission studied in this work was designed for use in bicycles. In this application, the input and output directions are the same, so to eliminate the need for a geartrain to reverse directions, a positive transmission ratio was desired. In addition, only relatively small gear ratios can be applied to the input or output rotations to achieve the correct system ratios. For example using off the shelf components, one can only expect to get a 2:1 or 1:2 advantage into or out of the transmission; therefore IVT ranges close to the system ratio were desired. Moreover, it was desirable to speed the input up, and slow the output down to reduce the torque load on the IVT. Therefore the system ratio range was set as 1:1 to 1:3. The two inversions which most closely met the requirements were 3 and 6. Inversion 3 though gives a larger transmission ratio change for the same change in cam lift, and because size and weight were a primary concern, this inversion was chosen.

3-7 Conclusions

In this chapter, a kinematic analysis of the Cam-based IVT was presented. The derivation of the kinematic equations built off the principles outlined in the theory of operations section. Specifically, the equations governing the motion of the CVT are derived from those of a planetary gearset, and for a constant output case, were shown to be relatively simple. Following this derivation, the equations for cam profile design are presented in which a zero acceleration active profile is combined with a trapezoidal acceleration return profile. The kinematic equations presented here were then used to study the characteristics of each inversion, in particular focusing on the achievable gear range of each inversion. Finally, several guidelines were given to choose a particular inversion for an application.

4 Numerical Optimization of the Cam-based IVT

In Chapters 1 and 2, the operation and kinematic principles of the Cam-based IVT were described. Chapter 3 looked at the various inversions of this device and the characteristics of each. The remaining portion of this work will now focus on the development of a specific inversion for use as a bicycle transmission. This development work was focused into two areas, mechanical and numerical. On the mechanical side, several mechanisms and novel transmission configurations were developed to increase the torque capacity of transmission, namely a cable differential system to double the number of active followers at any time and an inverted external cam to improve the contact stress geometry between the roller and cam. These developments are detailed in Chapter 5. This chapter will focus on the numerical optimization methods used to establish the various transmission parameters that would result in increased torque capacity, namely by reducing the contact stress. Three methods are discussed, first a parametric study is covered to understand the basic relationships between the follower velocity and position and the contact force between the roller and the cam. Following this, both a numerical search and a genetic algorithm are presented as a means of optimizing the transmission design while meeting the necessary design constraints.

As with many other infinitely variable transmission designs such as traction drives, a contact stress is the limiting stress in Cam-based IVT. Specifically, very large contact stresses are generated in two locations, within the sprag clutches and between the cam and rollers. These stresses limit the amount of torque that can be transmitted for a given size transmission. The stress in the sprags is a result of the large normal forces required to generate enough friction between the races and the sprags of the clutches. This is analogous to the clamping forces generated in traction drives that allow large torques to be transmitted. Because the sprag clutches are commercial units though, the designer has little control of them. The latter contact stress is generated as a reaction force to the torque on the sun gear shaft. Moreover, because this torque can be quite large, and the number of rollers generating a reaction force small (one to two), this contact stress is also high. The contact stress is so large in this location, that it is the limiting factor when reducing the transmission size or increasing its torque capacity. Therefore, the parametric study and the optimization algorithms of this chapter will focus on minimizing this stress under size and torque constraints.

The contact stress is sensitive to the size of the transmission, input torque, and transmission ratio. In that regard, because this IVT is designed for use in bicycles, it has rather strenuous specifications. The overall transmission size is not to exceed 150[mm] in either diameter or length to fit in the frame between the bicycle pedals. Bicycles also have very large gear ranges, up to a 600% difference between the lowest and highest gear. The aim of this project was only 300%, therefore the low gear was 1:1 while the highest transmission ratio was set as 1:3. A

cyclist can generate quite large input torques, up to 240[N-m]. Therefore, the transmission is designed to handle 120[N-m] with the expectation that the input will be geared up from the bicycle cranks to reduce the input torque to this level. These values are summarized in Table 5.

Table 5: Design specifications for optimization algorithms.

Specification	Value	Units
Torque Capacity	120	N-m
Gear range	100-300	%
Diameter	150	mm
Length	150	mm

In this chapter, a study of the factors influencing this stress is presented as a way of understanding how the geometry of the transmission affects it. Following the analysis, two optimization strategies are discussed. The first strategy presented is that of a numerical search, in which a broad design space is systematically searched for an optimum. A genetic algorithm optimization is then elaborated on as a comparison to and confirmation of the numerical search method's results. In the subsequent chapters, several mechanical solutions to the contact stress problem will be discussed as well.

4-1 Parametric Study

A parametric study is described here to better understand the relationship between the sun gear shaft torque and the contact stress between the rollers and the cam. From this study, the reader will see what transmission geometries affect the stress, and why it is so large relative to the other stresses in the transmission. Similarly, the design principles gleaned from it will be useful in interpreting the results of the two optimization algorithms.

Inversion 3 (input: sun; output carrier) is the subject of this parametric study. The maximum overall transmission ratio, *Tr,* is predetermined going into the design, which in this case is set to 300%, creating a 1:3 ratio between the input and output. From Equation 3-10, it can be seen that in order to meet this objective, the designer has the ability to manipulate either the gear ratio, r_p/r_3, or the maximum follower lift, θ_L. This particular study will focus on the relationship of the contact force to the follower lift and the angular position of the follower, θ_p, which from Equation *2-4* can be shown to vary the contact force by reducing the moment arm on which that force acts. From this study we should expect to find both the angular velocity and angular region in which to operate the follower to minimize the contact force, F_n.

To study the relationship between θ_L, θ_p and the contact force, F_n, an orthogonal coordinate system is established such that the z direction is parallel to the follower axis of rotation and the x and y axis are in a plane parallel to one swept by the carrier. It is necessary to know the unit vector normal to the surface of the cam at the contact point. Because the roller is spherical and therefore tangent to the cam surface at the contact point, this vector is the ray from the contact point to the center of the roller where the contact point is the same as determined from the cam surface. Using the same conventions as [12] and illustrated in Figure 4-1, the roller center is given by Equation 4-1 through 4-3:

$$x_r = r_2 \cos(\theta_2) - r_f \cos(\theta_p + \theta_2) \tag{4-1}$$

$$y_r = r_2 \sin(\theta_2) - r_f \sin(\theta_p + \theta_2) \tag{4-2}$$

$$z_r = z_{car} \tag{4-3}$$

where the subscript *r* denotes the roller center point, r_2 is the carrier radius, and r_f is the follower length. The unit normal vector from the contact point to the roller center is given as Equation 4-4:

$$\vec{v}_n = \frac{(x_r - x_c)\hat{i} + (y_r - y_c)\hat{j} + (z_r - z_c)\hat{k}}{\sqrt{(x_r - x_c)^2 + (y_r - y_c)^2 + (z_r - z_c)^2}}, \tag{4-4}$$

where the subscript *c* denotes the contact point between the roller and the cam and can be found using the profile determination methods mentioned previously [12, 13]. Defining $\vec{R}_f$ as the vector along the length of the follower, from its pivot to the roller center, will then reflect the position of the follower with respect to the carrier, θ_p.

$$\vec{R}_f = (x_r - r_2 \cos(\theta_2))\hat{i} + (y_r - r_2 \sin(\theta_2))\hat{j} + 0\hat{k} \tag{4-5}$$

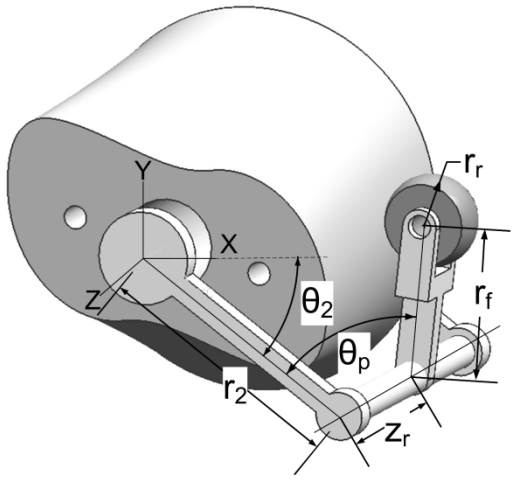

Figure 4-1. Reference for contact force equations.

Applying a torque balance as seen in Figure 4-2 to the follower around the $\hat{k}$ direction yields Equation 4-6:

$$\frac{T_2 r_p}{r_s} = \left(\vec{R}_f \times F_n \vec{v}_n\right) \bullet \hat{k}, \tag{4-6}$$

where T_2 is the torque applied to the sun gear shaft, F_n is the contact force between the roller and cam, and r_p/r_s is adjusted such that the maximum transmission ratio, *Tr*, is attained for the specific

ω_p, where ω_p is the follower velocity required to achieve the correct amount of follower lift. It is given as in Equation 4-7:

$$\omega_p = \frac{\theta_p n}{2\pi}. \tag{4-7}$$

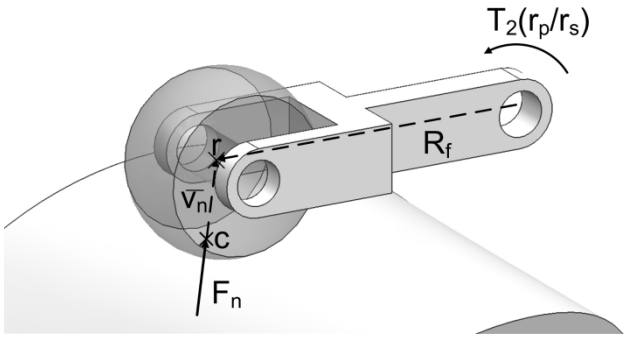

Figure 4-2. Sum of the moments on the follower about its axis of rotation.

Equation 4-6 shows that the normal force, F_n, is linearly proportional to the sun gear shaft torque, T_2, as well as the planet gear to sun gear ratio, r_p/r_s, which for this inversion is typically close in value to 2, and finally inversely proportional to the follower length. For a small transmission like that being studied here under large input torques, it can be seen how F_n will grow very large and lead to equally large contact stresses. To satisfy a given maximum overall transmission ratio requirement, ω_p and r_p/r_s must satisfy Equation 4-8:

$$TR = \left(1 - \omega_p \frac{r_p}{r_3}\right)^{-1}. \tag{4-8}$$

It should also be noted that only the maximum transmission ratio is studied here because it determines the necessary values of r_p/r_s and ω_p for the rest of the transmission ratios. In other words, once these two values are chosen to minimize the contact force at the maximum transmission ratio, only the follower position, θ_p, can be varied to minimize the contact stress at the other ratios. Therefore, the contact force is first studied at the maximum transmission ratio. Combining Equations 4-6 and 4-8 and rearranging yields:

$$F_n = \frac{(Tr-1)T_2}{Tr\,\omega_p\left(\vec{R}_f \times \vec{v}_n\right)\bullet \hat{k}}. \tag{4-9}$$

Equation 4-9 shows the relationship between the follower contact force, the transmission ratio, follower velocity, and the follower position (through the cross product of R_f and v_n). The follower angle, θ_p, was varied between 0.6 and 1.6 radians, and the follower velocity was varied between 0.2 and 0.5 while achieving an overall transmission ratio, Tr, of 3. The resulting contact force for an input torque of 113 [N-m] can be seen in Figure 4-3.

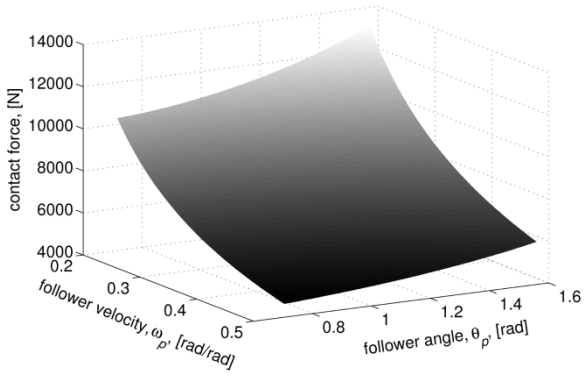

Figure 4-3. Contact force between roller and cam versus follower velocity and initial follower position.

What is significant about Figure 4-3 is that increasing ω_p will result in a lower contact force (because in effect a larger ω_p will result in a smaller value of r_p/r_s for that transmission ratio). In addition, at the lower values of θ_p, the contact force is reduced. Therefore, at the maximum transmission ratio it is best to operate the follower at small levels of θ_p indicating a smaller initial angle, $\theta_p(0)$, should be used when determining the cam profile. This is because at large follower velocities and small values of θ_p, the normal force between the roller and the cam is closer to perpendicular to the follower, and therefore smaller normal forces are needed to generate the necessary reaction torque. The drawback to raising the follower velocity is that higher values will necessitate higher levels of acceleration and stronger return springs. At a certain level, undercutting of the cam will result from the high follower acceleration. This may limit the maximum usable follower velocity.

When not at the maximum gear ratio, the trend is reversed, such that the pressure angle is reduced by operating at higher levels of θ_p, which reduces the contact force by minimizing the cross product of R_f and v_n. An absolute minimum value here though might not be desirable here though as it could affect the draft angle of the cam adversely.

4-2 Numerical Search

As one can see from the parametric study above, there are several of parameters that affect the contact force. There are even more though that affect the contact stress, such as the roller radius and the cam profile radius of curvature. In total, at least five parameters were chosen for optimization. Because of the complexity of the system and the myriad of restrictions imposed by mechanical constraints, a numerical optimization technique was written as opposed to an analytical one.

There are five main parameters to optimize, the roller radius, carrier radius, follower length, follower velocity at the maximum transmission ratio, and the initial position of the follower. For the numerical search method, a five dimensional design space was constructed upon which a coarse 'grid' was laid. At each grid point, the contact stress was computed for the active profile and the radius of curvature computed for the entire profile using an input torque of 120 [N-m]. The grid point with the lowest contact stress that also met all the constraints was then identified and around which a finer grid was laid. Every point on the finer grid was then evaluated. This process was repeated several times until little improvement was seen in the contact stress.

The search area of parameter values is presented in Table 4. Several different resources were used to determine appropriate bounds on these values. The parametric study provided a good base of experience for such things as the follower velocity and initial position. The carrier radius was largely based on the maximum permissible size of the transmission, and knowing that an increase carrier size decreases stress, two larger bounds were chosen. The roller radius and follower length were also largely based on experience from the parametric study, but in the case of the roller, also depended on the availability of common spherical stock pieces.

Table 6: Parameter bounds for the numerical search and genetic algorithm.

Parameter	Symbol	Lower bound	Upper bound	Units
follower velocity	ω_p	0.3	0.45	[rad/rad]
carrier radius	r_2	50	62	[mm]
follower length	r_f	30	50	[mm]
roller radius	r_r	12	20	[mm]
follower initial position	$\theta_p(0)$	.35	1.14	[rad]

In this optimization algorithm, it was necessary to enforce some constraints on the design to ensure a manufacturable and functioning transmission was chosen. These constraints included the overall diameter of the transmission, draft of the cam, shifter clearance, and both negative and positive radius of curvature limitations on the cam. If any of the constraints were violated the design in question was eliminated. The specific constraints enforced for the prototypes are discussed in Chapter 5.

An important factor in all cam design is the radius of curvature of the cam [35]. In all cases, undercutting must be avoided. Therefore the minimum positive radius of curvature of the pitch curve was required to be greater than the roller radius by 10[mm]. The additional 10[mm] buffer was added to smooth any sharp points on the profile. Also, the maximum negative radius of curvature at the roller center was maintained below -2[mm] to ensure there are no portions of the cam surface with a negative radius equal to that of the roller.

The radius of curvature for each pitch curve was found using Equation 4-10:

$$r = \frac{(x'^2 + y'^2)^{\frac{3}{2}}}{(x'y'' + x''y')} \tag{4-10}$$

where x and y are the Cartesian coordinates of the roller center and x' and x'' denote the first and second derivative respectively. It should be noted that because this is a three dimensional cam, the roller radius which is actually in contact with the cam varies as the draft of the cam changes along its circumference. The effects of this are small though, and are compensated by a buffer built into the aforementioned constraints. The first derivatives are given as:

$$x' = -r_2 \cdot \sin(\varphi_2) + b \cdot \sin(\alpha + \varphi_2 + \varphi_1)\,(1 + \omega) \tag{4-11}$$

$$y' = -r_2 \cdot \cos(\varphi_2) + b \cdot \cos(\alpha + \varphi_2 + \varphi_1)\,(1 + \omega) \tag{4-12}$$

The second derivatives are then computed as:

$$x'' = -r_2 \cdot \cos(\varphi_2) + b \cdot \cos(\alpha + \varphi_2 + \varphi_1)(1+\omega)^2 + b \cdot \sin(\alpha + \varphi_2 + \varphi_1) \cdot a \quad (4\text{-}13)$$

$$y' = -r_2 \cdot \sin(\varphi_2) + b \cdot \sin(\alpha + \varphi_2 + \varphi_1)(1+\omega)^2 + b \cdot \cos(\alpha + \varphi_2 + \varphi_1) \cdot a \quad (4\text{-}14)$$

where a is the follower acceleration, φ_1 is the carrier position, φ_2 is the follower position and α is the initial position offset of the follower.

The radius of the cam surface from the center of the transmission was also computed for every point on the cam profile. It was required that the roller radius be larger than the difference between the maximum and minimum of these values to ensure the follower shaft was able to clear the edges of the cam. The goal of this optimization was to find the combination of transmission parameters that minimized the contact stress. To that end, the contact stress was computed as in [36] for contact between a sphere (the roller) and a cylinder (the cam) with a contact force given by Equation 4-9.

The numerical algorithm first defines a coarse grid over the design space. For each parameter, a step size of one third of the maximum range was used. Therefore with five design parameters and four steps per parameter, the algorithm tested 4^5 (1024) designs in the first round alone. The best design that met all the constraints was saved, and a new finer grid was established around this point. The algorithm then tests all these new design points and stores the values with the lowest contact stress. The new parameter limits of each round are established according to Equations 4-15 and 4-16:

$$lowerlimit_n = best_{n-1} - \frac{step_{n-1}}{\delta}, \quad (4\text{-}15)$$

$$upperlimit_n = best_{n-1} + \frac{step_{n-1}}{\delta}, \quad (4\text{-}16)$$

where $best_{n-1}$ is the optimal parameter from the previous run, $step_{n-1}$ is the step size, and δ is a user defined parameter to vary the new grid area relative to the old step size. These equations are applied to all five of the parameters listed in Table 6. A δ value of unity will produce a new grid whose length is the same as the twice the previous step-size, anything smaller will produce a larger grid and a larger δ will reduce the size of grid. The effect of delta can be seen in Figure 4-5. The algorithm is shown in a flowchart in Figure 4-6.

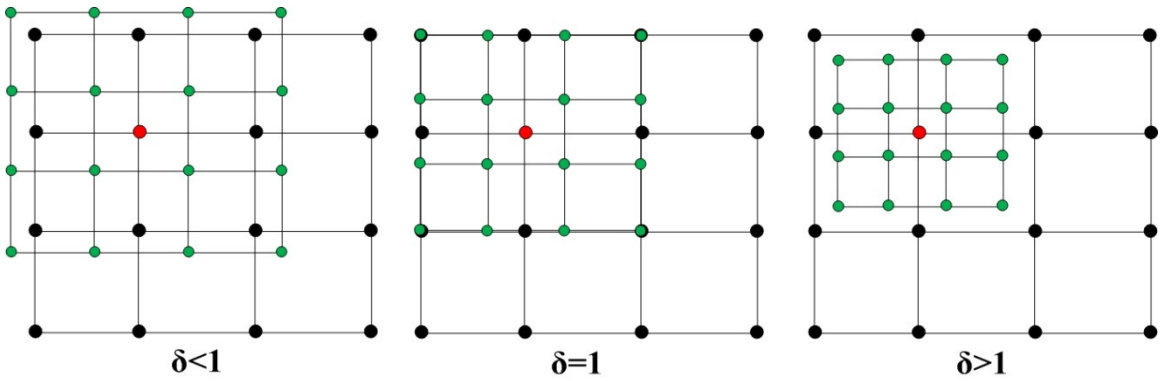

Figure 4-4. Graphical representation of a two dimensional search area and the effect δ has on the search area.

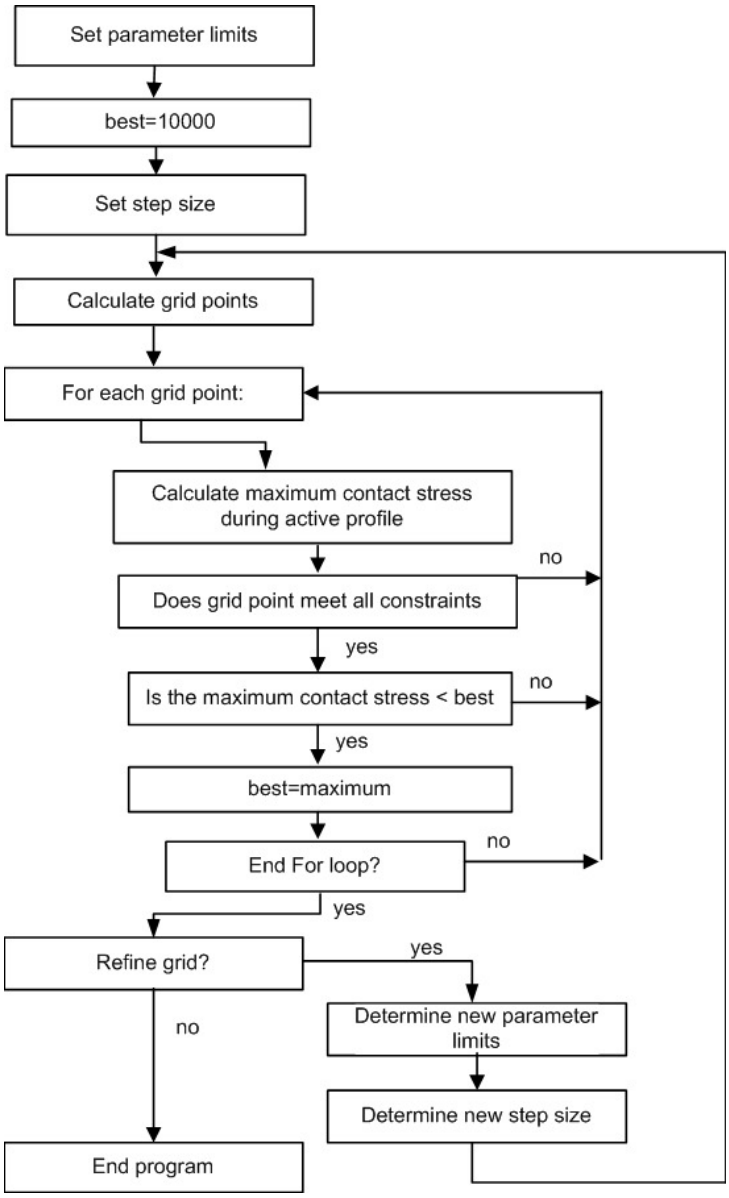

Figure 4-5. Contact force between roller and cam versus follower velocity and initial follower position

Upon finding the best viable design point, (that with the lowest stress), the design space was restricted to a region surrounding that point and subdivided into another 1024 points. All new design points were then evaluated. This iterative process was repeated four times, for a total of approximately 4000 designs. The final step size between design points was then approximately 1/32nd of the original limits.

The numerical search found a minimized the contact stress to 130[MPa] assuming an elastic modulus of 3 [GPa]. This is slightly above the compressive strength of 110[MPa], indicating the maximum torque level this transmission can sustain is slightly below the 120[N-m] desired input torque.

4-3 Genetic Algorithm

Genetic algorithms have in recent years been used for a wide variety of type and dimensional synthesis and optimization problems. They are unique among search algorithms in that they combine elements of both random and directed search routines. The genetic algorithm described here is applied to the Cam-based IVT

Genetic algorithms use the breeding and evolutionary mechanisms of natural systems to root out an optimal solution, where the optimal is determined by a user defined fitness function. The strength of these algorithms stems from the combination of elements from both random walk type searches and broader and more computationally intensive enumerative type algorithms. The result is a rigorous search which can be used for many types of optimizations of multi-criteria problems. [37]

The algorithm used here is applied to a dimensional type synthesis problem. In this approach, the various Cam-based IVT's parameters of significance, (carrier radius, follower length, and roller diameter for example) area coded into a series of bits which make up a chromosome. A large population is then built up of many different chromosomes. Each individual in the population is then scored for a fitness level using the fitness function. Members of the population are then combined and crossed using a mating function which gives priority to the individuals with higher fitness. Mutations are also allowed to occur in every generation. With each new generation, the population is rescored by the fitness function, and the cycle continues. The result is a powerful search algorithm built upon very basic and easy to program functions. A flowchart representing the structure of the genetic algorithm can be seen in Figure 4-6.

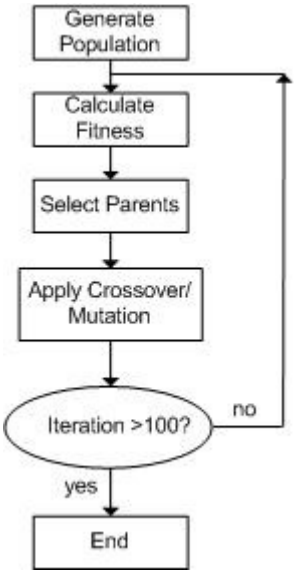

Figure 4-6. Flowchart of the Genetic Algorithm process.

4-3-1 Chromosome Coding

The coding of the population chromosomes is done as a binary representation. Each chromosome is made up of one or more genes, where each gene is a coding representing a transmission

parameter. For this transmission, there are five different parameters which are varied which are summarized in Table 7. The follower velocity is defined as the rotational speed of the follower relative to the carrier during the active portion of the cam. The follower length, roller radius, and carrier radius, and the follower starting position were also varied. The physical parameters can be seen in Figure 4-7.

Table 7: Parameter bounds for the numerical search and genetic algorithm.

Parameter	Symbol	Lower bound	Upper bound	Units
follower velocity	ω_p	0.3	0.45	[rad/rad]
carrier radius	r_2	50	62	[mm]
follower length	r_f	30	50	[mm]
roller radius	r_r	12	20	[mm]
follower initial position	$\theta_p(0)$	.35	1.14	[rad]

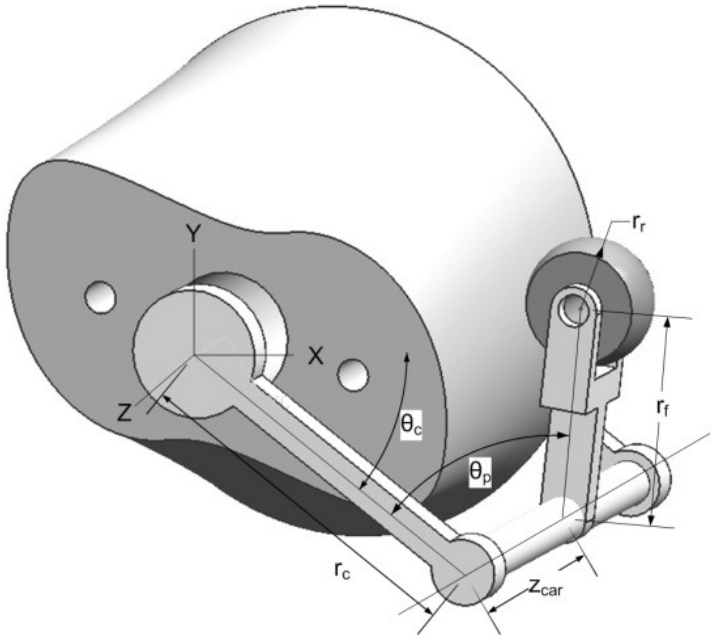

Figure 4-7. Variable relationships to the transmission model.

Each gene's parameter is transformed into a five bit number. The parameter value is determined by the user defined limits. Each value of the gene, a 0 or a 1, is randomly defined by a random number generator with equal probability given to each outcome. The region defined by the upper and lower limits of each parameter value are divided into 31 steps, (2^5-1), where each step is represented by an six bit binary number, the gene. For example, if for some parameter value the upper limit was 10, the lower limit was 5, and the gene was randomly generated as 01101, then the actual parameter value of that gene would be given as in Equation 4-17:

$$value = 5 + \frac{(10-5)}{2^5-1} * 01101_2 \tag{4-17}$$

where the subscript "2" indicates that it is a binary number. It is worth mentioning that the program deals strictly with the coded parameter value, only decoding the gene when it is necessary to use this value in the fitness scoring function. It is therefore easy to increase the resolution without greatly affecting the program runtime.

The upper and lower limits for each parameter were chosen based on experience from previous work with the transmission. This work showed a general range of acceptable values which would produce a viable transmission. The limits could be adjusted from run to run if it was found the algorithm chose the extremes more often than not.

The upper and lower limits for each parameter were chosen based on experience from previous work with the transmission. This work showed a general range of acceptable values which would produce a viable transmission. The limits could be adjusted from run to run if it was found the algorithm chose the extremes more often than not.

For the five parameters with a gene length of 6 bits, each member of the population has a chromosome length of 30. The first operation then performed by the program is to initialize the population. For this optimization, we used a population size of 100.

4-3-2 Fitness Scoring

Once the population has been established, it is necessary to assign a fitness value to each of the members of the population. The fitness values will then be used by the mating functions to determine the fittest specimens and give them a higher probability of mating. For the Cam-based IVT optimization, the scoring function was based first on reducing the contact stress, and secondly on maintaining the transmission limits described above.

Once the parameters were decoded using Equation 2, they are sent to the scoring function. The contact stress is then determined on the entire surface of the cam assuming a 120[N-m] input torque. The maximum value of this contact stress is then recorded.

In application, the lowest fitness value was 0.01 in order to allow even the poorest performing individuals to be allowed to reproduce, in case there was some valuable genetic information within the chromosome. The fitness value and the contact stress are related by Equation 4-18:

$$\boldsymbol{f(c) = \frac{(40000 - c)}{25000} + 0.01 \; when \; c \leq 40000}$$

$$f(c) = 0.01 \;\; when \; c > 40000 \qquad (4\text{-}18)$$

where c is the contact stress. This function was chose such that a desirable level of stress, 100[MPa], represented a unity fitness value. A graphical representation of the fitness function can be seen in Figure 4-8.

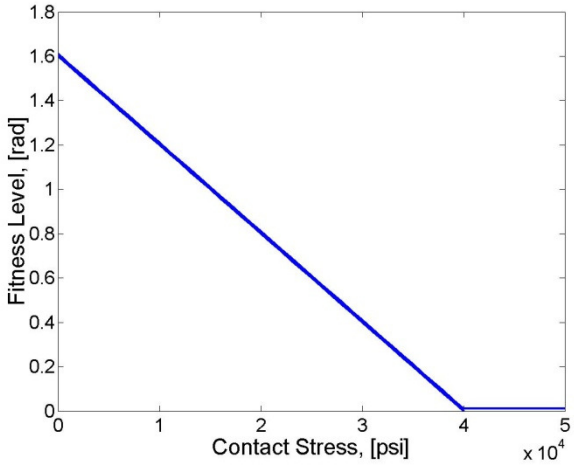

Figure 4-8. Fitness function used to evaluate individual fitness based on the contact stress.

It is necessary for the fitness function to also enforce the parameter limits. This is done by reducing the fitness value of the offending individual, either by a fixed value, or a percentage reduction. In this paper, we use a fixed value of 0.2 for each offense. Should there be too many individuals outside the limits, this value can be increased so as to inhibit reproduction further.

4-3-3 Fitness Scaling

Fitness scaling is an important part of the genetic algorithm. Its purpose is to modify the fitness values of the population to prevent the domination of reproduction by a few individuals in the early generations, and also to increase competition among the population in later generations. A linear scaling routine was implemented here. Given an original fitness value, the scaled value can be found from Equation 4-19:

$$f' = a \cdot f + b \tag{4-19}$$

where a and b are chosen such that the maximum original fitness is mapped to the twice the original average fitness but the original and scaled average fitness values remain the same. A graphical representation of this mapping can be seen in Figure 4-9.

In this way the fittest individual will reproduce on average twice as often as the average individual. Thus a healthy competition is maintained in both the early and later generations. In order to prevent negative fitness values, which may occur when using a scaling function, any scaled fitness value less than zero is mapped to a value of 0.1.

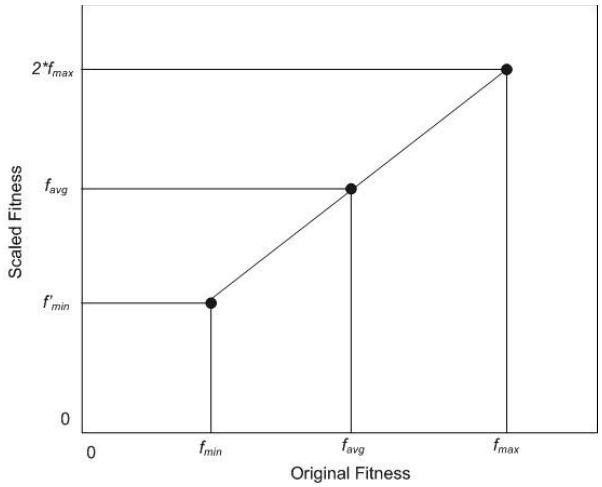

Figure 4-9. Fitness scaling used to promote healthy competition.

4-3-4 Selection and Mutation rate

Between each generation it is necessary to mate the population. A selection function chooses two members of the population for crossover. The probability that any member for reproduction is proportional to their fitness value. This routine is generally referred to as a "roulette wheel" style selection [38]. For every two selected members of the population, two offspring are generated. If the same individual is selected twice, it can be beneficial to cancel the mate and send the member back to the population through the mutation algorithm. It has been shown that this diversity monitor increases the number of acceptable solutions at the end of the program without lowering the maximum fitness level [38].

For every pair of mating individuals, a random number between one and the chromosome length is chosen. This is the crossover site. For reproduction, the two chromosomes are split at the crossover site, and the latter portions of the chromosomes are swapped between individuals. Put another way, each bit of the chromosome that occurs after the crossover site are swapped between the individuals.

Before the offspring are sent back to the population, they are passed through a mutation function. The purpose of this routine is to switch the value of one randomly selected bit within the chromosome. As implemented here, this mutation occurs with probability of 0.033. There is equal probability that any bit on the chromosome will be selected for mutation.

4-3-5 Stop Criteria

There is one stop criteria built into the genetic algorithm. This stop limits the maximum number of generations that can be produced, essentially a run-time limit on the program. No more than 100 generations were produced during this study. In addition, the member with the highest fitness throughout all generations is stored such that it can be retrieved when the program terminates.

4-4 Results

Both the genetic algorithm and the design space method were run on a 3[GHz] processor. The stress achieved through either method was comparable. The genetic algorithm achieved a lowest contact stress of 144[MPa], while the enumeration/design space method produced a design with a stress of 137[MPa]. The final parameters chosen for both methods can be seen in Table 8. The two designs are close, within five percent of each other except for the follower length. The genetic algorithm took nearly twice as long to run as the other program, which could be due to both the higher number of designs analyzed, and perhaps a higher overhead of processing required.

Table 8: Final parameter values resulting from the optimizations.

	w[r/r]	Rc[in]	Rf[in]	Rr[in]	$\theta_p(0)$[rad]
GA	0.33	2.45	1.25	0.68	5.68
Enum	0.34	2.40	1.43	0.70	5.54

It would appear that the enumeration method outperformed the genetic algorithm approach, but this would be underestimating the power of genetic algorithms. It is actually more indicative of the type of problem defined by this transmission than anything else. That is, the design space defined by the specified parameter ranges has few false peaks, such that the enumeration technique hones in on the global peak quickly, or there is a wide array of possible solutions, such that many designs achieve a minimum contact stress. Either case though would make it appear that the enumeration process is outperforming the genetic algorithm.

The power of the genetic algorithm though comes from its simplicity, flexibility, and efficiency. Once the primary functions have been written, which in itself is straightforward, they can be applied to a myriad of problems because they deal only with chromosomes. Only a new fitness function must be written for different optimizations.

5 Mechanical Design Improvements

The Cam-based IVT is a unique transmission with many capabilities beyond that of other current ratcheting drives and IVT technologies such as the torroidal and belt driven types. Much like the torroidial drives, in which most if not all of the driving torque passes through a small contact region, the entire reaction force to the driving torque of the Cam-based IVT is transmitted through the contact area between the rollers and cam. Therefore, this small region exhibits a very high Hertzian contact stress which is proportional to the input torque. For a given transmission size, it was found that this contact stress is the limiting factor of the torque capacity of the transmission. While other highly stressed components can be resized to accommodate high loads, such as the sprag clutches, input shaft, and planetary gear system, the cam and roller system has a much greater effect on the overall transmission size than the other components. So for a given input torque, the overall size of the transmission was determined such that this contact stress was within the limits of both the cam and roller material.

In the previous chapter, two optimization algorithms were employed to search a parameter space to minimize this contact stress. The results of these algorithms significantly reduced the contact stress to within acceptable levels thereby increasing the torque capacity of the transmission near to the desired capacity of 120[N-m]. This chapter addresses two major mechanical design improvements that were implemented on the Cam-based IVT to further reduce the contact stress through both the reduction of the contact force on the roller, and minimizing the stress resulting from this force. To reduce the contact force, increasing the number of followers, number of rollers, and/or changing the transmission parameters were studied. Aside from minimizing the contact force, changing the diameters of the contacting bodies, reducing the modulus of elasticity of the materials involved, or changing the geometry of the contact region were all suitable means of minimizing the stress for a given contact force.

The end approach was two pronged, to at least double the number of rollers under load at any time, and also to modify the overall topology of the mechanism to incorporate an inverted and external cam surface which surrounded the rest of the mechanism. Utilizing a unique cable differential, which splits the input torque evenly between two followers, allowed for two active followers and therefore loaded rollers. Inverting the cam provided a larger radius of curvature, and a more complimentary surface for the roller to follow. Both methods and their characteristics are presented here.

5-1 Contact Stress Model

A method for finding the contact force between the roller and cam has been presented in Chapter 4, and this method was used in these calculations for the active region of the cam considering only static loads. All design approaches and mechanisms were evaluated using these calculations. The transmission specifications called for a maximum input torque capacity of 120 [Nm] and an input rpm of 150 [rpm]. To correctly model the contact stress, the radius of curvature of the pitch curve and the cam surface itself were estimated as if the system was a planar cam mechanism[35]. Therefore, the effect of the draft angle of the cam was not modeled as part of the cam surface radius, but was taken into account within the contact force model. The effect of this draft angle on the radii calculation is small and so this is a safe assumption. In the calculation of the Hertzian contact stress, the roller and cam are assumed to be spherical. Therefore, the contact stress will be slightly over-estimated if one considers the cam surface is actually a ruled surface and could be more closely modeled as a cylinder.

5-1-1 Methods Contact Stress Reduction

A systematic approach was taken to minimizing this contact stress by beginning with a look at the Hertzian contact stress equations. Considering the geometry of the contacting bodies first, the effect of the diameters on the contacting area is given by Equation 5-1:

$$eff = \frac{1}{d_1} + \frac{1}{d_2} \tag{5-1}$$

where d_1 and d_2 are the diameters of the two contacting bodies[39]. Therefore, changing the diameters such that Equation 5-1 is minimized will result in the largest contact area and therefore smallest stress. Either increasing the diameter or using a negative diameter, equivalent to utilizing the inner surface of a hollow sphere, will suffice. Such was the goal of utilizing the inner surface of an inverted and external cam. This approach also reduces the contact stress through an improved topology which allows the highly stressed components to be made larger while transmission size remains the same.

Changing the geometry such that cylindrical contact is present as opposed to spherical will also introduce a significant reduction in the contact stress. This is a result of a larger contact area between bodies for a given deformation. Such an approach has been tried in a similar ratcheting IVT also based on a cam drive which can be seen in Figure 5-1.

While the use of cylindrical rollers in conjunction with a three dimensional cam can reduce the contact stress, the complexity is increased due to an additional degree of freedom that is required to allow the rollers to rock back and forth as they follow the draft of the cam. More significantly, sliding between the roller and the cam is also more prevalent as the ends of the rollers follow different cam profiles. Therefore this approach was not followed, but rather the design, materials, and other mechanisms within the transmission were emphasized.

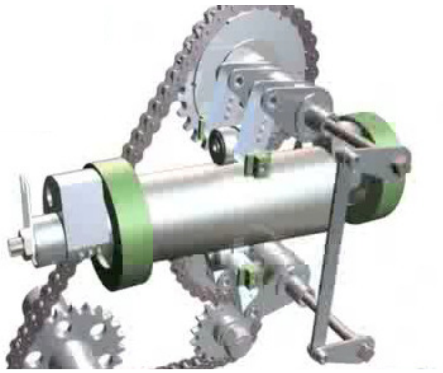

Figure 5-1. Model of Naude's cam driven IVT with cylindrical rollers [**33**].

When using aluminum or plastic as the cam and roller material, the roller contact region exhibits the highest stress within the transmission. If the design were to remain the same, higher performance materials could be substituted for the cam to achieve a greater torque capacity. In particular, titanium was investigated for its low modulus and high strength properties. Because of its high cost and the fact that it is difficult to machine, this approach was abandoned. Although, this could be implemented after other mechanism and design improvements to increase performance.

Minimizing the contact force is more difficult as it depends on transmission parameters which are more closely tied to the design criteria. To achieve this reduction then, distribution of the contact force was emphasized. In the following section, both a dual roller follower and a dual active follower system are investigated as means of accomplishing this. The unique mechanisms necessary for their utilization such as the cable differential are also presented here.

5-2 Dual active follower system

Increasing the number of active rollers in contact with the cam allows the input load to be distributed across more rollers and therefore decrease the contact stress. This can be accomplished in two different ways. Firstly, the number of followers can be increased, such that two followers, and hence rollers, will be active at any time. The second option is to add an additional roller to each follower, which can be seen in such as the model in Figure 5-2 next to the current follower design. In the latter case, each pair of rollers is mounted on a "truck" such that they are loaded equally. The former was researched first because the solution could be more readily implemented. In addition, at the time of writing, no literature was found regarding the method required to determine a cam surface for a dual roller follower. In the future, both solutions could be implemented simultaneously for further improvement and a method of finding the correct cam surface will be investigated.

5-2-1 Benefits

Aside from the reduction in contact stress the dual follower system allows, there are some additional benefits. Considering the static case, the net reaction on both the cam and the carrier will be reduced to a moment only, thereby reducing the load on any supports. Had there been only one active follower, or two active followers located adjacent to each other as opposed to

across, the normal forces from the followers on the cam would not cancel, and the resulting force can be very large, in our case almost 4000[N].

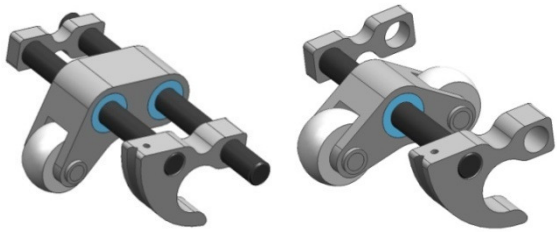

Figure 5-2. The current follower system on the left and the dual roller follower concept.

In addition, there are several advantages when looking at the dynamics of the mechanism. By placing the followers across from one another, the dynamic imbalances that could be present as the followers rotate with respect to the carrier are minimized or completely eliminated. This particular follower arrangement also produces an axial symmetrical cam, one which is dynamically balanced, which is ideal for inversions which require a rotating cam.

It was predicted that moving from one to two active followers would have a significant impact on the contact stress. It was necessary to test the hypothesis because although the followers would see a reduced load, the higher acceleration required of the shorter acting profile would decrease the cam surface curvature. The system was modeled in Matlab® with a carrier radius of 62[mm], follower length of 37[mm], and a roller radius of 12[mm]. A transmission ratio of 3 was achieved with a follower velocity of 0.30[rad/rad] and a planet to sun ratio of 2.2. With four total followers, one being active at a time, the maximum contact stress was 340[MPa] with a maximum shear stress of 102[MPa]. Using the cable differential with the same follower velocity, the stress is reduced by 41% to 199[MPa] and 52[MPa] respectively.

5-2-2 Differential System Requirements

Ideally, two followers could be engaged at any time by placing a second planet gear on the same sun gear as the opposite follower. The operation of this transmission though precludes this solution for two reasons. The first is that manufacturing tolerances in the cam, carrier, or follower may allow one follower to disengage from the cam, thereby overloading the second follower. This would occur for instance if the cam surface was undersized on one side of the cam. Secondly, because of the unique shifting mechanism of this design, which allows for shifting while stopped or under load, the followers may not necessarily be on the same cam profile. Therefore the roller on the more aggressive profile will become the sole active follower leading to a similar overloading situation as above. It is clear that a differential type mechanism is needed to split the load equally between the two while allowing them to move relative to each other. For this application, a unique planar cable differential was developed.

5-2-3 Prior Art

The constraints for the mechanism were a narrow width, light weight, ease of construction, and high torque capacity. Because of the nature of the transmission, the relative motion between the two inputs, the planet pulleys, would remain small. The maximum swing of the follower in this transmission is around 45 degrees; therefore, a continuous motion device was unnecessary. While a conventional differential would work and was investigated, these are generally more expensive (due to manufacturing), heavier, and complicated then a cable based system due to the nature of

force transmission through conventional gear teeth. In addition, a cable based system is less limited by the selection of stock gears.

The use of cable based differential and power transmission systems is commonly seen in robotic applications, where low backlash, high accuracy, and low weight are of primary concern [40]. These make the mechanisms ideal for transmission of power over a distance with few drawbacks. In both the Schillebeeckx and Jacobsen mechanisms, these differentials drive an output which is at a right angle to the inputs, as can be seen in Figure 5-3 [40,41]. In these cases, with a perpendicular drive, the difficulty becomes routing the cable through the pulleys while keeping the cable from becoming wedged between the pulleys themselves. In addition, because of the planar topology of the planetary gearset within the transmission, these existing cable differentials are not suitable.

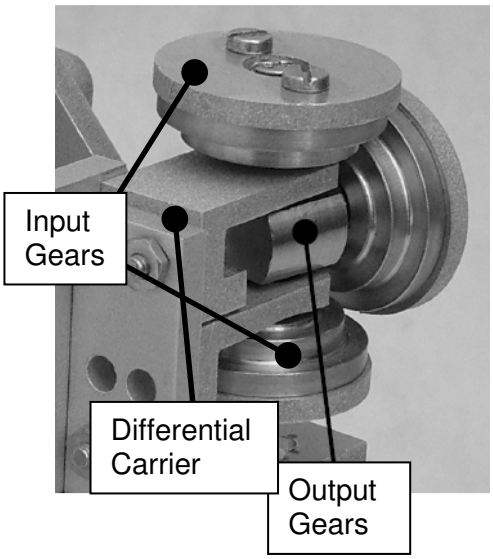

Figure 5-3. Cable driven differential drive mechanism. [**41**]

5-2-4 Cable Differential Design

The particular solution was chosen because of its simplicity, light weight, and high torque transmissibility. The design consists of a rope or cable wrapped around a pinion pulley, where the tension, *T* in both the ropes is equal, as seen in Figure 5-4, the force on the upper pinion pulley is then 2T. If the free ends of the cable are wrapped around two other input pulleys, such that a torque can be transmitted through them, the reaction force for the pinion pulley on its mounts is directly related to the input torques. Attaching the pinion pulley to a central sun pulley will result in a differentially geared pulley system as seen to the right in Figure 5-4. The cable differential system used in the CVT, right, is an adaptation of a conventional pulley system**.**. The center pulley then becomes analogous to the carrier of a conventional automotive differential while the small pulley attached to it is similar to the pinion gears. The output force then becomes an output torque, which is directly related to the input torques on the planet pulleys.

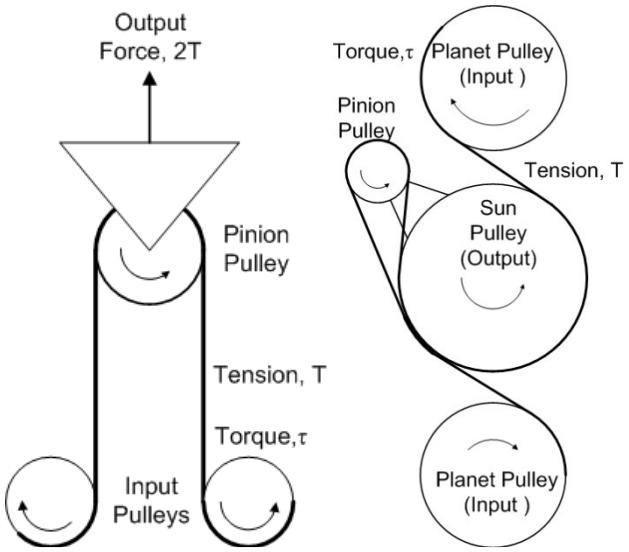

Figure 5-4. The cable differential system used in the CVT, right, is an adaptation of a conventional pulley system.

One of the primary concerns when incorporating the cable differential into the Cam-based IVT was the routing path of the cable around the pulleys. The path must allow for a sufficient range of motion of all three pulleys, be of narrow width, and must minimize additional components. Two such cable routing examples which were investigated can be seen in Figure 5-5; the difference being that one routes the cable through the inside of the sun pulley while the other is routed entirely around the sun pulley. In the most recent IVT prototype, the interior region of the sun pulley was occupied with a sprag clutch, and therefore the cable was routed around the sun gear, running back against itself for a portion of the circumference. The former routing option could be implemented if the width of the mechanism was a lower priority and the cable on cable interaction was a concern. They are otherwise identical in operation.

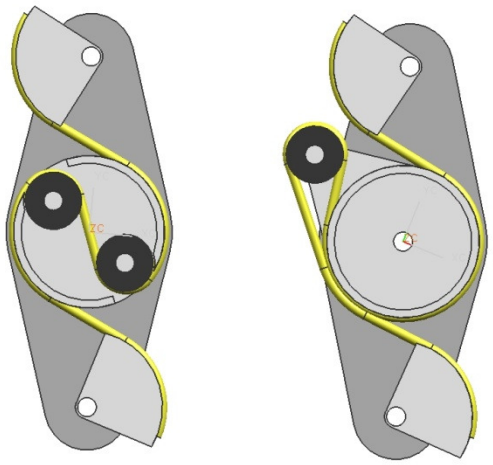

Figure 5-5. Two optional cable routes for the cable differential, one through the middle of the sun pulley, one which is routed around the sun.

5-2-5 Kinematic Equation

The equation of motion of this system is derived by assuming the chord is inextensible. Using this assumption, the total length of the chord at any pulley position is:

$$L = L_0 + 2r_3\theta_3 + r_{PA}\theta_{PA} + r_{PB}\theta_{PB} \tag{5-2}$$

where θ_{PA} and θ_{PB} are the amounts of cable wrap in radians of the planet pulleys, θ_3 the wrap around the sun pulley, r is the respective pulley's radius, L_0 is the sum of the lengths of cable not wrapped around a pulley, and L is the total length of the chord. Taking the derivative of Equation 5-2 yields:

$$r_{PA}\omega_{PA} + r_{PB}\omega_{PB} = -2r_3\omega_3 . \tag{5-3}$$

L_0 is constant because the cable is designed to remain tangent to the pulleys at all times and this tangency point will remain at the same location with respect to the carrier. Also, the pulley rotation axes do not move in relation to one another. A similar relationship can be derived by looking at the energy flow through the system. If power is give by torque times velocity, conservation of energy states that:

$$Tr_{PA}\omega_{PA} + Tr_{PB}\omega_{PB} + 2Tr_3\omega_3 = 0 \tag{5-4}$$

where T is the tension in the cable and can be divided out. The result will be the same as Equation 5-3. In practice, the differential is treated as a standard gearset because the followers are assumed to be on the same profile for most of the transmissions operation and this simplifies the calculations.

Studying Equation 5-4, it can be shown that a second advantage of the cable differential over a geared version is that the torque split can be varied by changing the relative pulley sizes. A comparable feature on a bevel gear differential would require gears cut at non-conventional angles. Also, with this cable differential, it is possible to vary the pulley size ratios throughout the travel of the mechanism, much like non-circular gears. The manufacturing of such pulleys though is considerably easier than that of non-circular gears. If such a design were to be used, the motion of the transmission would be the same as Equation 5-3, except r_p would be a function of the follower position. This characteristic is of particular interest because it would allow the pressure angle of the Cam-based IVT follower to be tailored to specific points of the follower motion for improved force transmission.

5-3 Mechanical Design

The experimental prototype seen in Figure 5-6 was constructed from aluminum and plastic to verify the operation of the differential under both normal operation and during shifting. A detail shot of the differential mechanism can be seen in Figure 5-6.

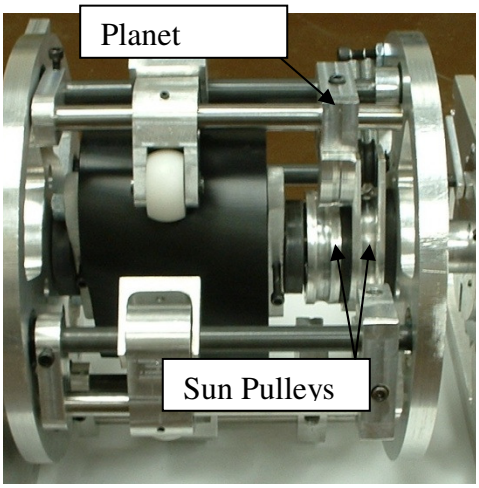

Figure 5-6.Transmission prototype with cable differential.

A dual active follower system requires a different cam profile then a single follower design. There are now two identical active profiles per revolution, as seen in Figure 5-7 for a follower velocity of 0.3[rad/rad]. This requires a much higher acceleration of the followers if no changes are made to the follower profile function. This also as the effect of reducing the angular range of travel of the follower, which is beneficial when using the cable based differential.

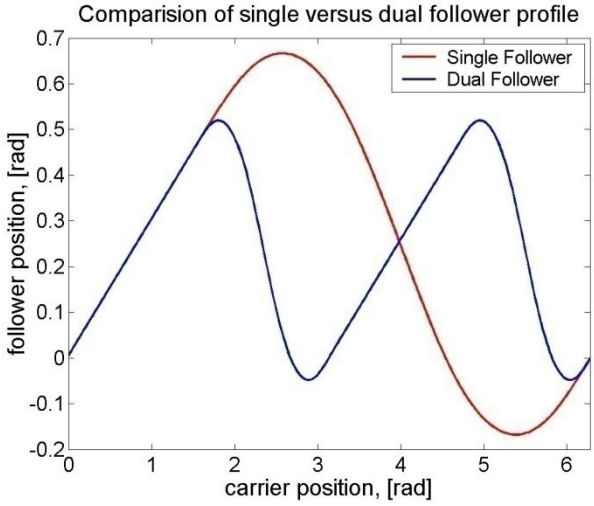

Figure 5-7. Comparison of the single follower cam profile to that of the dual follower design.

The performance of the differential system was found to be more than adequate. While the input load applied remained small due to the limits of the prototype, the performance of the differential was confirmed. At a constant gear ratio, the output of the transmission appeared smooth, and with a planet to sun ratio of 1.8, an overall transmission ratios between 1 and 2.5 was achieved. As can be seen in Figure 5-8, the flexibility of the shifter ring is confirmed, allowing the followers to be approximately half an inch apart on the cam surface. Such a situation occurs when the IVT is shifted while either under load or while stationary. Upon leaving the active region of the cam, the followers begin moving across the cam and finally reach the new cam profile as the ring moves through the shifter guides. As the transmission operates with followers at different positions, the differential is able to maintain contact between the rollers and cam. This is evidenced by the wear

present on the aluminum sun pulley from the cable sliding to adapt to the different follower velocities. This amount of wear though is not significant and it is believed this will not affect the durability of the mechanism.

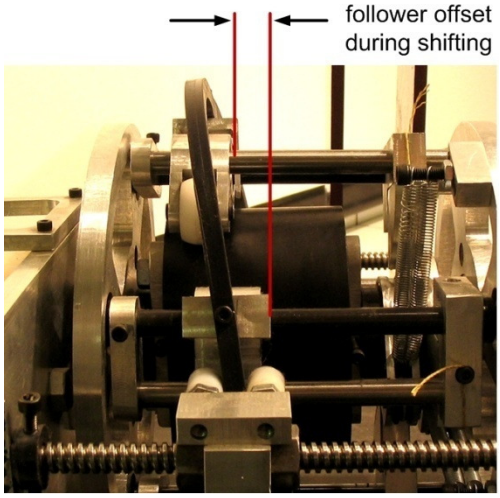

Figure 5-8. Maximum offset of followers during normal operation.

It was found that the maximum torque carrying capacity of this differential is primarily limited by the type of cord being used, which in general, is higher than a geared system of similar weight. This is the case because the system is non-continuous, and therefore all the connections between the cord and pulleys are hard, as opposed to friction based connections of an endless belt mechanism. In our case we are using a Kevlar® line with 500[N] working limit. Future versions though will call for Spectra® material based cable with a much higher strength. The polymer based cables are chosen for because they can be wrapped around smaller radii then a comparable metallic cable.

5-4 External Inverted Cam

While future versions will all incorporate the cable differential and dual active followers for their many improvements, development is continuing towards incorporating an external cam which dramatically reduces the contact stress for a given contact force. A partial model is presented in Figure 5-9 for reference.

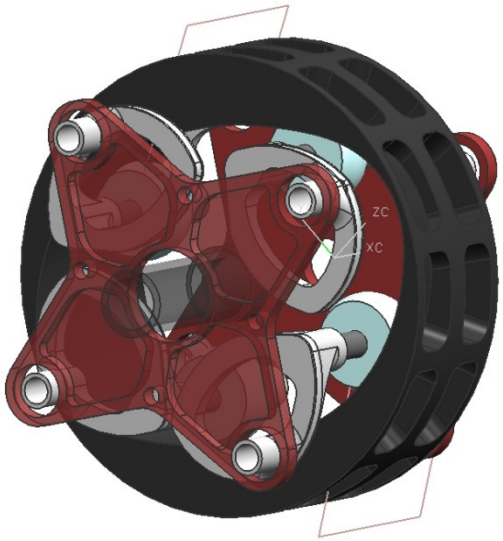

Figure 5-9. Partial CAD model of transmission including the external cam, followers, and carriers.

5-4-1 Benefits

In addition to the cam being larger as compared to an internal cam, the most dramatic improvement in contact stress results from a now negative radius of curvature as the spherical roller is now on the inner as opposed to the outer surface of the cam. Thus Equation 5-1 is reduced, and the resulting contact area between the roller and cam is increased with less deformation of the roller. For example, using a carrier radius of 62[mm], a follower length of 37[mm], and a roller of 12[mm], the older, internal cam produces a maximum pressure of 280[MPa] on the cam surface with a maximum shearing stress of 82[MPa]. Using the same dimensions and material properties, which is an unlikely situation as will be described later, the maximum pressure and shear stresses are reduced 37% to 172[MPa] and 52[MPa] respectively.

The use of an external cam offers several other improvements in terms of packaging. With an internal cam, there was a large region of space inside the cam which could not be utilized. With the external cam, this space is moved to the outside of the transmission, freeing up a large amount of space on the inside. Being as such, the shifting mechanism can be moved to the inside, and the size of the more highly stressed components can be increased while the overall transmission size remains the same. For example, with the external cam, the carrier radius can be increased from 62 to 68 [mm], and the roller from 12 to 17[mm], further reducing the contact pressure to 19.7[ksi] and the shear to 5.9[ksi].

Although this transmission has a uniform output velocity given a constant input, a significant problem with the early prototypes was the non-uniform torque output. This was the result of the heavy follower return springs storing and releasing energy as they held the followers to the cam. Because of the initial internal cam design, large springs were needed to hold the rather massive followers to the cam at high velocities. In addition, the higher follower acceleration required with the dual active followers exacerbated the problem. Indeed, it was experimentally determined that even heavier springs were needed then were built into the design. As such, the external cam will reduce or eliminate the need for large springs because the inertia of the followers will naturally force them onto the cam surface. Therefore lighter springs can be used which are required to only

maintain tension in the cables of the cable differential. The torque fluctuations can then be almost entirely eliminated in future prototypes.

5-4-2 Incorporation of the External Cam

The cam profile generation algorithm is almost identical to the internal cam; the same follower envelope equations were used with only a sign change as described in Tsay [42]. To maintain the correct follower rotation direction and force, the rollers now lead the follower, as opposed to trail. Also, to eliminate the interference between the follower and the cam, the follower has been redesigned from that seen in Figure 5-2 to that in Figure 5-10. The main body of the follow has been eliminated, and the roller now sits on the primary cross shaft. In addition to reducing the part count and the follower weight, this allows the carrier radius to be increased beyond the minimum inner radius of the cam, as can be seen in Figure 5-9. With this cross shaft going through the middle of the roller, the minimum roller radius is limited such that the shaft does not interfere with the cam surface. Although a larger roller radius is generally desired to reduce contact stress, this minimum limit becomes an issue when the roller size must be reduced to prevent undercutting of the cam.

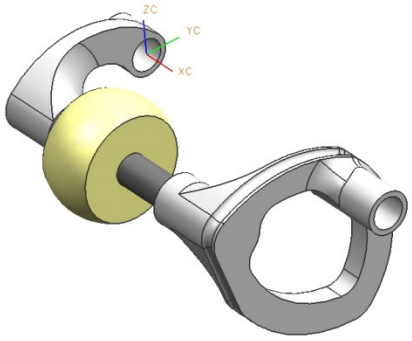

Figure 5-10. CAD model of the follower and roller assembly to be used with the external inverted cam design.

The shifter ring will remain similar to prior designs, but will most likely be made more flexible, as it will have to accommodate both the lateral movement of the roller along the cam as the current design does, as well as the movement of the roller due to the rotation of the follower. Because of this additional movement, the placement of the shifter becomes more critical. This corresponds to where the draft of the cam is zero, as illustrated in Figure 5-11. At this point, regardless of the particular profile the followers are on, the rollers and shifter ring will remain at a constant distance from the center and the shifter guide size can be minimized.

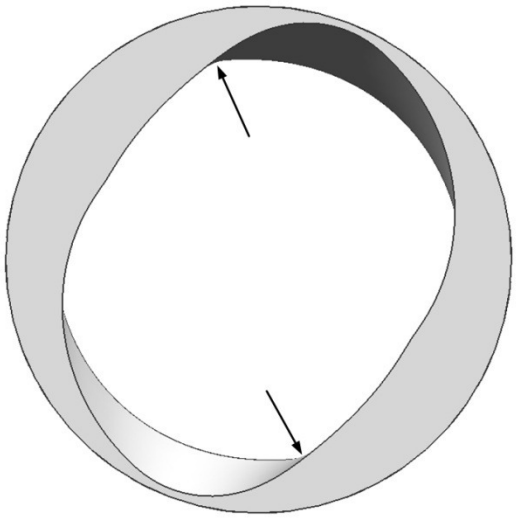

Figure 5-11 Points on the inactive profile of the cam of zero draft, also where the shifter guides should be located to minimize shifting loads.

5-5 Conclusions

In this chapter, several mechanisms and design approaches used to improve the torque and speed capacity of the unique Cam-based IVT have been presented. The number of active followers was doubled, allowing a greater distribution of the input reaction force, by the use of a compact, lightweight, and capable differential mechanism based on a cord and pulley system. This system also reduces the reaction forces on the carrier and sun gear bearings by creating pure moments as opposed to wrench type moments on these components. The contact stress between the followers and the cam surface was reduced by 41% due to this mechanism alone as compared to a single active follower arrangement. A kinematic model governing the motion of this differential was presented with a few experimental results from the prototype which showed a smooth output, a wide gear range, and shifting under load were all possible. An external cam mechanism was also presented which further reduced the contact stress another 21% through improved contact geometry and component resizing. The torque output of the transmission is also expected to improve through a reduction in the return spring size made possible by the inverted, external cam.

6 Prototype Testing

The previous two chapters have detailed the mechanical design changes and optimization approaches that were used to improve the torque capacity of the Cam-based IVT. This section describes the physical realization of those improvements. Specifically, a prototype was built to incorporate both the external cam and the cable differential mechanism for contact stress reduction. In addition, all major transmission parameters such as the carrier size, follower length, roller radius etc, were determined through the optimization algorithms. The entire design was modeled in a computer aided design software package and manufactured in house. This chapter will also describe an electric brake dynamometer that was fabricated to test the transmission prototype.

6-1 Prototype History

Several Cam-based IVT prototypes have been fabricated over the years. The first was a one speed demonstration model built from Lego® building blocks, as seen in Figure 6-1. From the Lego version evolved a three speed version, which was the first to be built from engineered materials such as aluminum and carbon fiber. This prototype, 'Alpha', also pictured in Figure 6-1, could not be shifted while in motion however, and the three cam profiles were shaped by hand which resulted in non-uniform output speeds and caused slipping between gears and their shafts due to very high torques. Later that year, the first fully functional continuously variable version was designed and built, called 'Beta'. This version featured a CNC machined cammoid made from Delrin® as well as high performance sprag clutches capable of transmitting 120[N-m]; it can be seen in Figure 6-1. As the first functional prototype, the Beta version was particularly valuable even though manufacturing errors and design shortcomings prohibited it from transmitting large loads. It was the first version with the dual follower cable differential system described in Chapter 5 and a shifting mechanism that would actively shift while the transmission was operating.

Following the completion of the 'Beta' prototype, development began on the 'Gamma' version, which was the first prototype to include both the cable differential mechanism as well as the external cam. In addition, all significant transmission parameters were decided upon through optimization algorithms. The Gamma version was also designed to meet the much tougher constraints described in Chapter 4, which were enforced so that the design could be implemented on an off-road bicycle. A detailed design review of the components in the Gamma prototype are described below.

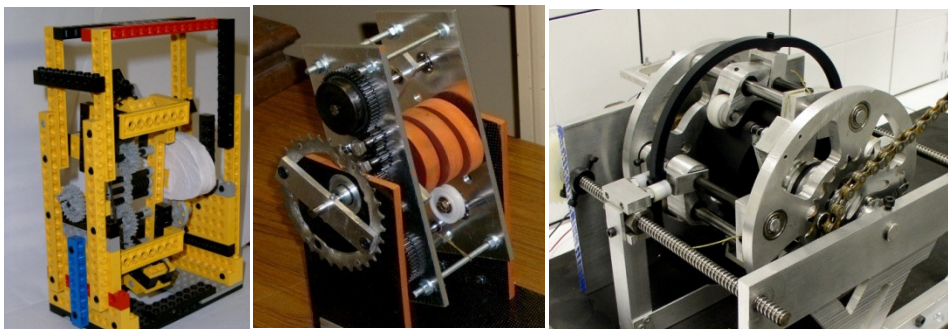

Figure 6-1. Prototypes from left to right: one speed Lego, three speed 'Alpha', fully functional 'Beta' version.

6-2 Gamma Prototype Design

The Gamma prototype, seen in Figure 6-2, was built for a fairly rigorous application, that of an off-road bicycle. As such the design took advantage of all available technologies for design and fabrication. The system was mathematically modeled for optimization, modeled in CAD as a complete system, and CNC machined. The design is a useful as a study of the analytical work reviewed in this work because it represents a culmination of all the theories and principles described above.

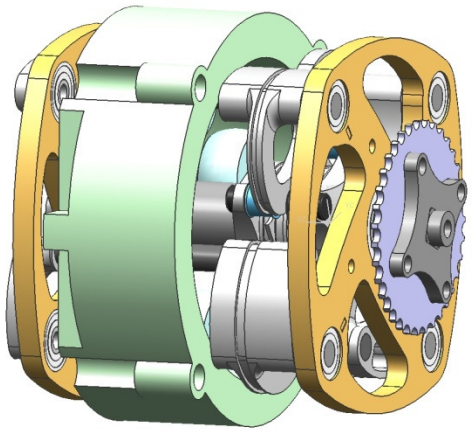

Figure 6-2. Gamma prototype with external cam and cable differential gear mechanism.

For the Gamma prototype, the application restricted the overall transmission size to not exceed 150[mm] in either diameter or length to fit in the frame between the bicycle pedals. Bicycles also have very large gear ranges, up to a 600% difference between the lowest and highest gear. While it is theoretically possible to create a Cam-based IVT with such a range, to limit the design challenges associated with such a large ratio change, a more conservative goal of 300% was set. A cyclist can generate quite large input torques, a conservative limit might be up to 240[N-m]. Therefore, the transmission is designed to handle 120[N-m] with the expectation that the input will be geared up from the bicycle cranks to reduce the input torque to this level. Although this limit may be low for some cyclist, it was again set on the low side to reduce the challenge while still producing an operable transmission for the vast majority of riders. These values are summarized in Table 9.

Table 9: Design specifications for optimization algorithms.

Specification	Value	Units
Torque Capacity	120	N-m
Gear range	100-300	%
Diameter	150	mm
Length	150	mm

Of the six possible inversions, the one using the sun as the input and the carrier as the output was again chosen, as it had been for all previous physical prototypes. This is because in this application, the input and output directions are the same, so to eliminate the need for a geartrain to reverse directions, a positive transmission ratio was desired. In addition, only relatively small gear ratios can be applied to the input or output to achieve the correct system ratios. Specifically, one can only expect to get a 2:1 or 1:2 advantage into or out of the transmission, therefore IVT ranges close to the system ratio were desired (where the total system ratios should be close to 1:1 to 1:3). Moreover, it was desirable to speed the input up, and slow the output down to reduce the torque load on the IVT. Therefore the system ratio range was set as 1:1 to 1:3. The two inversions which most closely met the requirements were 3 and 6. Inversion 3 though gives a larger transmission ratio change for the same change in cam lift, and because size and weight were a primary concern, this inversion was chosen.

Following the selection of the suitable inversion, the nest step of the design process was to establish the major design parameters. The numerical search was used at the time, and to ensure that the resulting transmission would meet the design specifications, the constraints were adjusted for this particular inversion. As was mentioned earlier, the maximum transmission size was kept below 150[mm]. In this design, an external cam is utilized to reduce the contact stress through the unique geometry. The external cam is the largest body in the transmission, and so the transmission size is controlled by the cam size. To this end, the radius of each point on the cam surface of the most extreme profile to the center of the cam was computed. This radius was maintained to below 70[mm] to allow for some thickness of the cam at the extremes.

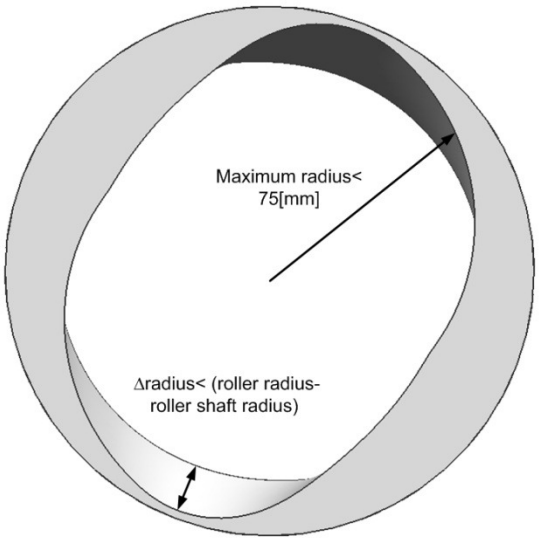

Figure 6-3. The maximum external radius of the cam surface was computed to allow for .1[in] at the thinnest section.

With the external cam mechanism, the shifting assembly is moved to the center of the transmission. To ensure there is no interference between this assembly and the rollers or followers at their most central point, the minimum radius of the pitch curve was required to greater than the sum of the roller radius and the maximum shifter assembly radius.

Also, to eliminate the interference between the follower and the cam, the follower has been redesigned that seen in Figure 6-4 to that in Figure 6-5. The main body of the follow has been eliminated, and the roller now sits on the primary cross shaft. In addition to reducing the part count and the follower weight, this allows the carrier radius to be increased beyond the minimum inner radius of the cam, as can be seen in Figure 6-3. With this cross shaft going through the middle of the roller, the minimum roller radius is limited such that the shaft does not interfere with the cam surface. That is, in order to prevent interference between the cam and the follower/roller support shaft, the roller radius size must be greater than the maximum difference in radius between the two edges of the cam profile minus the radius of the roller shaft.

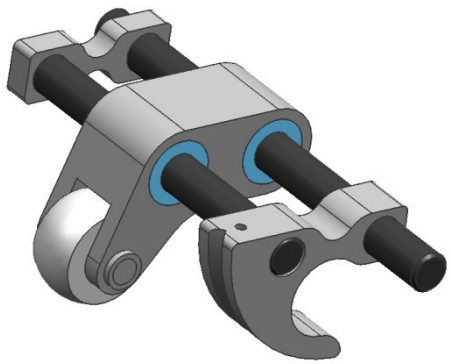

Figure 6-4. CAD model of the follower and roller assembly used with the internal cam design.

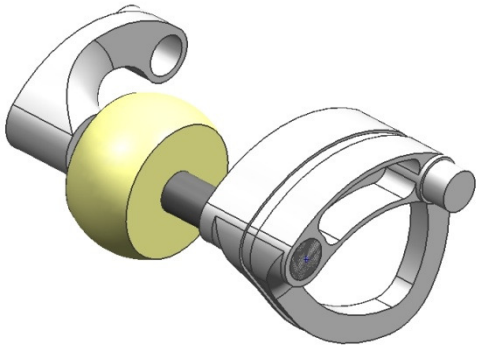

Figure 6-5. CAD model of the follower and roller assembly used with the external inverted cam design.

The numerical search optimized five parameters, the maximum follower velocity (analogous to the follower lift), the carrier radius, follower length, roller radius, and the follower initial position at the start of the active follower. The results of the optimization are seen in Table 10.

Table 10: Final parameter values resulting from the optimizations.

	w[r/r]	Rc[in]	Rf[in]	Rr[in]	$\theta_p(0)$[rad]
Numerical Results	0.33	2.45	1.25	0.68	5.68

As seen in Figure 6-2, and Figure 6-6, an external cam based continuously variable transmission includes four follower assemblies. As shown in Figure 6-5, a follower assembly includes a planet pulley, a roller shaft, a roller, and a roller shaft support. The roller shaft extends through holes in the planet pulleys, the roller bearing, and the roller shaft support, with the roller between the planet pulleys and the roller shaft support. The shaft is fixed to the pulley and the support through a light press fit and a pinned hole. Both ends of the follower assembly are rotatably fixed to the carrier at either end of the transmission via a ball bearing.

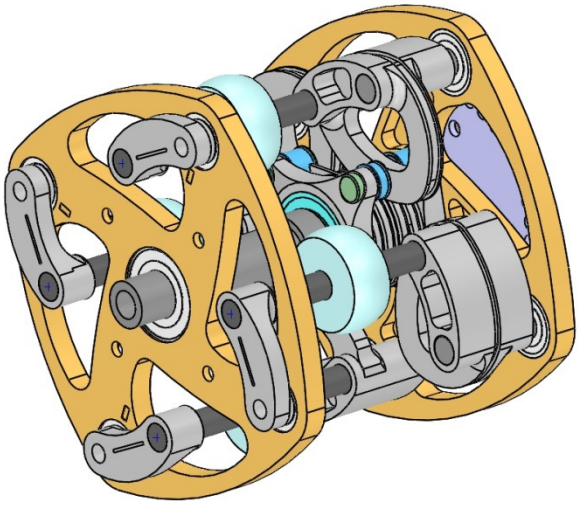

Figure 6-6. Gamma prototype with cam removed for clarity.

The planet pulley is generally stirrup-shaped, as seen in Figure 6-5 and includes a planet pulley groove. The planet pulley groove extends around the midsection on the side of the planet pulley in each follower assembly, and is parallel to the side edges of the planet pulley. When the transmission is in use, a cable extends around the periphery of the planet pulley, guided by the planet pulley groove. This cable is part of the cable differential system which equally distributes the reaction torque on the sun pulley to a pair of planet pulleys. Either end of the cable is affixed to one of the followers with a clamping bolt. There are four follower assemblies rotating when the transmission is engaged.

6-2-1 Sun Assembly

As seen in Figure 6-6, at the core of the transmission is what is called the sun assembly. As shown in Figure 6-7, a sun assembly comprises: a sun pulley, a sun pulley bearing, a sprag clutch, a differential pulley, and a differential cable guide. Both a sprag clutch and a bearing fit in the sun pulley with the outer race of the sprag clutch fixed to the sun pulley inner diameter. Similarly, the inner race of the sprag is pressed onto the sun pulley shaft. The purpose of the sun pulley bearing is to provide support of the sun pulley and therefore sun assembly as forces are applied to the sun assembly by the cable of the cable differential system. Fortunately, because the two ends of the cable leave the sun pulley in opposite directions, there will be little force on this bearing, so it is there mostly as a precaution against unequal loading events. Future versions will incorporate a bushing instead here to reduce the overall size.

This version of the sun pulley exemplifies one possible design for the cable differential system and is by no means the only method of accomplishing the torque splitting task. This sun pulley includes a set of cable grooves and a sun pulley fin. The cable grooves are in an outer wall of the sun pulley and extend all around the circumference. The cable grooves again act as a guide for the cable as the matching grooves do on the planet pulley.

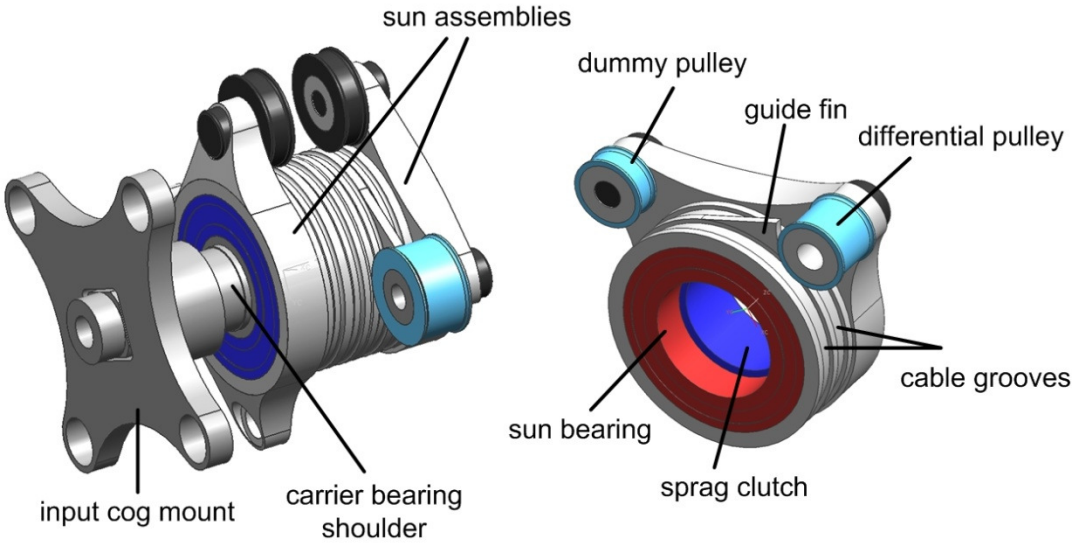

Figure 6-7. Sun assembly on left, and individual sun pulley on right.

The sun assembly includes a differential pulley and a differential cable guide for guiding the cable when the transmission is in use. The differential pulley and the differential cable guide are

each separately rotatably attached to the extended portion of the sun pulley extended portion. The sun pulley fin extends from between the grooves in the neck portion up toward the differential pulley. When the transmission is in use, one cable enters in a first groove of the sun pulley from the planet pulley, wraps around the differential pulley, and exits in a second groove of the sun pulley. The sun pulley fin prevents the cable from becoming entangled. A schematic of the cable routing can be seen in Figure 6-8.

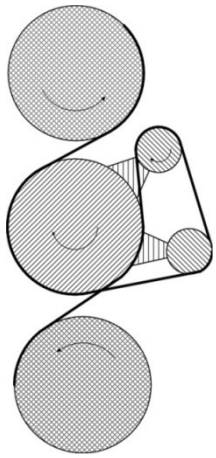

Figure 6-8. Schematic of cable routing from one planet pulley to another around the sun and differential pulleys.

A sprag clutch is a type of one way clutch which only allows relative rotation between two components in one direction. No relative motion is possible in the opposite direction and the two components will rotate together. The purpose of the sprag clutch is to allow the sun assembly to freewheel on the sun pulley shaft while the follower assembly rotates during the inactive profile. When the follower assembly in the opposite direction, as it does during the active region of the cam, the sprag clutch is engaged, causing the sun assembly, and sun pulley shaft to move as one.

6-2-2 Input Assembly

As seen in Figure 6-7, two sun pulley assemblies are mounted on a common shaft, the sun shaft. Together with a cog mount used to mount an input gear or sprocket, this assembly is called the input assembly. This unit is responsible for transferring the input power to one of the two sun pulleys. Ordinarily, a carrier is located between the input spider and the first sun assembly, as seen in Figure 6-6. For this reason, the carrier includes a central hole and bearing through which the sun shaft extends.

6-2-3 Carrier

There are two carriers on the Cam-based IVT, one on either side of the transmission. Only the input cog mount, output cog, and small portions of the center shaft and sun shaft are located outside. The cam, sun pulleys, followers, and shifter assemblies are all located between the carriers. The carriers serve two purposes in the Cam-based IVT. The first is to rotatably locate the four followers around the inside of the cam. For this purpose each end of the follower assembly is mounted through ball bearings to one of the two carriers. Because the output of this inversion is also the carriers, one of the two carriers is also designed with mounting holes to which an output gear or sprocket can be installed. In this way, a chain drive or gear train can be used to load the IVT. The carrier assembly can be seen below in Figure 6-9.

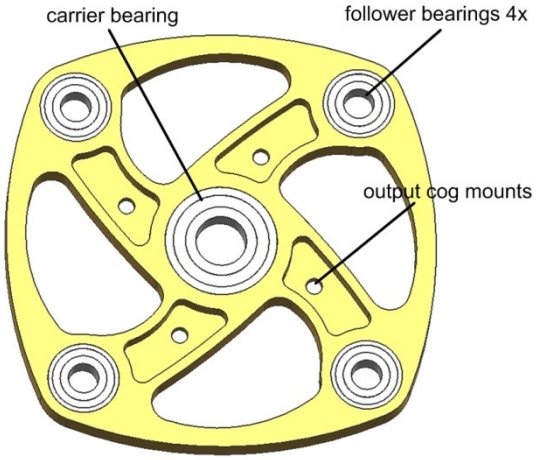

Figure 6-9. Carrier of the Cam-based IVT.

6-2-4 Shifter

The shifter assembly has one of the more complex tasks within the Cam-based IVT. Its primary purpose of course is to locate all four rollers onto the correct cam profile. The mechanics of such a task and the constraints on its dimensions though make the design of this component difficult. For instance, the shifter must allow three degrees of freedom to the roller, two DOFs for their translation around the cam as the followers move up and down around the cam and a third rotational DOF of the rollers about the roller shaft. Moreover, it is desirable to minimize the width of the shifter so as to minimize the width of the transmission.

The shifter should also allow some degree of compliance in the axial direction of the IVT at certain angular positions around the cam, specifically around the active regions of the cam profile. This compliance is reduces the force necessary to translate the rollers across the cam by allowing the loaded followers to remain on the same profile while the inactive followers are shifted to a new profile. In this way the shifter mechanism does not have to overcome the large amount of static friction between the active rollers and the cam. Then, when the active followers become inactive, they shifter will redirect them to the new desired profile.

Several shifter solutions have been proposed, and three different mechanisms have been experimentally tested. On the 'Beta' prototype, a large compliant nylon ring was used to interconnect all of the followers. Two guides were located radially around the cam near the inactive portion of the profile. The guides are positioned with leadscrews along the length of the cam and reposition the shifter using a pair of rollers. Because of the compliance of the shifter ring, a large amount of offset was possible between the active and inactive followers, as can be seen in Figure 6-10. For the Beta prototype, the kinematics were slightly simplified because the shifter ring was mounted to the followers at their axis of rotation, therefore it required one fewer DOFs than is present on the Gamma prototype.

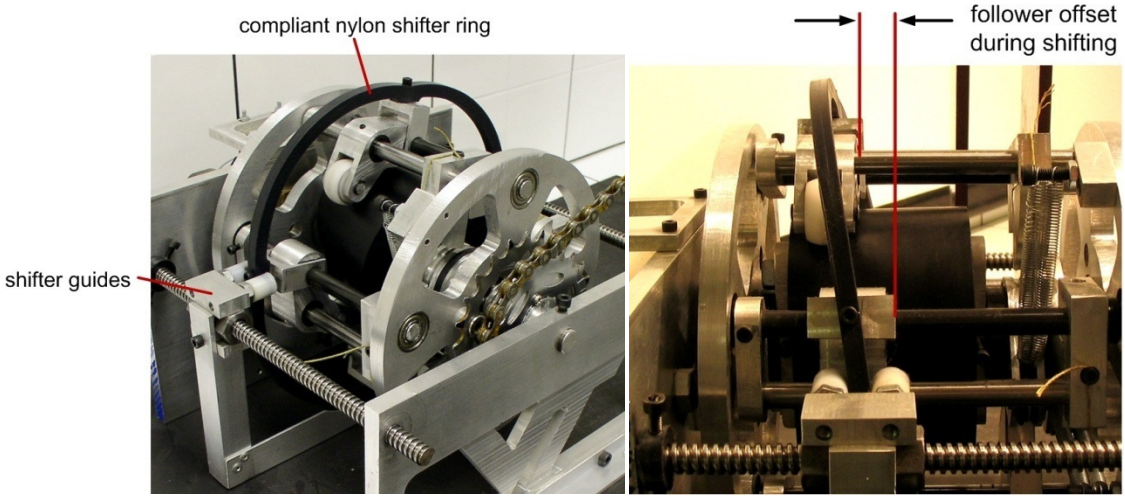

Figure 6-10. Shifter mechanism of the 'Beta' prototype on left, and its inherent compliance on right used to reduce shifting loads.

Two variations on the shifter design were implemented on the gamma prototype. The first and simpler of the two was comprised of two compliant nylon plates that sandwiched the rollers. The two plates were bolted together and were positioned with a shifting rod through the center shaft. Because the angular travel of the followers was limited by the interference with the edges of the cam, as described above, the shifting plates could be designed so that they constantly overlapped with the sides of the rollers. While this shifter functioned well, it generated drag against the rollers during shifting as the sides of the rollers slid along the non-rotating plates.

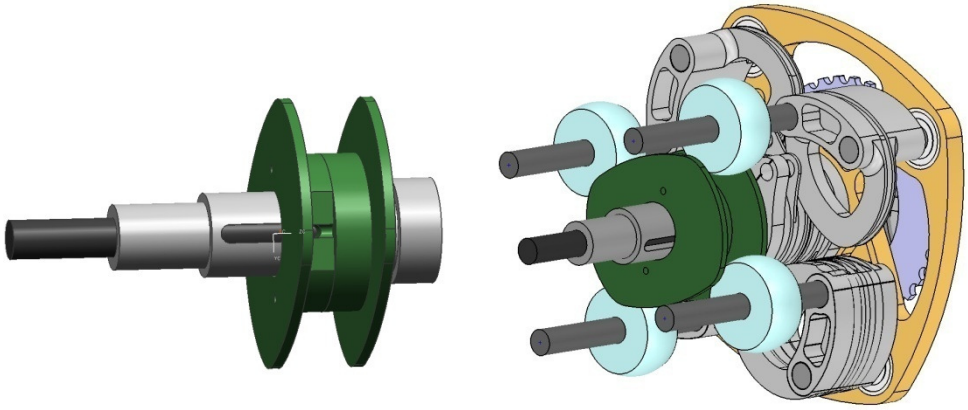

Figure 6-11. Shifter mechanism of the 'Gamma' prototype on left, and its position in the transmission on right.

A second generation shifter was designed to improve upon the efficiency of the first whilst maintaining the necessary performance. Therefore instead of a stationary plate, a rotating compliant shifting linkage was developed so as to eliminate most of the relative motion between the shifter and the rollers. There was also an additional bearing between the center shaft and the shifter to allow it to rotate. By eliminating the sliding between the rollers and the shifter that occurred with the first design, it was expected that this version of the shifter would be more efficient. Through experimental tests it was confirmed that the new shifter was quite a bit less noisy then the first, and would therefore support the hypothesis that it was more efficient. While the efficiency appears to be improved, observations show that the four independent flexible arms

that interact with the rollers do not locate the rollers as accurately as desired and therefore alternative solutions are still being sought.

6-2-5 Assembled Transmission

Figure 6-12 illustrates the fully assembled transmission including the base plate used for dynamometer testing. The transmission is supported on either end, on the driving side by the sun shaft, and on the opposite side by the end of the center shaft. There is a bearing located between the two, such that the input shaft can spin, while the center shaft remains fixed to the housing. This is done to ensure that the shifter can remain stationary if desired.

6-1 Dynamometer Design

The achievable efficiency of a CVT is often used as its defining characteristic. In that light, a test rig was developed by a senior design team under the guidance of the author. Using an electric gear motor and several load cells, the efficiency was experimentally determined. The design of the experiments and the results are presented here. Some final thoughts and possible future directions are presented lastly.

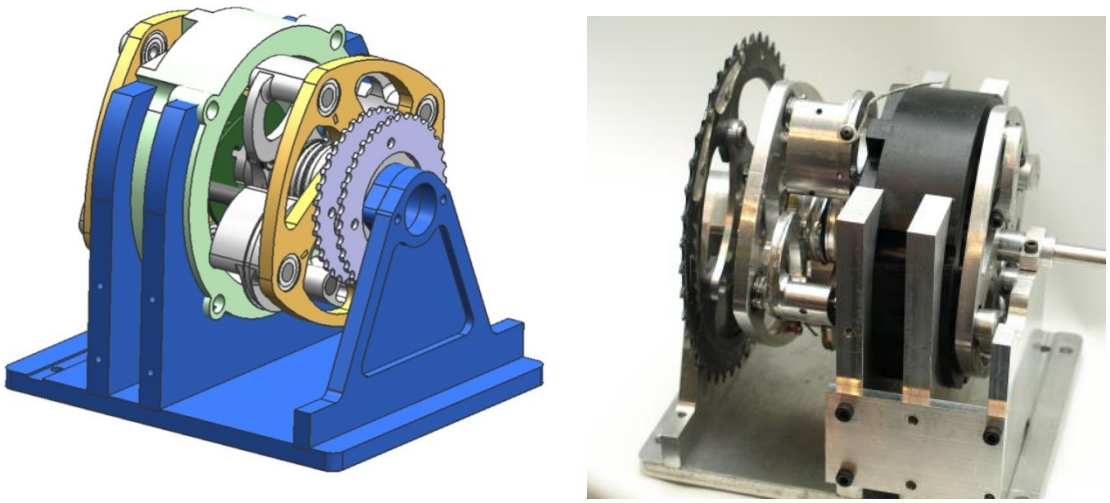

Figure 6-12. Assembled transmission on base with input and output cogs shown.

The dynamometer is comprised of three main components, motor, transmission and load [43]. The motor is a simple electric gearmotor from a hand drill and is used to supply power to the transmission via a chain drive. Connected to the output of the transmission is a load consisting of a disc brake and caliper. By measuring the input torque and speed and the speed and torque applied to the transmission by the load, the efficiency can be determined. The current configuration can be seen in Figure 6-13.

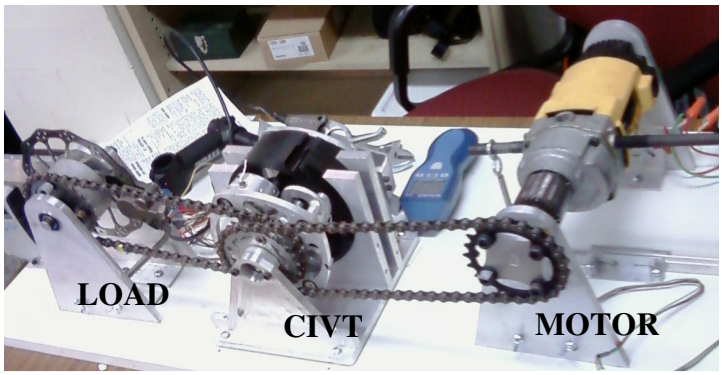

Figure 6-13. The current dynamometer setup including the current CIVT design. The three components of the design are connected together by a chain.

The input and output powers were calculated using data from Hall effect sensors for measured speed and load cells for measured torques. There are two load cells, both are S-bend type devices with integrated Wheatstone bridge from HBM, one on the input and another on the brake that measure the reaction torques generated by the respective components. Therefore both the motor and the brake caliper are mounted on free spinning bearings so the reaction can be measured via lever arms mounted to either component. Each load cell is connected to a National Instruments data acquisition board through a signal amplifier board. The Hall effect sensors record the change in a magnetic field that occurs at the passing of ferrous metals. Four bolts, that attach the sprockets to their mounts, are used as the 'encoder' wheels and trigger the Hall sensors. The speed of either the brake or motor can then be calculated knowing the position versus time data.

6-2 Testing procedure

Before measuring the efficiency of the Cam-based IVT, a baseline efficiency of the chain drives was established. The transmission was tested at an input speed of between 70 and 80 [rpm]. While the transmission is designed for ratios up to 300%, the upper gear ratios were impossible to reach due to the unexpected additional width of the shifter prohibiting its full range of motion. An input torque of only 5[N-m] was applied for all the tests. This is again significantly smaller than the designed torque capacity of the transmission, but larger magnitudes of torque were prohibited due to design and manufacturing flaws that presented themselves after assembly.

Data was recorded at 1[kHz] using a National Instruments data acquisition system and filtered after sampling using a discrete time low pass filter set to 30[Hz], also known as a 'exponential weighted moving average' as described in [44]. A frequency domain plot of the unfiltered and filtered data can be seen in Figure 6-14. The filter frequency was set low to reduce any electrical noise that may be present in the system, as well as keep the sampling time step sufficiently smaller then the filter time constant. [44]

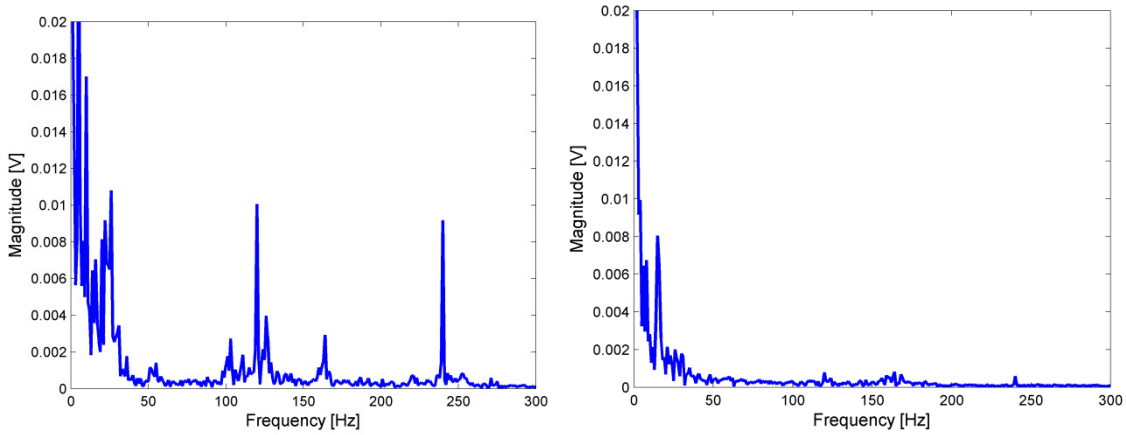

Figure 6-14. Unfiltered raw data on left, versus the data that has been averaged using a discrete time low-pass filter with a break frequency of 30 [Hz].

6-3 Results

A baseline run was performed with the two chain drives, one for the input and one for the output, connected to a free spinning dummy cog. It was found that the combination of chains were 95% efficient. Research shows that a single bicycle chain is around 98% efficient, and because there are two chains in series on dynamometer, one can expect at best an efficiency of 96% [45]. Therefore it is believed an efficiency of 95% is reasonable.

The Cam-based IVT was then assembled, installed on the dynamometer, and run at 75[rpm] with an input torque of 5[N-m]. While is a fairly small input torque, due to limitations of the cable attachment points of the cable differential system, this was the largest torque that could be transmitted. Similarly, only the lowest gear range could effectively be used to due interferences resulting from modifications made to adapt different shifting mechanisms. Nevertheless, given the early stage of development that the IVT is in, meaningful conclusions can be drawn from these results.

As before, the input and output torque and speed were recorded. Data was recorded over a 1[sec] period at 1[kHz]. The torque data can be seen in Figure 6-15, with torque on the y-axis and the sample number on the x-axis. The input torque is graphed in red, while the output is in blue. The output torque is adjusted in this case by the transmission ratio, therefore summing the torques over a sample period gives an indication of the amount of work that went into and out of the transmission. Using segments of ten samples, the efficiency was calculated to be 88% including the chain drives. Therefore, factoring out the efficiency of the chains yields an average transmission efficiency of 93%. The standard deviation of these samples though was large, 10%, indicating a large variation in measurements. Possible causes for these variations are discussed later.

Two things are noteworthy in Figure 6-15. One, there is a large amount of high frequency variation in the data, indicating roughness or vibration somewhere in the system. On the motor side, such vibration may originate in the gear train of the motor (a roughness which is apparent when the motor is spun by hand). This would explain why it is less apparent in the load data. There are also larger and lower frequency variations in both sets of data that are probably the result of either inconsistencies of the load brake or transmission. The second noteworthy point is

that the input torque drops below the adjusted output torque, indicating stored energy from somewhere in the system is driving the output during these phase. This is most likely due to inertial forces that result from rough spots in the transmission, for example parts catching on each other and releasing or sliding against one another and releasing. Regardless, the trend shows that at these levels of torque and speed, only a small portion of the energy is being lost in the transmission. It is these latter large variations in the energy flow that result in the large standard deviation of the results. Nevertheless, on a whole, the transmission shows promising efficiency numbers.

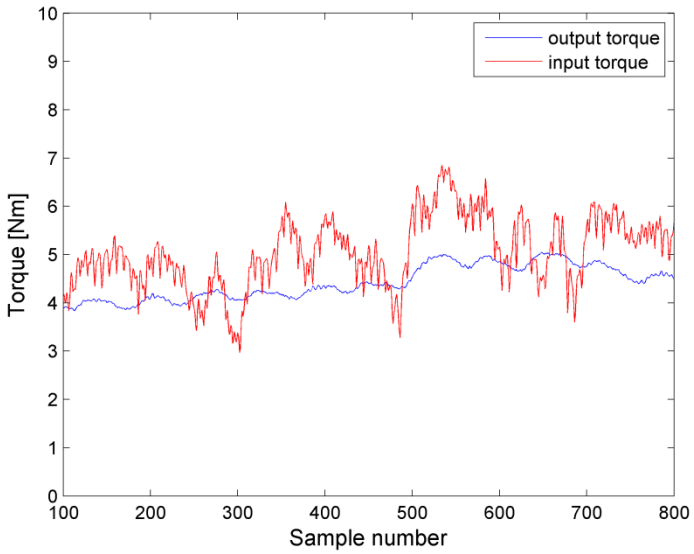

Figure 6-15. Filtered torque data from the dynamometer versus the sample number.

When further experimentation is done, several improvements should be made to the dynamometer to improve the quality of the data that results. Firstly, it is suggested an electric brake be used as opposed to the mechanical variety. This should produce smoother and more consistent loads on the transmission. Secondly, it would be interesting to be able to more closely see any variations in the speed of the output compared to the input. As it is, the hall sensors could only be effectively measured every quarter rotation, so variations in speed occurring at higher frequencies were impossible to measure. This would also improve the accuracy of the calculated power at any given time.

With some small improvements, the Cam-based IVT can be tested at much higher torques and speeds. Given the loss mechanisms in the transmission, these improved designs are expected to be competitive with conventional transmissions. As is, this IVT transmits 93% of the energy put through it.

6-4 Scalability of the Cam-based IVT

The transmission presented in the majority of this thesis was designed around a specific application, and while the analysis, optimization, and mechanisms presented here should be scalable, some discussion is necessary to address the change in performance that results when the transmission is scaled. This is of course of great importance as it indicates which applications are appropriate for the Cam-based IVT.

There are several factors used when determining the appropriateness of a transmission, including size, torque, and weight, but arguably the most important and encompassing parameter is the power that the transmission can transmit. Of course, power can be given described as in Equation 6-1:

$$Power = torque \times speed\ . \tag{6-1}$$

The scalability analysis will attempt to quantify how the torque and speed characteristics of the transmission change with its scale, where scale is defined as the transmissions linear dimensions.

Firstly, because the maximum contact pressure is the limiting stress in the transmission at the scales studied, it is assumed that the trend will continue at least around this design point for which this analysis is valid. The contact pressure is given by Equation 6-2:

$$P = c_1 {F_t}^{\frac{1}{3}} \left(\frac{1}{d_1} + \frac{1}{d_2}\right)^{-\frac{2}{3}}, \tag{6-2}$$

where P is the pressure, c_1 is a constant, F is the contact force, and d_1 and d_2 are the related diameters. For a given contact pressure not to exceed the material parameters, Equation 6-2 shows that the contact force, F, is proportional to the square of scale. This force is also inversely and linearly proportional to the transmission scale (the radius) as can be seen in Equation 6-3:

$$F_t = torque \times radius\ . \tag{6-3}$$

It follows that the torque capacity of the transmission is proportional to the cube of the scale, as in Equation 6-4:

$$torque \propto scale^3. \tag{6-4}$$

This is to be expected as the contact areas on which forces act go up with the square of scale and if the forces go down linearly with scale, the torque will go up with the cube of scale.

The stresses due to the rotational speed of the transmission now must be considered. The inertial forces of the rotating masses generate stresses by Equation 6-5:

$$\sigma_r = \frac{m \times \omega^2 \times r}{Area}, \tag{6-5}$$

where m is the mass, ω is the angular velocity, σ_r is the stress, and r is the radius. This equation generally applies to all the rotating masses including the oscillating followers under the assumption that the cam profile does not drastically change with scale. Given that the mass rises proportionally with the cube of the scale and area with the square of scale, this equation can be rewritten as Equation 6-6:

$$\sigma_r \propto \omega^2 \times r^2. \tag{6-6}$$

Therefore given a constant stress that does not exceed the material parameters, the maximum angular velocity of the transmission is linearly related to the inverse of the scale of the transmission, as in Equation 6-7:

$$speed \propto \frac{1}{scale}. \tag{6-7}$$

Finally, from Equation 6-1, 6-4, and 6-7, one can conclude that power throughput of the transmission is related by Equation 6-8:

$$Power \propto scale^2 \ . \tag{6-8}$$

Equation 6-8 shows that the power throughput of the transmission goes up with the square of the transmission scale. The preceding analysis also shows that as the transmission grows in size, it is beneficial to increase the torque throughput and reduce its operating speed to maximize its potential. Therefore initial estimates show that the Cam-based IVT will scale up well to fit applications with more demanding power requirements then those used in this thesis.

6-5 Conclusions

The Cam-based IVT concept has been continually developed since its inception using both optimization and mechanical design techniques. This section describes the physical realization of those improvements. Specifically, a prototype was built to incorporate both the external cam and the cable differential mechanism for contact stress reduction. In addition, all major transmission parameters such as the carrier size, follower length, roller radius etc, were determined through the optimization algorithms. The entire design was modeled in a computer aided design software package and manufactured in house. This chapter will also describe an electric brake dynamometer that was fabricated to test the transmission prototype. Under light loads and small gear ratios, the Cam-based IVT was found to be 93% efficient. It is expected that continuing development will yield similarly high efficiencies under larger loads and higher transmission ratios.

7 Conclusions

The goal of this thesis work was to analyze and design a continuously variable transmission of the ratcheting type. Both CVTs and IVTs are unique in their capability amongst transmission devices to produce any gear ratio within a certain range or even an infinite gear range. Therefore, CVTs do not have a finite number of gear ratios unlike conventional transmissions but rather, allow the attached devices to rotate at completely independent speeds. This capability makes them especially useful to improve the efficiency of both engines and generators among other things.

Of all the different types of CVTs, those most closely related to the Cam-based IVT are the traction, belt, and ratcheting drives types. Only these transmit motion through mechanical interactions as opposed to hydraulic or electrical ones. All mechanical CVTs must transmit motion through frictional interfaces. Traction drives do so with a number of discs and/or rollers. By changing the geometry between rollers, the gear ratio can be continuously changed. Belt drives on the other hand use adjustable pulleys and a belt to accomplish the same thing. Recent research has been directed at reducing excessive frictional and operating losses that result from the frictional interface of moving components. Ratcheting drives circumvent some of these losses by using mechanical diode type one way clutches as the frictional elements which transmit motion with no losses once engaged. Ratcheting drives though have traditionally suffered from a non-uniform output given a uniform input. The development of the Cam-based IVT has sought to alleviate this problem while maintaining the high efficiency and simplicity inherent to ratcheting CVTs.

The operation of the Cam-based IVT depends on six major components, those being the cam, followers, carrier, planet gears, sun gears, and the one way clutches. The cam is centrally positioned in the transmission, with at least two followers positioned around the cam and rotatably mounted to the carrier. Each follower is connected to a planet gear, and that planet gear connected to one sun gear. One way clutches are installed inside each sun gear with the inner race of the clutches being connected to a common shaft called the sun shaft. The operation of the transmission is very similar to a planetary gearset, in which either the cam, sun shaft, or the carrier can serve as either the input, output or ground. A description of the operation of two common inversions is given in this thesis.

A kinematic analysis was presented which builds off the principles of operation. The equations governing the motion of the CVT are derived from those of a planetary gearset, and for a constant output case, are relatively simple. The equations for the cam design are constructed from both a constant velocity and zero acceleration curve to generate the constant velocity transmission output with a trapezoidal acceleration curve for the return profile. This type of return profile is easy to work with and keeps jerk to acceptable levels. The derivations presented here are used to study the inversion characteristics.

As mentioned, there are six possible simple inversions of the Cam-based IVT, where each inversion is characterized by the components used as the input and output, whether it is the sun, carrier, or cam. Each inversion has special capabilities and limitations; of particular importance is the available gear ratio. A systematic method was developed to analyze the available gear range for each inversion that compares the direction of applied torque to the follower versus its direction of rotation. If the two are congruent, conclusions can be drawn about specific ratio ranges. Other factors such as the torque on the sun gear, cam eccentricity, and packaging are also

important when determining which inversion is most suitable for a particular application and some discussion was given to these factors.

As with many power transmission devices, the problem of contact stress is an issue with the Cam-based IVT as well. In this case, the problem arises as a result not of the frictional members in the transmission, but between the cam and follower rollers. A broad study of the factors influencing this stress is presented as a way of understanding the results from two optimization strategies that were implemented. The study shows that the major transmission parameters affecting the contact force are the follower radius, planet/sun gear ratio, follower velocity, and position. These results are used to frame and provide respective on two optimization strategies developed for this transmission.

The first strategy presented is that of an iterative brute force type numerical search, in which a broad design space is systematically searched for an optimum. This method searched a five dimensional design space over a course grid. At each iteration, the optimal point on the grid was chosen that met all the constraints, and a new finer grid used around this design point. A second optimization using a genetic algorithm was used as a comparison. This type of algorithm fills a population with random design parameters and successively mates and mutates members according to their fitness. After a certain amount of time, an optimal emerges from the population. Both of these algorithms showed similar results, indicating some type of global optimum was found. Significant improvement in transmission performance also resulted from these optimization techniques.

In addition to the optimization schemes, several mechanical solutions were developed as a way of reducing the contact stress. Firstly, a cable differential was designed to double the number of rollers under load at any time, nearly halving the stress. The cable transmission allowed the reaction force to the input torque to be distributed amongst a pair of rollers. So while the cam eccentricity was necessarily a little higher, an overall reduction of contact stress was achieved. In addition, the differential action of the cable system allowed for greater variation in machining tolerances as well as maintaining shifting ease. This system also generated a symmetric cam, which is important to in inversion in which the cam rotates, as well as reduce loads on other components within the transmission.

Secondly an external cam was devised to provide a more complementary contact surface for the roller, further reducing the stress. That is, instead of two contacting convex bodies, (the cam and roller), a concave and convex body will be in contact. This dramatically improves the contact stress for a given contact force. In addition, the larger and more heavily stressed components are moved to the periphery of the transmission, and the more light loaded shifting mechanisms are moved inwards resulting in better overall use of the available transmission space. The cable differential mechanism, the external inverted cam, and the optimization results were incorporated into a prototype transmission. Along with the design presented, a discussion is included on the scalability of the transmission concept which indicates the input power should scale linearly with size.

The achievable efficiency of a CVT is often used as its defining characteristic. In that light, a test rig was developed by a senior design team under the guidance of the author. Using a cradled electric gear motor and a disc brake as a Prony dynamometer, the input and output torque and speeds could be measured. The transmission was run at fairly low input torques, 5[Nm], and at 80[rpm] due to limitations with the prototype. From this, the efficiency was experimentally determined to be 93%.

8 References

1) Carson, R.W., "New and Better Traction Drives are Here," Machine Design, Vol. 46, no. 10, Apr. 1974 pp 148-155.

2) "Reduce energy consumption of belt-driven engine accessories with a NuVinci® crankshaft mounted Continuously Variable Accessory Drive (CVAD)," http://www.fallbrooktech.com/docs/CVAD_crank.pdf, September 8, 2009.

3) A. Kluger, D.M. Long, An overview of Current Automatic Manual and Continuously Variable Tramsmission Efficiencies and Their Projected Future Improvement, SAE Technical Paper Series, No. 1999-01-1259 (Mar. 1999), pp. 1-6.

4) P. Carlin, A. Laxson, E. Muljadi, The History and State of the Art of Variable-Speed Wind Turbine Technology, NREL/TP-500-28607, February 2001.

5) J. Cotrell, Motion Technologies CRADACRD-03-130: Assessing the Potential of a Mechanical Continuously Variable Transmission, NREL/TP-500-36371, September 2004.

6) P.G. Gott, Changing Gears, The development of the Automotive Transmissions, SAE.

7) Hewko, L., 1986, ‘‘Automotive Traction Drive CVTs–An Overview,’’ SAE 861355.

8) Carbone, G., Mangialardi, L., and Mantriot, G., 2004, “A Comparison of the Performances of Full and Half Toroidal Traction Drives,” Mech. Mach.Theory, 39, pp. 921–942.

9) Raghavan, M., "Kinematics of the Full-Toroidal Traction Drive Variator," Journal of Mechanical Design, Vol 124, Sept. 2002, pp 448-455.

10) Yamamoto, T., Matsuda, K., and Hibi, T., 2001, “Analysis of the Efficiency of a Half Toroidal CVT,” JSAE Rev., 22-4, pp. 565–570.

11) Carter, J., and Miller, D., “The Design And Analysis of an Alternative Traction Drive CVT,” SAE Paper No. 2003-01-0970.

12) Smithson, R., Miller, D., and Allen, D., “Scalability for an Alternative Rolling Traction CVT,” SAE Paper 2004-01-0355.

13) "Nuvinci Overview," http://www.fallbrooktech.com/Nuvinci.asp, September 9, 2009.

14) Cretu, O.S., Glovnea, R.P. "Traction Drive with Reduced Spin Losses," Journal Of Tribology, Vol. 125, July 2003, 507-512.

15) Akehurst, S., Parker, D.A., Schaaf, S., "Dynamic Modeling of the Milner Continuously Variable Transmission—The Basic Kinematics," Journal of Mechanical Design, Vol 129, Nov. 2007, pp 1170-1178.

16) Akehurst, S., Brace, C. J., Vaughan, N. D., Milner, P. J., and Hosoi, Y., 2001, “Performance Investigations of a Novel Rolling Traction Drive CVT,” SAE Paper No. 2001-01-0874.

17) Milner, P.J., "Milner CVT for high torque applications, VDI Berichte, n. 1709, 2002, pp 543-554.

18) Cretu, O.S., Glovnea, R.P., "Constant Power Continuously Variable Transmission: Operating Principle and Analysis" Journal of mechanical Design, Vol 127, Jan, 2005, 114-120.

19)Younes, Y.K., "A design Scheme for Multidisk Beier Traction Variators," Journal of Mechanical Design, Vol 114, March 1992, pp 17-23.

20) Loewenthal, S., and Zaretsky, E., 1985, “Design of Traction Drives,” *NASA Reference Publication 1154*.

21) Micklem, J.D., Lonmore, D.K., Burrows, C.R., "The magnitude of the loses in the steel pushing V-belt continuously variable transmission", Proceedings of the Institution of Mechanical Engineers, Vol. 210, No. 1, 1996, pp. 57-62.

22) Guebeli, M., Micklem, J.D., Burrows, C.R., "Maximum Transmission Efficiency of a Steel Belt Continuously Variable Transmission," J. Mech. Design, Vol. 115, No. 4, 1993, pp 1044-1049.

23) F.G. Benitez, J.M. Madrigal, J.M. del Castillo, Infinitely variable transmission of ratcheting drive type based on one-way clutches, Journal of Mechancial Design, July 2004, Vol. 126, pg. 673-682.

24) F. G. Benitez, J. Gutierrez, G. Campillo, P. Madronal, Variable Continuous Transmission System, US Patent, 6,371,881 B1, 2002.

25) F.A. Fitz, P.B. Pires, A geared infinitely variable transmission for automotive applications, SAE paper no. 910407, pp. 1-7 1991.

26) P.B. Pires, Transmission Ratio Changing Apparatus and Method, US Patent 4,983,151, 2001.

27) S. Matsumoto, N. Inoue, Y. Tsukada, Continuously variable transmission for bicycles, United States Patent Application 20030221892, 2003.

28)Yates, W.A., "Design Principles of a Four bar crank continuously variable transmission" ASME 2008 2nd International Conference on Energy Sustainability, Vol. 1, Jacksonville, Florida, August, 2008, pp. 419-438.

29) "Zero-Max motion control products," http://www.zero-max.com/products/drives/drivesmain.asp, September 8, 2009.

30) Centeno, G., Morales, F., Perez, F.B., Benitez, F.G., "Continuous Variable Transmission with an Inertia Regulating System," ASME Journal of Mechanical Design, Pending Publication.

31) Constantinesco G., “An improved method and means for transmitting power from prime movers such as internal combustion engines to driven shafts, particularly for locomotives or other vehicles driven by internal combustion engines,” GB Patent 185,022; 1922.

32) "1900 Commodity Air Cart Technical Manual," John Deere Seeding Group, TM1711, September 1998.

33) Naude, J., "Rotor controlled transmission," US Patent 7,416,506, August, 2008.

34) Report of U.S. Department of Energy, 1982, Advanced Automotive Transmission Development Status and Research Needs, DOE/CS/50286-1.

35) J.J. Uicker, G.R. Pennock, J.E. Shigley, Theory of Machines and Mechanisms, Oxford University Press, New York, 2003.

36) Boresi, A.P., Schmidt, R.J., *Advanced Mechanics of Materials*, 6th ed. Wiley, New York, 2003.

37) W.M. Szydlowski, C. A. Nelson, Synthesis of adaptive pliers mechanism using genetic algorithms, ASME IDETC Conference, Las Vegas, Nevada, September 2007.

38) D.E. Goldberg, Genetic algorithms in search, optimization, and machine learning, Addison-Wesley, Reading, MA, 1989.

39) J.E. Shigley, C.R. Mischke, R.G. Budynas, Mechanical Engineering Design, McGraw-Hill, New York, 2004.

40) J.K. Salisbury Jr., W.T. Townsend, et al, Compact Cable Transmission with Cable Differential, US Patent, 5,046,375, 1991.

41) F. Schillebeeckx, J. Peirs. Compact Zero-Backlash Tilt-Pan Mechanism Based on Differential Gear Technology, Proc. 9th International Conference on New Actuators, Bremen, Germany, June 2004.

42) D.M. Tsay, G.S. Hwang, The profile determination and machining of camoids with oscillating spherical followers, Journal of Engineering for Industry, ASME, August 1994, Vol. 116, p. 355.

43) Figliola, R.S., Beasley, D.E., *Theory and Design for Mechanical Measurements,* John Wiley and Sons, Danvers, MA., 2000.

44) Haugen, F., "Derivation of a Discrete-Time Lowpass Filter," http://techteach.no/simview/, October 20, 2009.

45) Spicer, J.B., "On the Efficiency of Bicycle Chain Drives," Human Power Journal, 50, Spring 2000.

46) H.A. Rothbart, Cam design handbook, McGraw-Hill, New York, 2004.

47) J. Chakraborty, S.G. Ghande, Kinematics and geometry of planar ad spatial cam mechanism, John Wiley & Sons, 1977.

48) Lahr, D. and Hong, D. W., “Contact Stress Reduction Mechanisms for the Cam-based Infinitely Variable Transmission”, 31st ASME Mechanisms and Robotics Conference, Las Vegas, Nevada, September 4-7, 2007.

49) Lahr, D. and Hong, D., “Dimensional Synthesis of a Cam-Based Infinitely Variable Transmission Using Genetic Algorithms”, US-Korea Conference on Science, Technology and Entrepreneurship (UKC2007), Mechanical Engineering & Robotics Symposium, Washington DC, August 9-12, 2007.

50) Lahr, D. F. and Hong, D. W., “The Operation and Kinematic Analysis of a Novel Cam-Based Infinitely Variable Transmission”, 30th ASME Mechanisms and Robotics Conference, Philadelphia, Pennsylvania, September 10-13, 2006.

9 Appendix

9-1 Nomenclature

Nomenclature:
a, maximum level of follower acceleration;
F_n, contact force between roller and cam;
n, number of followers;
r_3, sun gear radius;
r_a, r_b, gear radii;
r_p, planet gear radius;
R_f, vector along length of follower;
θ_1, angular position of the cam;
θ_2, angular position of the carrier;
θ_3, angular position of the sun gear;
θ_L, magnitude of follower lift during acting profile;
θ_p, angular position of the follower and planet gear;
T_{in}, input torque;
v_n, normal vector to surface of cam at the point of contact;
ω_1, angular velocity of the cam;
ω_2, angular velocity of the carrier;
ω_3, angular velocity of the sun gear;
ω_p, angular velocity of the followers and planet gears;
(x_r, y_r, z_r), coordinates of the roller center;
(x_c, y_c, z_c), coordinates of contact point between roller and cam;

9-2 Inversion Analysis Continued

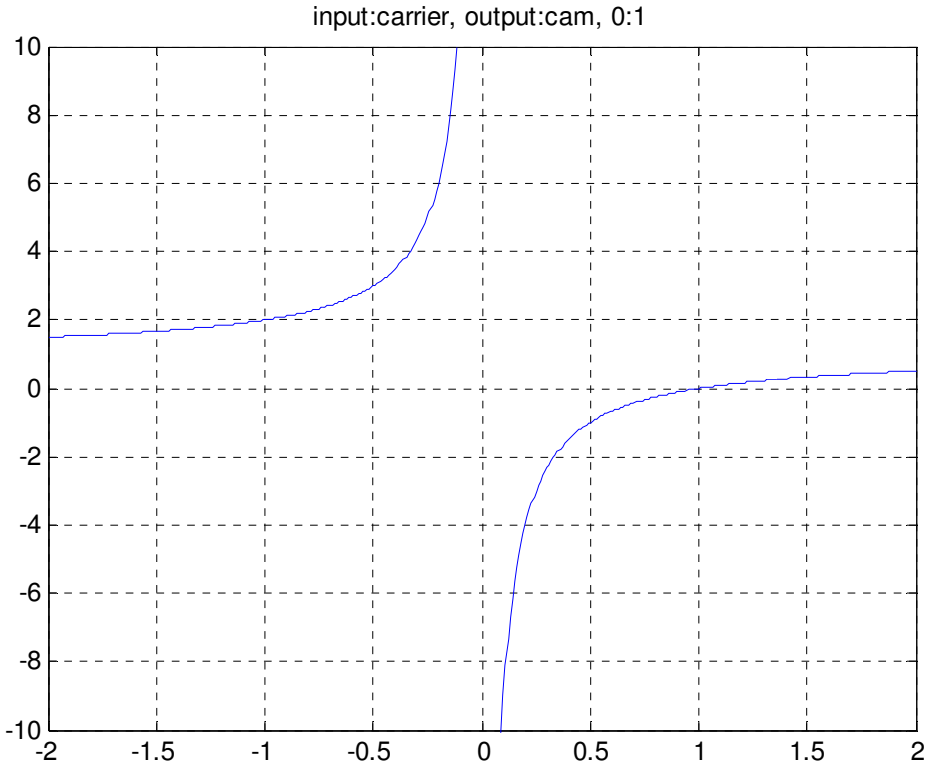

Figure 9-1. Input Carrier, Output Cam

The analysis of all four quadrants of Figure 9-1 are shown below.

Quadrant 1: The transmission ratio is positive and less than one, so the carrier rotates CW as the input. The cam also rotates CW but at a rate slower than the carrier as the output. To maintain a positive internal ratio, a negative value of θ_L is necessary. By Figure 3-9, configuration 'd' must be used (rule 4). For this inversion, the reaction torque generated on the sun must be determined. A CW torque is applied to the input (rule 3), and a CCW torque larger in magnitude than the input is applied to the output. Therefore the reaction force on the sun must be in the CW direction. This torque rotates the followers into the cam, and therefore the transmission ratios in this quadrant are valid.

Quadrant 2: The transmission ratio is positive and greater than one, so the carrier rotates CW as the input and the cam rotates CW at a rate faster than the carrier as the output. To maintain a negative internal ratio, a positive value of θ_L is necessary. By Figure 3-9, configuration 'a' must be used (rule 4). A CW torque is still applied to the input (rule 3), but a CCW torque smaller in magnitude than the input is applied to the output. Therefore the reaction force on the sun must be in the CCW direction. This torque rotates the followers away from the cam, and therefore the transmission ratios in this quadrant are invalid.

Quadrant 3: There are no possible transmission ratios in this quadrant, so no analysis is necessary.

Quadrant 4: The transmission ratio is negative, so the carrier rotates CW as the input and the cam rotates CCW as the output. To maintain a positive internal ratio, a negative value of θ_L is necessary. By Figure 3-9, configuration 'd' must be used (rule 4). A CW torque is still applied to the input (rule 3), and a CW torque is applied to the output. Therefore the reaction force on the sun must be in the CCW direction. This torque rotates the followers away from the cam, and therefore the transmission ratios in this quadrant are invalid.

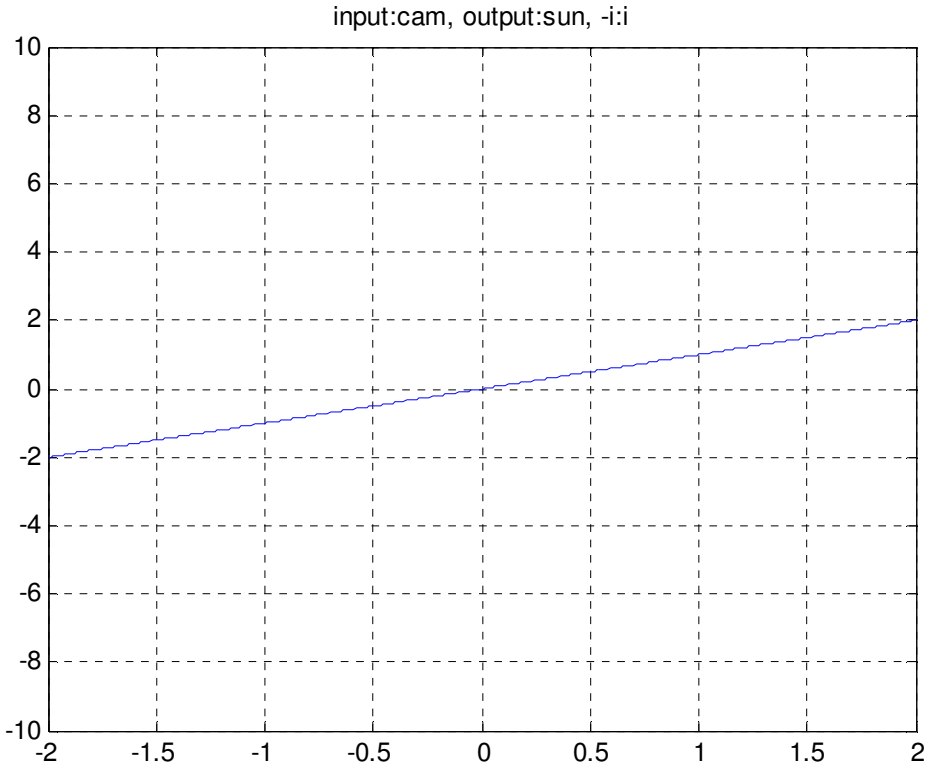

Figure 9-2. Input cam, Output sun

The analysis of all four quadrants of Figure 9-2 are shown below.

Quadrant 1: The transmission ratio is positive, so the cam rotates CW as the input and the sun rotates CW as the output. To maintain a positive internal ratio, a negative value of θ_L is necessary. By Figure 3-9, configuration 'b' must be used (rule 4). As the output, a CCW torque is applied to the sun (rule 3). This torque rotates the followers into the cam, and therefore the transmission ratios in this quadrant are valid.

Quadrant 2: There are no possible transmission ratios in this quadrant, so no analysis is necessary.

Quadrant 3: The transmission ratio is negative, so the cam rotates CW as the input and the sun rotates CCW as the output. To maintain a negative internal ratio, a positive value of θ_L is necessary. By Figure 3-9, configuration 'b' must be used (rule 4). As the output, a CW torque is applied to the sun (rule 3). This torque rotates the followers into the cam, and therefore the transmission ratios in this quadrant are valid.

Quadrant 4: There are no possible transmission ratios in this quadrant, so no analysis is necessary.

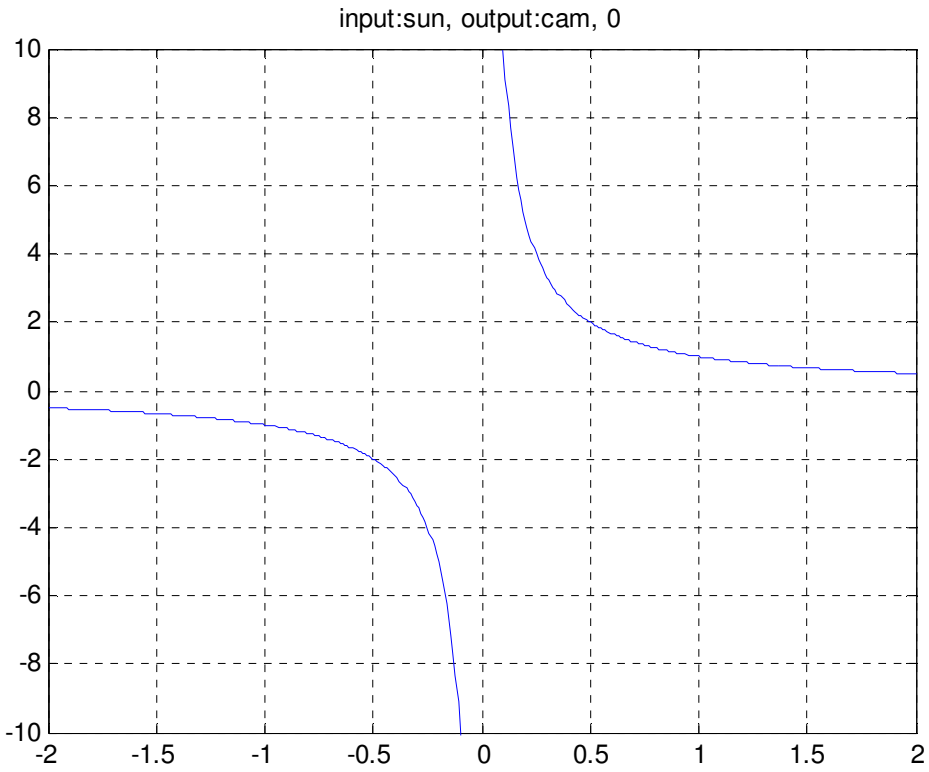

Figure 9-3. Input sun, Output cam

The analysis of all four quadrants of Figure 9-3 are shown below.

Quadrant 1: The transmission ratio is positive, so the sun rotates CW as the input and the cam rotates CW as the output. To maintain a positive internal ratio, a negative value of θ_L is necessary. By Figure 3-9, configuration 'b' must be used (rule 4). As the input, a CW torque is applied to the sun (rule 3). This torque rotates the followers away from the cam, and therefore the transmission ratios in this quadrant are invalid.

Quadrant 2: There are no possible transmission ratios in this quadrant, so no analysis is necessary.

Quadrant 3: The transmission ratio is negative, so the sun rotates CW as the input and the cam rotates CCW as the output. To maintain a negative internal ratio, a positive value of θ_L is necessary. By Figure 3-9, configuration 'c' must be used (rule 4). As the input, a CW torque is applied to the sun (rule 3). This torque rotates the followers away from the cam, and therefore the transmission ratios in this quadrant are invalid.

Quadrant 4: There are no possible transmission ratios in this quadrant, so no analysis is necessary.

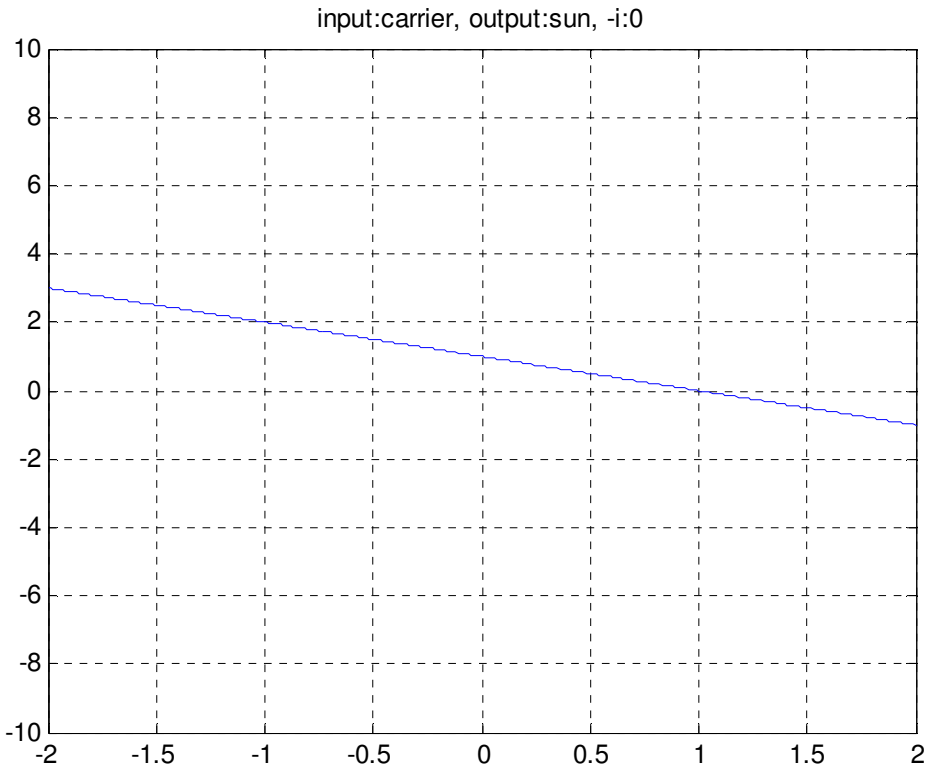

Figure 9-4. Input carrier, Output sun

The analysis of all four quadrants of Figure 9-4 are shown below.

Quadrant 1: The transmission ratio is positive, so the carrier rotates CW as the input and the sun rotates CW as the output. To maintain a positive internal ratio, a negative value of θ_L is necessary. By Figure 3-9, configuration 'd' must be used (rule 4). As the output, a CCW torque is applied to the sun (rule 3). This torque rotates the followers away from the cam, and therefore the transmission ratios in this quadrant are invalid.

Quadrant 2: The transmission ratio is positive, so the carrier rotates CW as the input and the sun rotates CW as the output. To maintain a negative internal ratio, a positive value of θ_L is necessary. By Figure 3-9, configuration 'c' must be used (rule 4). As the output, a CCW torque is applied to the sun (rule 3). This torque rotates the followers into the cam, and therefore the transmission ratios in this quadrant are valid.

Quadrant 3: There are no possible transmission ratios in this quadrant, so no analysis is necessary.

Quadrant 4: The transmission ratio is negative, so the carrier rotates CW as the input and the sun rotates CCW as the output. To maintain a positive internal ratio, a negative value of θ_L is necessary. By Figure 3-9, configuration 'd' must be used (rule 4). As the output, a CW torque is applied to the sun (rule 3). This torque rotates the followers into the cam, and therefore the transmission ratios in this quadrant are valid.